

## 15-7 Worm-Gear Analysis

Compared to other gearing systems worm-gear meshes have a much lower mechanical efficiency. Cooling, for the benefit of the lubricant, becomes a design constraint sometimes resulting in what appears to be an oversize gear case in light of its contents. If the heat can be dissipated by natural cooling, or simply with a fan on the wormshaft, simplicity persists. Water coils within the gear case or lubricant outpumping to an external cooler is the next level of complexity. For this reason, gear-case area is a design decision.

To reduce cooling load, use multiple-thread worms. Also keep the worm pitch diameter as small as possible.

Multiple-thread worms can remove the self-locking feature of many worm-gear drives. When the worm drives the gearset, the mechanical efficiency  $e_W$  is given by

$$e_W = \frac{\cos \phi_n - f \tan \lambda}{\cos \phi_n + f \cot \lambda} \quad (15-54)$$

With the gear driving the gearset, the mechanical efficiency  $e_G$  is given by

$$e_G = \frac{\cos \phi_n - f \cot \lambda}{\cos \phi_n + f \tan \lambda} \quad (15-55)$$

To ensure that the worm gear will drive the worm,

$$f_{\text{stat}} < \cos \phi_n \tan \lambda \quad (15-56)$$

where values of  $f_{\text{stat}}$  can be found in ANSI/AGMA 6034-B92. To prevent the worm gear from driving the worm, refer to clause 9 of 6034-B92 for a discussion of self-locking in the static condition.

It is important to have a way to relate the tangential component of the gear force  $W_G^t$  to the tangential component of the worm force  $W_W^t$ , which includes the role of friction and the angularities of  $\phi_n$  and  $\lambda$ . Refer to Eq. (13-45) solved for  $W_W^t$ :

$$W_W^t = W_G^t \frac{\cos \phi_n \sin \lambda + f \cos \lambda}{\cos \phi_n \cos \lambda - f \sin \lambda} \quad (15-57)$$

In the absence of friction

$$W_W^t = W_G^t \tan \lambda$$

The mechanical efficiency of most gearing is very high, which allows power in and power out to be used almost interchangeably. Worm gearsets have such poor efficiencies that we work with, and speak of, output power. The magnitude of the gear transmitted force  $W_G^t$  can be related to the output horsepower  $H_0$ , the application factor  $K_a$ , the efficiency  $e$ , and design factor  $n_d$  by

$$W_G^t = \frac{33\,000 n_d H_0 K_a}{V_G e} \quad (15-58)$$

We use Eq. (15-57) to obtain the corresponding worm force  $W_W^t$ . It follows that

$$H_W = \frac{W_W^t V_W}{33\,000} = \frac{\pi d_W n_W W_W^t}{12(33\,000)} \text{ hp} \quad (15-59)$$

$$H_G = \frac{W_G^t V_G}{33\,000} = \frac{\pi d_G n_G W_G^t}{12(33\,000)} \text{ hp} \quad (15-60)$$

**Table 15-9**

Largest Lead Angle  
Associated with a  
Normal Pressure Angle  
 $\phi_n$  for Worm Gearing

$\phi_n$	Maximum Lead Angle $\lambda_{\max}$
14.5°	16°
20°	25°
25°	35°
30°	45°

From Eq. (13-44),

$$W_f = \frac{f W_G^t}{f \sin \lambda - \cos \phi_n \cos \lambda} \quad (15-61)$$

The sliding velocity of the worm at the pitch cylinder  $V_s$  is

$$V_s = \frac{\pi d n_w}{12 \cos \lambda} \quad (15-62)$$

and the friction power  $H_f$  is given by

$$H_f = \frac{|W_f| V_s}{33\,000} \text{ hp} \quad (15-63)$$

Table 15-9 gives the largest lead angle  $\lambda_{\max}$  associated with normal pressure angle  $\phi_n$ .

### EXAMPLE 15-3

A single-thread steel worm rotates at 1800 rev/min, meshing with a 24-tooth worm gear transmitting 3 hp to the output shaft. The worm pitch diameter is 3 in and the tangential diametral pitch of the gear is 4 teeth/in. The normal pressure angle is 14.5°. The ambient temperature is 70°F. The application factor is 1.25 and the design factor is 1; gear face width is 2 in, lateral case area 600 in<sup>2</sup>, and the gear is chill-cast bronze.

- Find the gear geometry.
- Find the transmitted gear forces and the mesh efficiency.
- Is the mesh sufficient to handle the loading?
- Estimate the lubricant sump temperature.

### Solution

(a)  $m_G = N_G/N_W = 24/1 = 24$ , gear:  $D = N_G/P_t = 24/4 = 6.000$  in, worm:  $d = 3.000$  in. The axial circular pitch  $p_x$  is  $p_x = \pi/P_t = \pi/4 = 0.7854$  in.  $C = (3 + 6)/2 = 4.5$  in.

$$\text{Eq. (15-39):} \quad a = p_x/\pi = 0.7854/\pi = 0.250 \text{ in}$$

$$\text{Eq. (15-40):} \quad b = 0.3683 p_x = 0.3683(0.7854) = 0.289 \text{ in}$$

$$\text{Eq. (15-41):} \quad h_t = 0.6866 p_x = 0.6866(0.7854) = 0.539 \text{ in}$$

$$\text{Eq. (15-42):} \quad d_0 = 3 + 2(0.250) = 3.500 \text{ in}$$

$$\text{Eq. (15-43):} \quad d_r = 3 - 2(0.289) = 2.422 \text{ in}$$

$$\text{Eq. (15-44):} \quad D_t = 6 + 2(0.250) = 6.500 \text{ in}$$

$$\text{Eq. (15-45):} \quad D_r = 6 - 2(0.289) = 5.422 \text{ in}$$

$$\text{Eq. (15-46):} \quad c = 0.289 - 0.250 = 0.039 \text{ in}$$

$$\text{Eq. (15-47):} \quad (F_W)_{\max} = 2\sqrt{2(6)0.250} = 3.464 \text{ in}$$

The tangential speeds of the worm,  $V_W$ , and gear,  $V_G$ , are, respectively,

$$V_W = \pi(3)1800/12 = 1414 \text{ ft/min} \quad V_G = \frac{\pi(6)1800/24}{12} = 117.8 \text{ ft/min}$$

The lead of the worm, from Eq. (13–27), is  $L = p_x N_W = 0.7854(1) = 0.7854$  in. The lead angle  $\lambda$ , from Eq. (13–28), is

$$\lambda = \tan^{-1} \frac{L}{\pi d} = \tan^{-1} \frac{0.7854}{\pi(3)} = 4.764^\circ$$

The normal diametral pitch for a worm gear is the same as for a helical gear, which from Eq. (13–18) with  $\psi = \lambda$  is

$$P_n = \frac{P_t}{\cos \lambda} = \frac{4}{\cos 4.764^\circ} = 4.014$$

$$p_n = \frac{\pi}{P_n} = \frac{\pi}{4.014} = 0.7827 \text{ in}$$

The sliding velocity, from Eq. (15–62), is

$$V_s = \frac{\pi d n_W}{12 \cos \lambda} = \frac{\pi(3)1800}{12 \cos 4.764^\circ} = 1419 \text{ ft/min}$$

(b) The coefficient of friction, from Eq. (15–38), is

$$f = 0.103 \exp[-0.110(1419)^{0.450}] + 0.012 = 0.0178$$

The efficiency  $e$ , from Eq. (13–46), is

Answer 
$$e = \frac{\cos \phi_n - f \tan \lambda}{\cos \phi_n + f \cot \lambda} = \frac{\cos 14.5^\circ - 0.0178 \tan 4.764^\circ}{\cos 14.5^\circ + 0.0178 \cot 4.764^\circ} = 0.818$$

The designer used  $n_d = 1$ ,  $K_a = 1.25$  and an output horsepower of  $H_0 = 3$  hp. The gear tangential force component  $W_G^t$ , from Eq. (15–58), is

Answer 
$$W_G^t = \frac{33\,000 n_d H_0 K_a}{V_G e} = \frac{33\,000(1)3(1.25)}{117.8(0.818)} = 1284 \text{ lbf}$$

Answer The tangential force on the worm is given by Eq. (15–57):

$$\begin{aligned} W_W^t &= W_G^t \frac{\cos \phi_n \sin \lambda + f \cos \lambda}{\cos \phi_n \cos \lambda - f \sin \lambda} \\ &= 1284 \frac{\cos 14.5^\circ \sin 4.764^\circ + 0.0178 \cos 4.764^\circ}{\cos 14.5^\circ \cos 4.764^\circ - 0.0178 \sin 4.764^\circ} = 131 \text{ lbf} \end{aligned}$$

(c)

Eq. (15–34):  $C_s = 1000$

Eq. (15–36):  $C_m = 0.0107 \sqrt{-24^2 + 56(24) + 5145} = 0.823$

Eq. (15–37):  $C_v = 13.31(1419)^{-0.571} = 0.211^4$

<sup>4</sup>Note: From ANSI/AGMA 6034-B92, the rating factors are  $C_s = 1000$ ,  $C_m = 0.825$ ,  $C_v = 0.214$ , and  $f = 0.0185$ .

$$\begin{aligned}\text{Eq. (15-28): } (W^t)_{\text{all}} &= C_s D^{0.8} (F_e)_G C_m C_v \\ &= 1000(6)^{0.8} (2) 0.823 (0.211) = 1456 \text{ lbf}\end{aligned}$$

Since  $W_G^t < (W^t)_{\text{all}}$ , the mesh will survive at least 25 000 h. The friction force  $W_f$  is given by Eq. (15-61):

$$\begin{aligned}W_f &= \frac{f W_G^t}{f \sin \lambda - \cos \phi_n \cos \lambda} = \frac{0.0178(1284)}{0.0178 \sin 4.764^\circ - \cos 14.5^\circ \cos 4.764^\circ} \\ &= -23.7 \text{ lbf}\end{aligned}$$

The power dissipated in frictional work  $H_f$  is given by Eq. (15-63):

$$H_f = \frac{|W_f| V_s}{33\,000} = \frac{|-23.7| 1419}{33\,000} = 1.02 \text{ hp}$$

The worm and gear powers,  $H_W$  and  $H_G$ , are given by

$$H_W = \frac{W_W^t V_W}{33\,000} = \frac{131(1414)}{33\,000} = 5.61 \text{ hp} \quad H_G = \frac{W_G^t V_G}{33\,000} = \frac{1284(117.8)}{33\,000} = 4.58 \text{ hp}$$

**Answer** Gear power is satisfactory. Now,

$$P_n = P_t / \cos \lambda = 4 / \cos 4.764^\circ = 4.014$$

$$p_n = \pi / P_n = \pi / 4.014 = 0.7827 \text{ in}$$

The bending stress in a gear tooth is given by Buckingham's adaptation of the Lewis equation, Eq. (15-53), as

$$(\sigma)_G = \frac{W_G^t}{p_n F_G y} = \frac{1284}{0.7827(2)(0.1)} = 8200 \text{ psi}$$

**Answer** Stress in gear satisfactory.

(d)

$$\text{Eq. (15-52): } A_{\text{min}} = 43.2 C^{1.7} = 43.2(4.5)^{1.7} = 557 \text{ in}^2$$

The gear case has a lateral area of 600 in<sup>2</sup>.

$$\begin{aligned}\text{Eq. (15-49): } H_{\text{loss}} &= 33\,000(1 - e) H_{\text{in}} = 33\,000(1 - 0.818) 5.61 \\ &= 33\,690 \text{ ft} \cdot \text{lbf/min}\end{aligned}$$

$$\text{Eq. (15-50): } \dot{h}_{\text{CR}} = \frac{n_W}{3939} + 0.13 = \frac{1800}{3939} + 0.13 = 0.587 \text{ ft} \cdot \text{lbf}/(\text{min} \cdot \text{in}^2 \cdot ^\circ\text{F})$$

**Answer**

$$\text{Eq. (15-51): } t_s = t_a + \frac{H_{\text{loss}}}{\dot{h}_{\text{CR}} A} = 70 + \frac{33\,690}{0.587(600)} = 166^\circ\text{F}$$

## 15–8 Designing a Worm-Gear Mesh

A usable decision set for a worm-gear mesh includes

- |   |   |                    |
|---|---|--------------------|
| • Function: power, speed, $m_G$ , $K_a$ | } | A priori decisions |
| • Design factor: $n_d$                  |   |                    |
| • Tooth system                          |   |                    |
| • Materials and processes               |   |                    |
| • Number of threads on the worm: $N_W$  | } | Design variables   |
| • Axial pitch of worm: $p_x$            |   |                    |
| • Pitch diameter of the worm: $d_W$     |   |                    |
| • Face width of gear: $F_G$             |   |                    |
| • Lateral area of case: $A$             |   |                    |

Reliability information for worm gearing is not well developed at this time. The use of Eq. (15–28) together with the factors  $C_s$ ,  $C_m$ , and  $C_v$ , with an alloy steel case-hardened worm together with customary nonferrous worm-wheel materials, will result in lives in excess of 25 000 h. The worm-gear materials in the experience base are principally bronzes:

- Tin- and nickel-bronzes (chilled-casting produces hardest surfaces)
- Lead-bronze (high-speed applications)
- Aluminum- and silicon-bronze (heavy load, slow-speed application)

The factor  $C_s$  for bronze in the spectrum sand-cast, chilled-cast, and centrifugally cast increases in the same order.

Standardization of tooth systems is not as far along as it is in other types of gearing. For the designer this represents freedom of action, but acquisition of tooling for tooth-forming is more of a problem for in-house manufacturing. When using a subcontractor the designer must be aware of what the supplier is capable of providing with on-hand tooling.

Axial pitches for the worm are usually integers, and quotients of integers are common. Typical pitches are  $\frac{1}{4}$ ,  $\frac{5}{16}$ ,  $\frac{3}{8}$ ,  $\frac{1}{2}$ ,  $\frac{3}{4}$ , 1,  $\frac{5}{4}$ ,  $\frac{6}{4}$ ,  $\frac{7}{4}$ , and 2, but others are possible. Table 15–8 shows dimensions common to both worm gear and cylindrical worm for proportions often used. Teeth frequently are stubbed when lead angles are  $30^\circ$  or larger.

Worm-gear design is constrained by available tooling, space restrictions, shaft center-to-center distances, gear ratios needed, and the designer's experience. ANSI/AGMA 6022-C93, *Design Manual for Cylindrical Wormgearing* offers the following guidance. Normal pressure angles are chosen from  $14.5^\circ$ ,  $17.5^\circ$ ,  $20^\circ$ ,  $22.5^\circ$ ,  $25^\circ$ ,  $27.5^\circ$ , and  $30^\circ$ . The recommended minimum number of gear teeth is given in Table 15–10. The normal range of the number of threads on the worm is 1 through 10. Mean worm pitch diameter is usually chosen in the range given by Eq. (15–27).

A design decision is the axial pitch of the worm. Since acceptable proportions are couched in terms of the center-to-center distance, which is not yet known, one chooses a trial axial pitch  $p_x$ . Having  $N_W$  and a trial worm diameter  $d$ ,

$$N_G = m_G N_W \quad P_t = \frac{\pi}{p_x} \quad D = \frac{N_G}{P_t}$$

**Table 15-10**

Minimum Number of  
Gear Teeth for Normal  
Pressure Angle  $\phi_n$

$\phi_n$	$(N_G)_{\min}$
14.5	40
17.5	27
20	21
22.5	17
25	14
27.5	12
30	10

Then

$$(d)_{\text{lo}} = C^{0.875}/3 \quad (d)_{\text{hi}} = C^{0.875}/1.6$$

Examine  $(d)_{\text{lo}} \leq d \leq (d)_{\text{hi}}$ , and refine the selection of mean worm-pitch diameter to  $d_1$  if necessary. Recompute the center-to-center distance as  $C = (d_1 + D)/2$ . There is even an opportunity to make  $C$  a round number. Choose  $C$  and set

$$d_2 = 2C - D$$

Equations (15-39) through (15-48) apply to one usual set of proportions.

#### EXAMPLE 15-4

Design a 10-hp 11:1 worm-gear speed-reducer mesh for a lumber mill planer feed drive for 3- to 10-h daily use. A 1720-rev/min squirrel-cage induction motor drives the planer feed ( $K_a = 1.25$ ), and the ambient temperature is 70°F.

#### Solution

*Function:*  $H_0 = 10$  hp,  $m_G = 11$ ,  $n_W = 1720$  rev/min.

*Design factor:*  $n_d = 1.2$ .

*Materials and processes:* case-hardened alloy steel worm, sand-cast bronze gear.

*Worm threads:* double,  $N_W = 2$ ,  $N_G = m_G N_W = 11(2) = 22$  gear teeth acceptable for  $\phi_n = 20^\circ$ , according to Table 15-10.

*Decision 1:* Choose an axial pitch of worm  $p_x = 1.5$  in. Then,

$$P_t = \pi/p_x = \pi/1.5 = 2.0944$$

$$D = N_G/P_t = 22/2.0944 = 10.504 \text{ in}$$

$$\text{Eq. (15-39): } a = 0.3183p_x = 0.3183(1.5) = 0.4775 \text{ in (addendum)}$$

$$\text{Eq. (15-40): } b = 0.3683(1.5) = 0.5525 \text{ in (dedendum)}$$

$$\text{Eq. (15-41): } h_t = 0.6866(1.5) = 1.030 \text{ in}$$

*Decision 2:* Choose a mean worm diameter  $d = 2.000$  in. Then

$$C = (d + D)/2 = (2.000 + 10.504)/2 = 6.252 \text{ in}$$

$$(d)_{\text{lo}} = 6.252^{0.875}/3 = 1.657 \text{ in}$$

$$(d)_{\text{hi}} = 6.252^{0.875}/1.6 = 3.107 \text{ in}$$

The range, given by Eq. (15-27), is  $1.657 \leq d \leq 3.107$  in, which is satisfactory. Try  $d = 2.500$  in. Recompute  $C$ :

$$C = (2.5 + 10.504)/2 = 6.502 \text{ in}$$

The range is now  $1.715 \leq d \leq 3.216$  in, which is still satisfactory. Decision:  $d = 2.500$  in. Then

$$\text{Eq. (13-27):} \quad L = p_x N_W = 1.5(2) = 3.000 \text{ in}$$

$$\text{Eq. (13-28):}$$

$$\lambda = \tan^{-1}[L/(\pi d)] = \tan^{-1}[3/(\pi 2.5)] = 20.905^\circ \quad (\text{from Table 15-9 lead angle OK})$$

$$\text{Eq. (15-62):} \quad V_s = \frac{\pi d n_W}{12 \cos \lambda} = \frac{\pi (2.5) 1720}{12 \cos 20.905^\circ} = 1205.1 \text{ ft/min}$$

$$V_W = \frac{\pi d n_W}{12} = \frac{\pi (2.5) 1720}{12} = 1125.7 \text{ ft/min}$$

$$V_G = \frac{\pi D n_G}{12} = \frac{\pi (10.504) 1720/11}{12} = 430.0 \text{ ft/min}$$

$$\text{Eq. (15-33):} \quad C_s = 1190 - 477 \log 10.504 = 702.8$$

$$\text{Eq. (15-36):} \quad C_m = 0.02\sqrt{-11^2 + 40(11) - 76} + 0.46 = 0.772$$

$$\text{Eq. (15-37):} \quad C_v = 13.31(1205.1)^{-0.571} = 0.232$$

$$\text{Eq. (15-38):} \quad f = 0.103 \exp[-0.11(1205.1)^{0.45}] + 0.012 = 0.0191^5$$

$$\text{Eq. (15-54):} \quad e_W = \frac{\cos 20^\circ - 0.0191 \tan 20.905^\circ}{\cos 20^\circ + 0.0191 \cot 20.905^\circ} = 0.942$$

(If the worm gear drives,  $e_G = 0.939$ .) To ensure nominal 10-hp output, with adjustments for  $K_a$ ,  $n_d$ , and  $e$ ,

$$\text{Eq. (15-57):} \quad W_W^t = 1222 \frac{\cos 20^\circ \sin 20.905^\circ + 0.0191 \cos 20.905^\circ}{\cos 20^\circ \cos 20.905^\circ - 0.0191 \sin 20.905^\circ} = 495.4 \text{ lbf}$$

$$\text{Eq. (15-58):} \quad W_G^t = \frac{33\,000(1.2)10(1.25)}{430(0.942)} = 1222 \text{ lbf}$$

$$\text{Eq. (15-59):} \quad H_W = \frac{\pi (2.5) 1720 (495.4)}{12(33\,000)} = 16.9 \text{ hp}$$

$$\text{Eq. (15-60):} \quad H_G = \frac{\pi (10.504) 1720/11 (1222)}{12(33\,000)} = 15.92 \text{ hp}$$

$$\text{Eq. (15-61):} \quad W_f = \frac{0.0191(1222)}{0.0191 \sin 20.905^\circ - \cos 20^\circ \cos 20.905^\circ} = -26.8 \text{ lbf}$$

$$\text{Eq. (15-63):} \quad H_f = \frac{|-26.8|1205.1}{33\,000} = 0.979 \text{ hp}$$

With  $C_s = 702.8$ ,  $C_m = 0.772$ , and  $C_v = 0.232$ ,

$$(F_e)_{\text{req}} = \frac{W_G^t}{C_s D^{0.8} C_m C_v} = \frac{1222}{702.8(10.504)^{0.8} 0.772(0.232)} = 1.479 \text{ in}$$

<sup>5</sup>Note: From ANSI/AGMA 6034-B92, the rating factors are  $C_s = 703$ ,  $C_m = 0.773$ ,  $C_v = 0.2345$ , and  $f = 0.01995$ .

*Decision 3:* The available range of  $(F_e)_G$  is  $1.479 \leq (F_e)_G \leq 2d/3$  or  $1.479 \leq (F_e)_G \leq 1.667$  in. Set  $(F_e)_G = 1.5$  in.

$$\text{Eq. (15-28): } W_{\text{all}}^t = 702.8(10.504)^{0.8} 1.5(0.772)0.232 = 1239 \text{ lbf}$$

This is greater than 1222 lbf. There is a little excess capacity. The force analysis stands.

*Decision 4:*

$$\text{Eq. (15-50): } h_{\text{CR}} = \frac{n_W}{6494} + 0.13 = \frac{1720}{6494} + 0.13 = 0.395 \text{ ft} \cdot \text{lbf}/(\text{min} \cdot \text{in}^2 \cdot ^\circ\text{F})$$

$$\text{Eq. (15-49): } H_{\text{loss}} = 33\,000(1 - e)H_W = 33\,000(1 - 0.942)16.9 = 32\,347 \text{ ft} \cdot \text{lbf}/\text{min}$$

The AGMA area, from Eq. (15-52), is  $A_{\text{min}} = 43.2C^{1.7} = 43.2(6.502)^{1.7} = 1041.5 \text{ in}^2$ . A rough estimate of the lateral area for 6-in clearances:

$$\begin{aligned} \text{Vertical: } d + D + 6 &= 2.5 + 10.5 + 6 = 19 \text{ in} \\ \text{Width: } D + 6 &= 10.5 + 6 = 16.5 \text{ in} \\ \text{Thickness: } d + 6 &= 2.5 + 6 = 8.5 \text{ in} \\ \text{Area: } 2(19)16.5 + 2(8.5)19 + 16.5(8.5) &\doteq 1090 \text{ in}^2 \end{aligned}$$

Expect an area of  $1100 \text{ in}^2$ . Choose: Air-cooled, no fan on worm, with an ambient temperature of  $70^\circ\text{F}$ .

$$t_s = t_a + \frac{H_{\text{loss}}}{h_{\text{CR}}A} = 70 + \frac{32\,350}{0.395(1100)} = 70 + 74.5 = 144.5^\circ\text{F}$$

Lubricant is safe with some margin for smaller area.

$$\text{Eq. (13-18): } P_n = \frac{P_t}{\cos \lambda} = \frac{2.094}{\cos 20.905^\circ} = 2.242$$

$$p_n = \frac{\pi}{P_n} = \frac{\pi}{2.242} = 1.401 \text{ in}$$

Gear bending stress, for reference, is

$$\text{Eq. (15-53): } \sigma = \frac{W_G^t}{p_n F_e y} = \frac{1222}{1.401(1.5)0.125} = 4652 \text{ psi}$$

The risk is from wear, which is addressed by the AGMA method that provides  $(W_G^t)_{\text{all}}$ .

## 15-9 Buckingham Wear Load

A precursor to the AGMA method was the method of Buckingham, which identified an allowable wear load in worm gearing. Buckingham showed that the allowable gear-tooth loading for wear can be estimated from

$$(W_G^t)_{\text{all}} = K_w d_G F_e \quad (15-64)$$

where  $K_w$  = worm-gear load factor

$d_G$  = gear-pitch diameter

$F_e$  = worm-gear effective face width



**Table 15–11**Wear Factor  $K_w$  for Worm  
Gearing*Source:* Earle Buckingham,  
*Design of Worm and Spiral  
Gears*, Industrial Press,  
New York, 1981.

Worm	Gear	Thread Angle $\phi_n$			
		$14\frac{1}{2}^\circ$	$20^\circ$	$25^\circ$	$30^\circ$
Hardened steel*	Chilled bronze	90	125	150	180
Hardened steel*	Bronze	60	80	100	120
Steel, 250 BHN (min.)	Bronze	36	50	60	72
High-test cast iron	Bronze	80	115	140	165
Gray iron†	Aluminum	10	12	15	18
High-test cast iron	Gray iron	90	125	150	180
High-test cast iron	Cast steel	22	31	37	45
High-test cast iron	High-test cast iron	135	185	225	270
Steel 250 BHN (min.)	Laminated phenolic	47	64	80	95
Gray iron	Laminated phenolic	70	96	120	140

\*Over 500 BHN surface.

†For steel worms, multiply given values by 0.6.

Table 15–11 gives values for  $K_w$  for worm gearsets as a function of the material pairing and the normal pressure angle.

**EXAMPLE 15–5**

Estimate the allowable gear wear load  $(W_G^t)_{\text{all}}$  for the gearset of Ex. 15–4 using Buckingham's wear equation.

**Solution**

From Table 15–11 for a hardened steel worm and a bronze gear,  $K_w$  is given as 80 for  $\phi_n = 20^\circ$ . Equation (15–64) gives

$$(W_G^t)_{\text{all}} = 80(10.504)1.5 = 1260 \text{ lbf}$$

which is larger than the 1239 lbf of the AGMA method. The method of Buckingham does not have refinements of the AGMA method. [Is  $(W_G^t)_{\text{all}}$  linear with gear diameter?]

For material combinations not addressed by AGMA, Buckingham's method allows quantitative treatment.

**PROBLEMS****15–1**

An uncrowned straight-bevel pinion has 20 teeth, a diametral pitch of 6 teeth/in, and a transmission accuracy number of 6. Both the pinion and gear are made of through-hardened steel with a Brinell hardness of 300. The driven gear has 60 teeth. The gearset has a life goal of  $10^9$  revolutions of the pinion with a reliability of 0.999. The shaft angle is  $90^\circ$ ; the pinion speed is 900 rev/min. The face width is 1.25 in, and the normal pressure angle is  $20^\circ$ . The pinion is mounted outboard of its bearings, and the gear is straddle-mounted. Based on the AGMA bending strength, what is the power rating of the gearset? Use  $K_0 = 1$ ,  $S_F = 1$ , and  $S_H = 1$ .

- 15-2** For the gearset and conditions of Prob. 15-1, find the power rating based on the AGMA surface durability.
- 15-3** An uncrowned straight-bevel pinion has 30 teeth, a diametral pitch of 6, and a transmission accuracy number of 6. The driven gear has 60 teeth. Both are made of No. 30 cast iron. The shaft angle is  $90^\circ$ . The face width is 1.25 in, the pinion speed is 900 rev/min, and the normal pressure angle is  $20^\circ$ . The pinion is mounted outboard of its bearings; the bearings of the gear straddle it. What is the power rating based on AGMA bending strength? (For cast iron gearsets reliability information has not yet been developed. We say the life is greater than  $10^7$  revolutions; set  $K_L = 1$ ,  $C_L = 1$ ,  $C_R = 1$ ,  $K_R = 1$ ; and apply a factor of safety. Use  $S_F = 2$  and  $S_H = \sqrt{2}$ .)
- 15-4** For the gearset and conditions of Prob. 15-3, find the power rating based on AGMA surface durability. For the solutions to Probs. 15-3 and 15-4, what is the power rating of the gearset?
- 15-5** An uncrowned straight-bevel pinion has 22 teeth, a module of 4 mm, and a transmission accuracy number of 5. The pinion and the gear are made of through-hardened steel, both having core and case hardnesses of 180 Brinell. The pinion drives the 24-tooth bevel gear. The shaft angle is  $90^\circ$ , the pinion speed is 1800 rev/min, the face width is 25 mm, and the normal pressure angle is  $20^\circ$ . Both gears have an outboard mounting. Find the power rating based on AGMA pitting resistance if the life goal is  $10^9$  revolutions of the pinion at 0.999 reliability.
- 15-6** For the gearset and conditions of Prob. 15-5, find the power rating for AGMA bending strength.
- 15-7** In straight-bevel gearing, there are some analogs to Eqs. (14-44) and (14-45). If we have a pinion core with a hardness of  $(H_B)_{11}$  and we try equal power ratings, the transmitted load  $W_t$  can be made equal in all four cases. It is possible to find these relations:

	Core	Case
Pinion	$(H_B)_{11}$	$(H_B)_{12}$
Gear	$(H_B)_{21}$	$(H_B)_{22}$

(a) For carburized case-hardened gear steel with core AGMA bending strength  $(s_{at})_G$  and pinion core strength  $(s_{at})_P$ , show that the relationship is

$$(s_{at})_G = (s_{at})_P \frac{J_P}{J_G} m_G^{-0.0323}$$

This allows  $(H_B)_{21}$  to be related to  $(H_B)_{11}$ .

(b) Show that the AGMA contact strength of the gear case  $(s_{ac})_G$  can be related to the AGMA core bending strength of the pinion core  $(s_{at})_P$  by

$$(s_{ac})_G = \frac{C_p}{(C_L)_G C_H} \sqrt{\frac{S_H^2}{S_F} \frac{(s_{at})_P (K_L)_P K_x J_P K_T C_s C_{xc}}{N_P I K_s}}$$

If factors of safety are applied to the transmitted load  $W_t$ , then  $S_H = \sqrt{S_F}$  and  $S_H^2/S_F$  is unity. The result allows  $(H_B)_{22}$  to be related to  $(H_B)_{11}$ .

(c) Show that the AGMA contact strength of the gear  $(s_{ac})_G$  is related to the contact strength of the pinion  $(s_{ac})_P$  by

$$(s_{ac})_P = (s_{ac})_G m_G^{0.0602} C_H$$

**15-8** Refer to your solution to Probs. 15-1 and 15-2, which is to have a pinion core hardness of 300 Brinell. Use the relations from Prob. 15-7 to establish the hardness of the gear core and the case hardnesses of both gears.

**15-9** Repeat Probs. 15-1 and 15-2 with the hardness protocol

	Core	Case
Pinion	300	372
Gear	352	344

which can be established by relations in Prob. 15-7, and see if the result matches transmitted loads  $W^t$  in all four cases.

**15-10** A catalog of stock bevel gears lists a power rating of 5.2 hp at 1200 rev/min pinion speed for a straight-bevel gearset consisting of a 20-tooth pinion driving a 40-tooth gear. This gear pair has a  $20^\circ$  normal pressure angle, a face width of 0.71 in, and a diametral pitch of 10 teeth/in and is through-hardened to 300 BHN. Assume the gears are for general industrial use, are generated to a transmission accuracy number of 5, and are uncrowned. Given these data, what do you think about the stated catalog power rating?

**15-11** Apply the relations of Prob. 15-7 to Ex. 15-1 and find the Brinell case hardness of the gears for equal allowable load  $W^t$  in bending and wear. Check your work by reworking Ex. 15-1 to see if you are correct. How would you go about the heat treatment of the gears?

**15-12** Your experience with Ex. 15-1 and problems based on it will enable you to write an interactive computer program for power rating of through-hardened steel gears. Test your understanding of bevel-gear analysis by noting the ease with which the coding develops. The hardness protocol developed in Prob. 15-7 can be incorporated at the end of your code, first to display it, then as an option to loop back and see the consequences of it.

**15-13** Use your experience with Prob. 15-11 and Ex. 15-2 to design an interactive computer-aided design program for straight-steel bevel gears, implementing the ANSI/AGMA 2003-B97 standard. It will be helpful to follow the decision set in Sec. 15-5, allowing the return to earlier decisions for revision as the consequences of earlier decisions develop.

**15-14** A single-threaded steel worm rotates at 1725 rev/min, meshing with a 56-tooth worm gear transmitting 1 hp to the output shaft. The pitch diameter of the worm is 1.50. The tangential diametral pitch of the gear is 8 teeth per inch and the normal pressure angle is  $20^\circ$ . The ambient temperature is  $70^\circ\text{F}$ , the application factor is 1.25, the design factor is 1, the gear face is 0.5 in, the lateral case area is  $850\text{ in}^2$ , and the gear is sand-cast bronze.

(a) Determine and evaluate the geometric properties of the gears.

(b) Determine the transmitted gear forces and the mesh efficiency.

(c) Is the mesh sufficient to handle the loading?

(d) Estimate the lubricant sump temperature.

**15-15 to 15-22** As in Ex. 15-4, design a cylindrical worm-gear mesh to connect a squirrel-cage induction motor to a liquid agitator. The motor speed is 1125 rev/min, and the velocity ratio is to be 10:1. The output power requirement is 25 hp. The shaft axes are  $90^\circ$  to each other. An overload factor  $K_o$  (see Table 15-2) makes allowance for external dynamic excursions of load from the nominal or average load  $W^t$ . For this service  $K_o = 1.25$  is appropriate. Additionally, a design factor  $n_d$  of 1.1 is to be included to address other unquantifiable risks. For Probs. 15-15 to 15-17 use the AGMA method for  $(W_G^t)_{\text{all}}$  whereas for Probs. 15-18 to 15-22, use the Buckingham method. See Table 15-12.

**Table 15-12**

Table Supporting  
Problems 15-15 to  
15-22

Problem No.	Method	<i>Materials</i>	
		Worm	Gear
15-15	AGMA	Steel, HRC 58	Sand-cast bronze
15-16	AGMA	Steel, HRC 58	Chilled-cast bronze
15-17	AGMA	Steel, HRC 58	Centrifugal-cast bronze
15-18	Buckingham	Steel, 500 Bhn	Chilled-cast bronze
15-19	Buckingham	Steel, 500 Bhn	Cast bronze
15-20	Buckingham	Steel, 250 Bhn	Cast bronze
15-21	Buckingham	High-test cast iron	Cast bronze
15-22	Buckingham	High-test cast iron	High-test cast iron

# 16

## Clutches, Brakes, Couplings, and Flywheels

### Chapter Outline

<b>16-1</b>	Static Analysis of Clutches and Brakes	<b>807</b>
<b>16-2</b>	Internal Expanding Rim Clutches and Brakes	<b>812</b>
<b>16-3</b>	External Contracting Rim Clutches and Brakes	<b>820</b>
<b>16-4</b>	Band-Type Clutches and Brakes	<b>824</b>
<b>16-5</b>	Frictional-Contact Axial Clutches	<b>825</b>
<b>16-6</b>	Disk Brakes	<b>829</b>
<b>16-7</b>	Cone Clutches and Brakes	<b>833</b>
<b>16-8</b>	Energy Considerations	<b>836</b>
<b>16-9</b>	Temperature Rise	<b>837</b>
<b>16-10</b>	Friction Materials	<b>841</b>
<b>16-11</b>	Miscellaneous Clutches and Couplings	<b>844</b>
<b>16-12</b>	Flywheels	<b>846</b>

This chapter is concerned with a group of elements usually associated with rotation that have in common the function of storing and/or transferring rotating energy. Because of this similarity of function, clutches, brakes, couplings, and flywheels are treated together in this book.

A simplified dynamic representation of a friction clutch or brake is shown in Fig. 16–1*a*. Two inertias,  $I_1$  and  $I_2$ , traveling at the respective angular velocities  $\omega_1$  and  $\omega_2$ , one of which may be zero in the case of brakes, are to be brought to the same speed by engaging the clutch or brake. Slippage occurs because the two elements are running at different speeds and energy is dissipated during actuation, resulting in a temperature rise. In analyzing the performance of these devices we shall be interested in:

- 1 The actuating force
- 2 The torque transmitted
- 3 The energy loss
- 4 The temperature rise

The torque transmitted is related to the actuating force, the coefficient of friction, and the geometry of the clutch or brake. This is a problem in statics, which will have to be studied separately for each geometric configuration. However, temperature rise is related to energy loss and can be studied without regard to the type of brake or clutch, because the geometry of interest is that of the heat-dissipating surfaces.

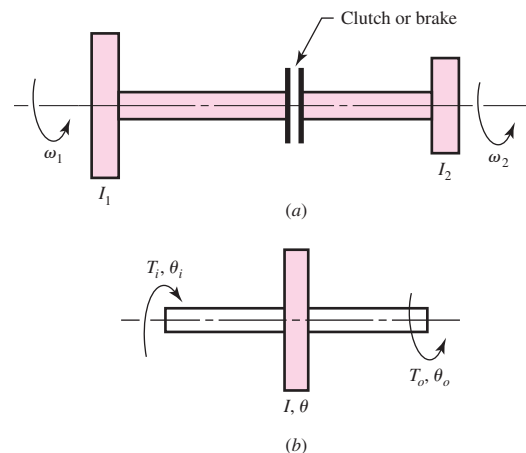
The various types of devices to be studied may be classified as follows:

- 1 Rim types with internal expanding shoes
- 2 Rim types with external contracting shoes
- 3 Band types
- 4 Disk or axial types
- 5 Cone types
- 6 Miscellaneous types

A flywheel is an inertial energy-storage device. It absorbs mechanical energy by increasing its angular velocity and delivers energy by decreasing its velocity. Figure 16–1*b* is a mathematical representation of a flywheel. An input torque  $T_i$ , corresponding to a coordinate  $\theta_i$ , will cause the flywheel speed to increase. And a load or output torque  $T_o$ , with coordinate  $\theta_o$ , will absorb energy from the flywheel and cause it to slow down. We shall be interested in designing flywheels so as to obtain a specified amount of speed regulation.

**Figure 16–1**

(*a*) Dynamic representation of a clutch or brake;  
(*b*) mathematical representation of a flywheel.



## 16-1 Static Analysis of Clutches and Brakes

Many types of clutches and brakes can be analyzed by following a general procedure. The procedure entails the following tasks:

- Estimate, model, or measure the pressure distribution on the friction surfaces.
- Find a relationship between the largest pressure and the pressure at any point.
- Use the conditions of static equilibrium to find the braking force or torque and the support reactions.

Let us apply these tasks to the doorstep depicted in Fig. 16-2a. The stop is hinged at pin A. A normal pressure distribution  $p(u)$  is shown under the friction pad as a function of position  $u$ , taken from the right edge of the pad. A similar distribution of shearing frictional traction is on the surface, of intensity  $fp(u)$ , in the direction of the motion of the floor relative to the pad, where  $f$  is the coefficient of friction. The width of the pad into the page is  $w_2$ . The net force in the  $y$  direction and moment about C from the pressure are respectively,

$$N = w_2 \int_0^{w_1} p(u) du = p_{av} w_1 w_2 \quad (a)$$

$$w_2 \int_0^{w_1} p(u)u du = \bar{u} w_2 \int_0^{w_1} p(u) du = p_{av} w_1 w_2 \bar{u} \quad (b)$$

We sum the forces in the  $x$ -direction to obtain

$$\sum F_x = R_x \mp w_2 \int_0^{w_1} fp(u) du = 0$$

where  $-$  or  $+$  is for rightward or leftward relative motion of the floor, respectively. Assuming  $f$  constant, solving for  $R_x$  gives

$$R_x = \pm w_2 \int_0^{w_1} fp(u) du = \pm f w_1 w_2 p_{av} \quad (c)$$

Summing the forces in the  $y$  direction gives

$$\sum F_y = -F + w_2 \int_0^{w_1} p(u) du + R_y = 0$$

from which

$$R_y = F - w_2 \int_0^{w_1} p(u) du = F - p_{av} w_1 w_2 \quad (d)$$

for either direction. Summing moments about the pin located at A we have

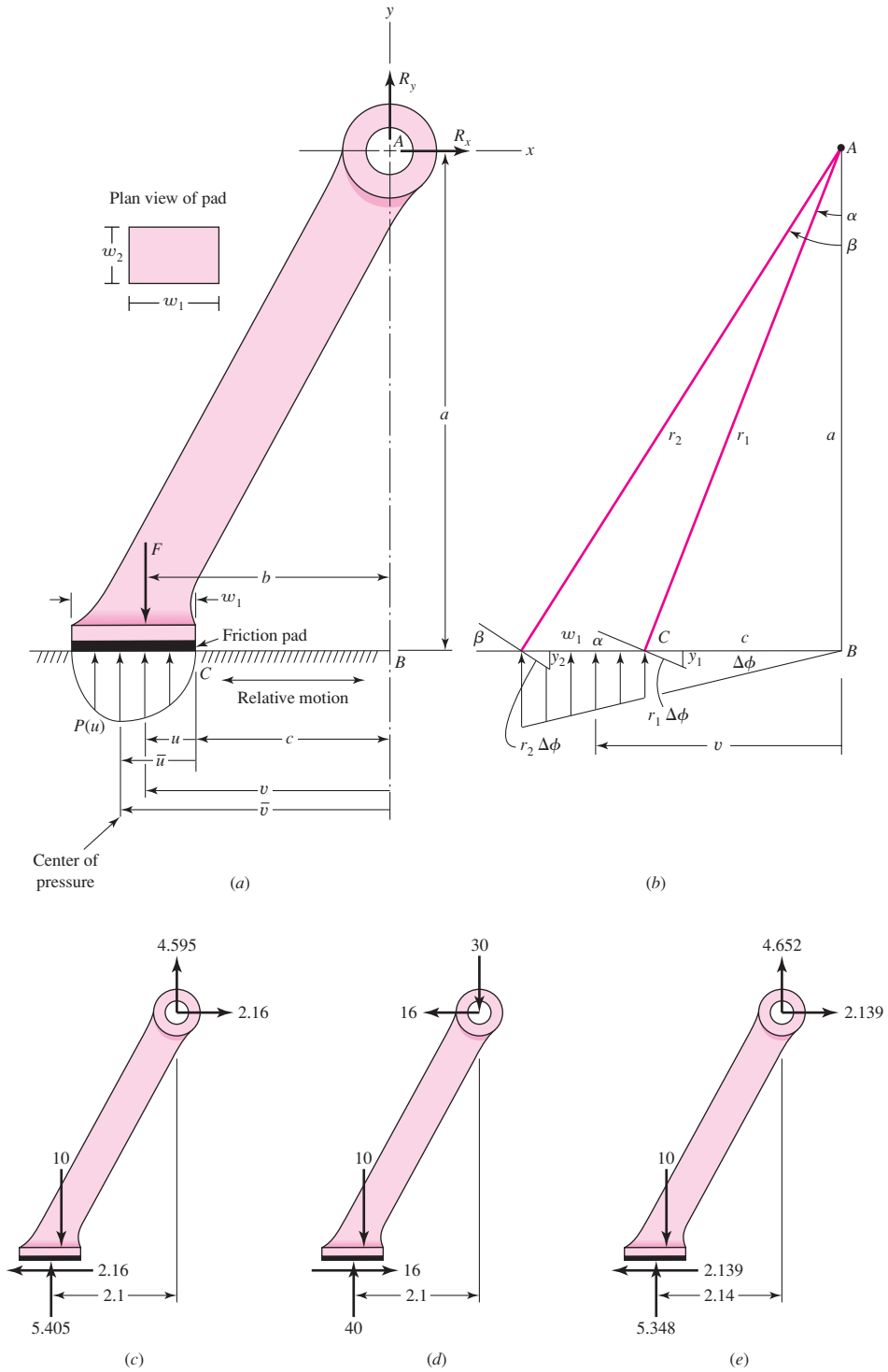
$$\sum M_A = Fb - w_2 \int_0^{w_1} p(u)(c + u) du \mp af w_2 \int_0^{w_1} p(u) du = 0$$

A brake shoe is *self-energizing* if its moment sense helps set the brake, *self-deenergizing* if the moment resists setting the brake. Continuing,

$$F = \frac{w_2}{b} \left[ \int_0^{w_1} p(u)(c + u) du \pm af \int_0^{w_1} p(u) du \right] \quad (e)$$

**Figure 16-2**

A common doorstep.  
(a) Free body of the doorstep.  
(b) Trapezoidal pressure distribution on the foot pad based on linear deformation of pad. (c) Free-body diagram for leftward movement of the floor, uniform pressure, Ex. 16-1. (d) Free-body diagram for rightward movement of the floor, uniform pressure, Ex. 16-1. (e) Free-body diagram for leftward movement of the floor, trapezoidal pressure, Ex. 16-1.





Can  $F$  be equal to or less than zero? Only during rightward motion of the floor when the expression in brackets in Eq. (e) is equal to or less than zero. We set the brackets to zero or less:

$$\int_0^{w_1} p(u)(c+u) du - af \int_0^{w_1} p(u) du \leq 0$$

from which

$$f_{cr} \geq \frac{\frac{1}{a} \int_0^{w_1} p(u)(c+u) du}{\int_0^{w_1} p(u) du} = \frac{\frac{1}{a} c \int_0^{w_1} p(u) du + \int_0^{w_1} p(u)u du}{\int_0^{w_1} p(u) du}$$

$$f_{cr} \geq \frac{c + \bar{u}}{a} \quad (f)$$

where  $\bar{u}$  is the distance of the center of pressure from the right edge of the pad. The conclusion that a *self-acting* or *self-locking* phenomenon is present is independent of our knowledge of the normal pressure distribution  $p(u)$ . Our ability to *find* the critical value of the coefficient of friction  $f_{cr}$  is dependent on our knowledge of  $p(u)$ , from which we derive  $\bar{u}$ .

### EXAMPLE 16-1

The doorstep depicted in Fig. 16-2a has the following dimensions:  $a = 4$  in,  $b = 2$  in,  $c = 1.6$  in,  $w_1 = 1$  in,  $w_2 = 0.75$  in, where  $w_2$  is the depth of the pad into the plane of the paper.

(a) For a leftward relative movement of the floor, an actuating force  $F$  of 10 lbf, a coefficient of friction of 0.4, use a uniform pressure distribution  $p_{av}$ , find  $R_x$ ,  $R_y$ ,  $p_{av}$ , and the largest pressure  $p_a$ .

(b) Repeat part a for rightward relative movement of the floor.

(c) Model the normal pressure to be the “crush” of the pad, much as if it were composed of many small helical coil springs. Find  $R_x$ ,  $R_y$ ,  $p_{av}$ , and  $p_a$  for leftward relative movement of the floor and other conditions as in part a.

(d) For rightward relative movement of the floor, is the doorstep a self-acting brake?

### Solution

(a)

$$\text{Eq. (c):} \quad R_x = fp_{av}w_1w_2 = 0.4(1)(0.75)p_{av} = 0.3p_{av}$$

$$\text{Eq. (d):} \quad R_y = F - p_{av}w_1w_2 = 10 - p_{av}(1)(0.75) = 10 - 0.75p_{av}$$

$$\begin{aligned} \text{Eq. (e):} \quad F &= \frac{w_2}{b} \left[ \int_0^1 p_{av}(c+u) du + af \int_0^1 p_{av} du \right] \\ &= \frac{w_2}{b} \left( p_{av}c \int_0^1 du + p_{av} \int_0^1 u du + afp_{av} \int_0^1 du \right) \\ &= \frac{w_2 p_{av}}{b} (c + 0.5 + af) = \frac{0.75}{2} [1.6 + 0.5 + 4(0.4)] p_{av} \\ &= 1.3875 p_{av} \end{aligned}$$

Solving for  $p_{av}$  gives

$$p_{av} = \frac{F}{1.3875} = \frac{10}{1.3875} = 7.207 \text{ psi}$$

We evaluate  $R_x$  and  $R_y$  as

**Answer**  $R_x = 0.3(7.207) = 2.162 \text{ lbf}$

**Answer**  $R_y = 10 - 0.75(7.207) = 4.595 \text{ lbf}$

The normal force  $N$  on the pad is  $F - R_y = 10 - 4.595 = 5.405 \text{ lbf}$ , upward. The line of action is through the center of pressure, which is at the center of the pad. The friction force is  $fN = 0.4(5.405) = 2.162 \text{ lbf}$  directed to the left. A check of the moments about  $A$  gives

$$\begin{aligned} \sum M_A &= Fb - fNa - N(w_1/2 + c) \\ &= 10(2) - 0.4(5.405)4 - 5.405(1/2 + 1.6) \doteq 0 \end{aligned}$$

**Answer** The maximum pressure  $p_a = p_{av} = 7.207 \text{ psi}$ .  
(b)

Eq. (c):  $R_x = -fp_{av}w_1w_2 = -0.4(1)(0.75)p_{av} = -0.3p_{av}$

Eq. (d):  $R_y = F - p_{av}w_1w_2 = 10 - p_{av}(1)(0.75) = 10 - 0.75p_{av}$

Eq. (e): 
$$\begin{aligned} F &= \frac{w_2}{b} \left[ \int_0^1 p_{av}(c + u) du + af \int_0^1 p_{av} du \right] \\ &= \frac{w_2}{b} \left( p_{av}c \int_0^1 du + p_{av} \int_0^1 u du + afp_{av} \int_0^1 du \right) \\ &= \frac{0.75}{2} p_{av} [1.6 + 0.5 - 4(0.4)] = 0.1875 p_{av} \end{aligned}$$

from which

$$p_{av} = \frac{F}{0.1875} = \frac{10}{0.1875} = 53.33 \text{ psi}$$

which makes

**Answer**  $R_x = -0.3(53.33) = -16 \text{ lbf}$

**Answer**  $R_y = 10 - 0.75(53.33) = -30 \text{ lbf}$

The normal force  $N$  on the pad is  $10 + 30 = 40 \text{ lbf}$  upward. The friction shearing force is  $fN = 0.4(40) = 16 \text{ lbf}$  to the right. We now check the moments about  $A$ :

$$M_A = fNa + Fb - N(c + 0.5) = 16(4) + 10(2) - 40(1.6 + 0.5) = 0$$

Note the change in average pressure from 7.207 psi in part *a* to 53.3 psi. Also note how directions of forces have changed. The maximum pressure  $p_a$  is the same as  $p_{av}$ , which has changed from 7.207 psi to 53.3 psi.

(c) We will model the deformation of the pad as follows. If the doorstep rotates  $\Delta\phi$  counterclockwise, the right and left edges of the pad will deform down  $y_1$  and  $y_2$ , respectively (Fig. 16-2*b*). From similar triangles,  $y_1/(r_1 \Delta\phi) = c/r_1$  and  $y_2/(r_2 \Delta\phi) = (c + w_1)/r_2$ . Thus,  $y_1 = c \Delta\phi$  and  $y_2 = (c + w_1) \Delta\phi$ . This means that  $y$  is directly

proportional to the horizontal distance from the pivot point  $A$ ; that is,  $y = C_1 v$ , where  $C_1$  is a constant (see Fig. 16–2*b*). Assuming the pressure is directly proportional to deformation, then  $p(v) = C_2 v$ , where  $C_2$  is a constant. In terms of  $u$ , the pressure is  $p(u) = C_2(c + u) = C_2(1.6 + u)$ .

Eq. (e):

$$\begin{aligned} F &= \frac{w_2}{b} \left[ \int_0^{w_1} p(u)c \, du + \int_0^{w_1} p(u)u \, du + af \int_0^{w_1} p(u) \, du \right] \\ &= \frac{0.75}{2} \left[ \int_0^1 C_2(1.6 + u)1.6 \, du + \int_0^1 C_2(1.6 + u)u \, du + af \int_0^1 C_2(1.6 + u) \, du \right] \\ &= 0.375C_2[(1.6 + 0.5)1.6 + (0.8 + 0.3333) + 4(0.4)(1.6 + 0.5)] = 2.945C_2 \end{aligned}$$

Since  $F = 10$  lbf, then  $C_2 = 10/2.945 = 3.396$  psi/in, and  $p(u) = 3.396(1.6 + u)$ . The average pressure is given by

**Answer** 
$$p_{av} = \frac{1}{w_1} \int_0^{w_1} p(u) \, du = \frac{1}{1} \int_0^1 3.396(1.6 + u) \, du = 3.396(1.6 + 0.5) = 7.132 \text{ psi}$$

The maximum pressure occurs at  $u = 1$  in, and is

**Answer** 
$$p_a = 3.396(1.6 + 1) = 8.83 \text{ psi}$$

Equations (c) and (d) of Sec. 16–1 are still valid. Thus,

**Answer** 
$$\begin{aligned} R_x &= 0.3p_{av} = 0.3(7.131) = 2.139 \text{ lbf} \\ R_y &= 10 - 0.75p_{av} = 10 - 0.75(7.131) = 4.652 \text{ lbf} \end{aligned}$$

The average pressure is  $p_{av} = 7.13$  psi and the maximum pressure is  $p_a = 8.83$  psi, which is approximately 24 percent higher than the average pressure. The presumption that the pressure was uniform in part *a* (because the pad was small, or because the arithmetic would be easier?) underestimated the peak pressure. Modeling the pad as a one-dimensional springset is better, but the pad is really a three-dimensional continuum. A theory of elasticity approach or a finite element modeling may be overkill, given uncertainties inherent in this problem, but it still represents better modeling.

(d) To evaluate  $\bar{u}$  we need to evaluate two integrations

$$\begin{aligned} \int_0^c p(u)u \, du &= \int_0^1 3.396(1.6 + u)u \, du = 3.396(0.8 + 0.3333) = 3.849 \text{ lbf} \\ \int_0^c p(u) \, du &= \int_0^1 3.396(1.6 + u) \, du = 3.396(1.6 + 0.5) = 7.132 \text{ lbf/in} \end{aligned}$$

Thus  $\bar{u} = 3.849/7.132 = 0.5397$  in. Then, from Eq. (f) of Sec. 16–1, the critical coefficient of friction is

**Answer** 
$$f_{cr} \geq \frac{c + \bar{u}}{a} = \frac{1.6 + 0.5397}{4} = 0.535$$

The doorstep friction pad does not have a high enough coefficient of friction to make the doorstep a self-acting brake. The configuration must change and/or the pad material specification must be changed to sustain the function of a doorstep.

## 16-2 Internal Expanding Rim Clutches and Brakes

The internal-shoe rim clutch shown in Fig. 16-3 consists essentially of three elements: the mating frictional surface, the means of transmitting the torque to and from the surfaces, and the actuating mechanism. Depending upon the operating mechanism, such clutches are further classified as *expanding-ring*, *centrifugal*, *magnetic*, *hydraulic*, and *pneumatic*.

The expanding-ring clutch is often used in textile machinery, excavators, and machine tools where the clutch may be located within the driving pulley. Expanding-ring clutches benefit from centrifugal effects; transmit high torque, even at low speeds; and require both positive engagement and ample release force.

The centrifugal clutch is used mostly for automatic operation. If no spring is used, the torque transmitted is proportional to the square of the speed. This is particularly useful for electric-motor drives where, during starting, the driven machine comes up to speed without shock. Springs can also be used to prevent engagement until a certain motor speed is reached, but some shock may occur.

Magnetic clutches are particularly useful for automatic and remote-control systems. Such clutches are also useful in drives subject to complex load cycles (see Sec. 11-7).

Hydraulic and pneumatic clutches are also useful in drives having complex loading cycles and in automatic machinery, or in robots. Here the fluid flow can be controlled remotely using solenoid valves. These clutches are also available as disk, cone, and multiple-plate clutches.

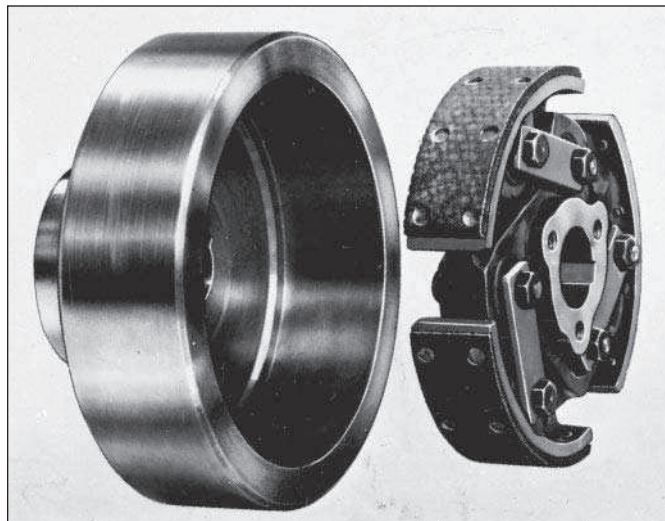
In braking systems, the *internal-shoe* or *drum* brake is used mostly for automotive applications.

To analyze an internal-shoe device, refer to Fig. 16-4, which shows a shoe pivoted at point A, with the actuating force acting at the other end of the shoe. Since the shoe is long, we cannot make the assumption that the distribution of normal forces is uniform. The mechanical arrangement permits no pressure to be applied at the heel, and we will therefore assume the pressure at this point to be zero.

It is the usual practice to omit the friction material for a short distance away from the heel (point A). This eliminates interference, and the material would contribute little to the performance anyway, as will be shown. In some designs the hinge pin is made movable to provide additional heel pressure. This gives the effect of a floating shoe.

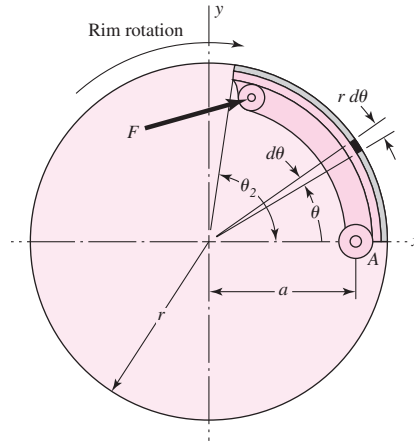
**Figure 16-3**

An internal expanding centrifugal-acting rim clutch.  
(Courtesy of the Hilliard Corporation.)

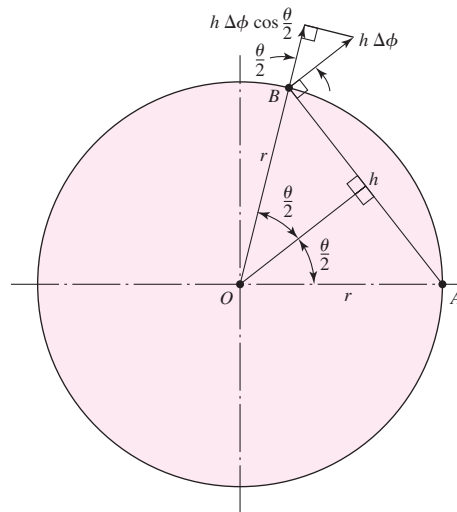


**Figure 16-4**

Internal friction shoe geometry.

**Figure 16-5**

The geometry associated with an arbitrary point on the shoe.



(Floating shoes will not be treated in this book, although their design follows the same general principles.)

Let us consider the pressure  $p$  acting upon an element of area of the frictional material located at an angle  $\theta$  from the hinge pin (Fig. 16-4). We designate the maximum pressure  $p_a$  located at an angle  $\theta_a$  from the hinge pin. To find the pressure distribution on the periphery of the internal shoe, consider point  $B$  on the shoe (Fig. 16-5). As in Ex. 16-1, if the shoe deforms by an infinitesimal rotation  $\Delta\phi$  about the pivot point  $A$ , deformation perpendicular to  $AB$  is  $h \Delta\phi$ . From the isosceles triangle  $AOB$ ,  $h = 2r \sin(\theta/2)$ , so

$$h \Delta\phi = 2r \Delta\phi \sin(\theta/2)$$

The deformation perpendicular to the rim is  $h \Delta\phi \cos(\theta/2)$ , which is

$$h \Delta\phi \cos(\theta/2) = 2r \Delta\phi \sin(\theta/2) \cos(\theta/2) = r \Delta\phi \sin \theta$$

Thus, the deformation, and consequently the pressure, is proportional to  $\sin \theta$ . In terms of the pressure at  $B$  and where the pressure is a maximum, this means

$$\frac{p}{\sin \theta} = \frac{p_a}{\sin \theta_a} \quad (a)$$

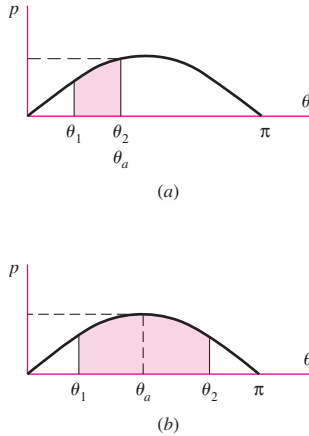


**Figure 16-6**

Defining the angle  $\theta_a$  at which the maximum pressure  $p_a$  occurs when (a) shoe exists in zone  $\theta_1 \leq \theta_2 \leq \pi/2$  and (b) shoe exists in zone  $\theta_1 \leq \pi/2 \leq \theta_2$ .

Rearranging gives

$$p = \frac{p_a}{\sin \theta_a} \sin \theta \quad (16-1)$$

This pressure distribution has interesting and useful characteristics:

- The pressure distribution is sinusoidal with respect to the angle  $\theta$ .
- If the shoe is short, as shown in Fig. 16-6a, the largest pressure on the shoe is  $p_a$  occurring at the end of the shoe,  $\theta_2$ .
- If the shoe is long, as shown in Fig. 16-6b, the largest pressure on the shoe is  $p_a$  occurring at  $\theta_a = 90^\circ$ .

Since limitations on friction materials are expressed in terms of the largest allowable pressure on the lining, the designer wants to think in terms of  $p_a$  and not about the amplitude of the sinusoidal distribution that addresses locations off the shoe.

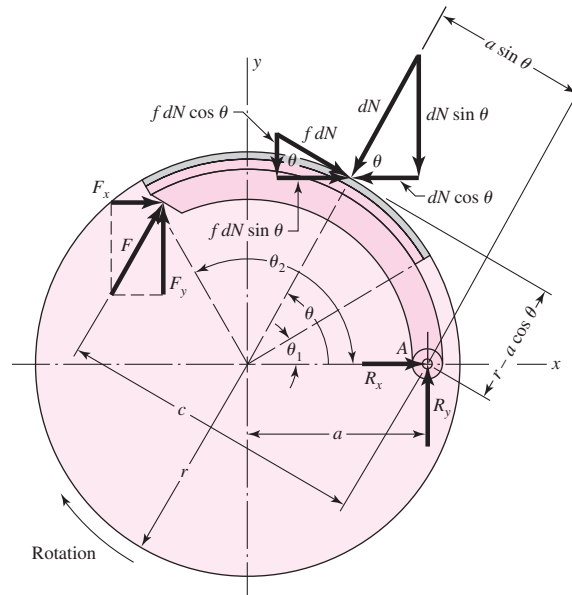
When  $\theta = 0$ , Eq. (16-1) shows that the pressure is zero. The frictional material located at the heel therefore contributes very little to the braking action and might as well be omitted. A good design would concentrate as much frictional material as possible in the neighborhood of the point of maximum pressure. Such a design is shown in Fig. 16-7. In this figure the frictional material begins at an angle  $\theta_1$ , measured from the hinge pin A, and ends at an angle  $\theta_2$ . Any arrangement such as this will give a good distribution of the frictional material.

Proceeding now (Fig. 16-7), the hinge-pin reactions are  $R_x$  and  $R_y$ . The actuating force  $F$  has components  $F_x$  and  $F_y$  and operates at distance  $c$  from the hinge pin. At any angle  $\theta$  from the hinge pin there acts a differential normal force  $dN$  whose magnitude is

$$dN = pbr d\theta \quad (b)$$

**Figure 16-7**

Forces on the shoe.



where  $b$  is the face width (perpendicular to the paper) of the friction material. Substituting the value of the pressure from Eq. (16-1), the normal force is

$$dN = \frac{p_a b r \sin \theta d\theta}{\sin \theta_a} \quad (c)$$

The normal force  $dN$  has horizontal and vertical components  $dN \cos \theta$  and  $dN \sin \theta$ , as shown in the figure. The frictional force  $f dN$  has horizontal and vertical components whose magnitudes are  $f dN \sin \theta$  and  $f dN \cos \theta$ , respectively. By applying the conditions of static equilibrium, we may find the actuating force  $F$ , the torque  $T$ , and the pin reactions  $R_x$  and  $R_y$ .

We shall find the actuating force  $F$ , using the condition that the summation of the moments about the hinge pin is zero. The frictional forces have a moment arm about the pin of  $r - a \cos \theta$ . The moment  $M_f$  of these frictional forces is

$$M_f = \int f dN (r - a \cos \theta) = \frac{f p_a b r}{\sin \theta_a} \int_{\theta_1}^{\theta_2} \sin \theta (r - a \cos \theta) d\theta \quad (16-2)$$

which is obtained by substituting the value of  $dN$  from Eq. (c). It is convenient to integrate Eq. (16-2) for each problem, and we shall therefore retain it in this form. The moment arm of the normal force  $dN$  about the pin is  $a \sin \theta$ . Designating the moment of the normal forces by  $M_N$  and summing these about the hinge pin give

$$M_N = \int dN (a \sin \theta) = \frac{p_a b r a}{\sin \theta_a} \int_{\theta_1}^{\theta_2} \sin^2 \theta d\theta \quad (16-3)$$

The actuating force  $F$  must balance these moments. Thus

$$F = \frac{M_N - M_f}{c} \quad (16-4)$$

We see here that a condition for zero actuating force exists. In other words, if we make  $M_N = M_f$ , self-locking is obtained, and no actuating force is required. This furnishes us with a method for obtaining the dimensions for some self-energizing action. Thus the dimension  $a$  in Fig. 16-7 must be such that

$$M_N > M_f \quad (16-5)$$

The torque  $T$  applied to the drum by the brake shoe is the sum of the frictional forces  $f dN$  times the radius of the drum:

$$\begin{aligned} T &= \int f r dN = \frac{f p_a b r^2}{\sin \theta_a} \int_{\theta_1}^{\theta_2} \sin \theta d\theta \\ &= \frac{f p_a b r^2 (\cos \theta_1 - \cos \theta_2)}{\sin \theta_a} \end{aligned} \quad (16-6)$$

The hinge-pin reactions are found by taking a summation of the horizontal and vertical forces. Thus, for  $R_x$ , we have

$$\begin{aligned} R_x &= \int dN \cos \theta - \int f dN \sin \theta - F_x \\ &= \frac{p_a b r}{\sin \theta_a} \left( \int_{\theta_1}^{\theta_2} \sin \theta \cos \theta d\theta - f \int_{\theta_1}^{\theta_2} \sin^2 \theta d\theta \right) - F_x \end{aligned} \quad (d)$$

The vertical reaction is found in the same way:

$$\begin{aligned} R_y &= \int dN \sin \theta + \int f dN \cos \theta - F_y \\ &= \frac{p_a b r}{\sin \theta_a} \left( \int_{\theta_1}^{\theta_2} \sin^2 \theta d\theta + f \int_{\theta_1}^{\theta_2} \sin \theta \cos \theta d\theta \right) - F_y \end{aligned} \quad (e)$$

The direction of the frictional forces is reversed if the rotation is reversed. Thus, for counterclockwise rotation the actuating force is

$$F = \frac{M_N + M_f}{c} \quad (16-7)$$

and since both moments have the same sense, the self-energizing effect is lost. Also, for counterclockwise rotation the signs of the frictional terms in the equations for the pin reactions change, and Eqs. (d) and (e) become

$$R_x = \frac{p_a b r}{\sin \theta_a} \left( \int_{\theta_1}^{\theta_2} \sin \theta \cos \theta d\theta + f \int_{\theta_1}^{\theta_2} \sin^2 \theta d\theta \right) - F_x \quad (f)$$

$$R_y = \frac{p_a b r}{\sin \theta_a} \left( \int_{\theta_1}^{\theta_2} \sin^2 \theta d\theta - f \int_{\theta_1}^{\theta_2} \sin \theta \cos \theta d\theta \right) - F_y \quad (g)$$

Equations (d), (e), (f), and (g) can be simplified to ease computations. Thus, let

$$\begin{aligned} A &= \int_{\theta_1}^{\theta_2} \sin \theta \cos \theta d\theta = \left( \frac{1}{2} \sin^2 \theta \right)_{\theta_1}^{\theta_2} \\ B &= \int_{\theta_1}^{\theta_2} \sin^2 \theta d\theta = \left( \frac{\theta}{2} - \frac{1}{4} \sin 2\theta \right)_{\theta_1}^{\theta_2} \end{aligned} \quad (16-8)$$

Then, for clockwise rotation as shown in Fig. 16–7, the hinge-pin reactions are

$$\begin{aligned} R_x &= \frac{p_a b r}{\sin \theta_a} (A - f B) - F_x \\ R_y &= \frac{p_a b r}{\sin \theta_a} (B + f A) - F_y \end{aligned} \quad (16-9)$$

For counterclockwise rotation, Eqs. (f) and (g) become

$$\begin{aligned} R_x &= \frac{p_a b r}{\sin \theta_a} (A + f B) - F_x \\ R_y &= \frac{p_a b r}{\sin \theta_a} (B - f A) - F_y \end{aligned} \quad (16-10)$$

In using these equations, the reference system always has its origin at the center of the drum. The positive  $x$  axis is taken through the hinge pin. The positive  $y$  axis is always in the direction of the shoe, even if this should result in a left-handed system.

The following assumptions are implied by the preceding analysis:

- 1 The pressure at any point on the shoe is assumed to be proportional to the distance from the hinge pin, being zero at the heel. This should be considered from the standpoint that pressures specified by manufacturers are averages rather than maxima.



- 2 The effect of centrifugal force has been neglected. In the case of brakes, the shoes are not rotating, and no centrifugal force exists. In clutch design, the effect of this force must be considered in writing the equations of static equilibrium.
- 3 The shoe is assumed to be rigid. Since this cannot be true, some deflection will occur, depending upon the load, pressure, and stiffness of the shoe. The resulting pressure distribution may be different from that which has been assumed.
- 4 The entire analysis has been based upon a coefficient of friction that does not vary with pressure. Actually, the coefficient may vary with a number of conditions, including temperature, wear, and environment.

**EXAMPLE 16-2**

The brake shown in Fig. 16-8 is 300 mm in diameter and is actuated by a mechanism that exerts the same force  $F$  on each shoe. The shoes are identical and have a face width of 32 mm. The lining is a molded asbestos having a coefficient of friction of 0.32 and a pressure limitation of 1000 kPa. Estimate the maximum

- (a) Actuating force  $F$ .
- (b) Braking capacity.
- (c) Hinge-pin reactions.

**Solution**

(a) The right-hand shoe is self-energizing, and so the force  $F$  is found on the basis that the maximum pressure will occur on this shoe. Here  $\theta_1 = 0^\circ$ ,  $\theta_2 = 126^\circ$ ,  $\theta_a = 90^\circ$ , and  $\sin \theta_a = 1$ . Also,

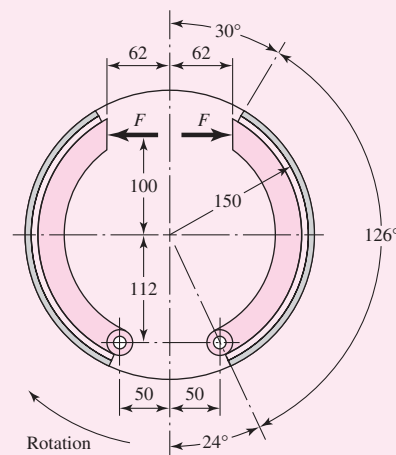
$$a = \sqrt{(112)^2 + (50)^2} = 122.7 \text{ mm}$$

Integrating Eq. (16-2) from 0 to  $\theta_2$  yields

$$\begin{aligned} M_f &= \frac{f p_a b r}{\sin \theta_a} \left[ \left( -r \cos \theta \right)_0^{\theta_2} - a \left( \frac{1}{2} \sin^2 \theta \right)_0^{\theta_2} \right] \\ &= \frac{f p_a b r}{\sin \theta_a} \left( r - r \cos \theta_2 - \frac{a}{2} \sin^2 \theta_2 \right) \end{aligned}$$

**Figure 16-8**

Brake with internal expanding shoes; dimensions in millimeters.



Changing all lengths to meters, we have

$$\begin{aligned} M_f &= (0.32)[1000(10)^3](0.032)(0.150) \\ &\quad \times \left[ 0.150 - 0.150 \cos 126^\circ - \left( \frac{0.1227}{2} \right) \sin^2 126^\circ \right] \\ &= 304 \text{ N} \cdot \text{m} \end{aligned}$$

The moment of the normal forces is obtained from Eq. (16–3). Integrating from 0 to  $\theta_2$  gives

$$\begin{aligned} M_N &= \frac{p_a b r a}{\sin \theta_a} \left( \frac{\theta}{2} - \frac{1}{4} \sin 2\theta \right)_0^{\theta_2} \\ &= \frac{p_a b r a}{\sin \theta_a} \left( \frac{\theta_2}{2} - \frac{1}{4} \sin 2\theta_2 \right) \\ &= [1000(10)^3](0.032)(0.150)(0.1227) \left\{ \frac{\pi}{2} \frac{126}{180} - \frac{1}{4} \sin[(2)(126^\circ)] \right\} \\ &= 788 \text{ N} \cdot \text{m} \end{aligned}$$

From Eq. (16–4), the actuating force is

**Answer** 
$$F = \frac{M_N - M_f}{c} = \frac{788 - 304}{100 + 112} = 2.28 \text{ kN}$$

(b) From Eq. (16–6), the torque applied by the right-hand shoe is

$$\begin{aligned} T_R &= \frac{f p_a b r^2 (\cos \theta_1 - \cos \theta_2)}{\sin \theta_a} \\ &= \frac{0.32[1000(10)^3](0.032)(0.150)^2 (\cos 0^\circ - \cos 126^\circ)}{\sin 90^\circ} = 366 \text{ N} \cdot \text{m} \end{aligned}$$

The torque contributed by the left-hand shoe cannot be obtained until we learn its maximum operating pressure. Equations (16–2) and (16–3) indicate that the frictional and normal moments are proportional to this pressure. Thus, for the left-hand shoe,

$$M_N = \frac{788 p_a}{1000} \quad M_f = \frac{304 p_a}{1000}$$

Then, from Eq. (16–7),

$$F = \frac{M_N + M_f}{c}$$

or

$$2.28 = \frac{(788/1000)p_a + (304/1000)p_a}{100 + 112}$$

Solving gives  $p_a = 443 \text{ kPa}$ . Then, from Eq. (16–6), the torque on the left-hand shoe is

$$T_L = \frac{f p_a b r^2 (\cos \theta_1 - \cos \theta_2)}{\sin \theta_a}$$

Since  $\sin \theta_a = \sin 90^\circ = 1$ , we have

$$T_L = 0.32[443(10)^3](0.032)(0.150)^2 (\cos 0^\circ - \cos 126^\circ) = 162 \text{ N} \cdot \text{m}$$

The braking capacity is the total torque:

**Answer**

$$T = T_R + T_L = 366 + 162 = 528 \text{ N} \cdot \text{m}$$

(c) In order to find the hinge-pin reactions, we note that  $\sin \theta_a = 1$  and  $\theta_1 = 0$ . Then Eq. (16–8) gives

$$A = \frac{1}{2} \sin^2 \theta_2 = \frac{1}{2} \sin^2 126^\circ = 0.3273$$

$$B = \frac{\theta_2}{2} - \frac{1}{4} \sin 2\theta_2 = \frac{\pi(126)}{2(180)} - \frac{1}{4} \sin[(2)(126^\circ)] = 1.3373$$

Also, let

$$D = \frac{p_a b r}{\sin \theta_a} = \frac{1000(0.032)(0.150)}{1} = 4.8 \text{ kN}$$

where  $p_a = 1000 \text{ kPa}$  for the right-hand shoe. Then, using Eq. (16–9), we have

$$\begin{aligned} R_x &= D(A - fB) - F_x = 4.8[0.3273 - 0.32(1.3373)] - 2.28 \sin 24^\circ \\ &= -1.410 \text{ kN} \end{aligned}$$

$$\begin{aligned} R_y &= D(B + fA) - F_y = 4.8[1.3373 + 0.32(0.3273)] - 2.28 \cos 24^\circ \\ &= 4.839 \text{ kN} \end{aligned}$$

The resultant on this hinge pin is

**Answer**

$$R = \sqrt{(-1.410)^2 + (4.839)^2} = 5.04 \text{ kN}$$

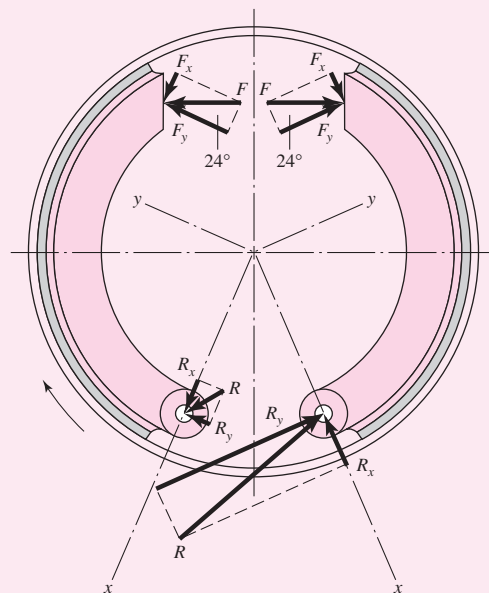
The reactions at the hinge pin of the left-hand shoe are found using Eqs. (16–10) for a pressure of 443 kPa. They are found to be  $R_x = 0.678 \text{ kN}$  and  $R_y = 0.538 \text{ kN}$ . The resultant is

**Answer**

$$R = \sqrt{(0.678)^2 + (0.538)^2} = 0.866 \text{ kN}$$

The reactions for both hinge pins, together with their directions, are shown in Fig. 16–9.

**Figure 16–9**



This example dramatically shows the benefit to be gained by arranging the shoes to be self-energizing. If the left-hand shoe were turned over so as to place the hinge pin at the top, it could apply the same torque as the right-hand shoe. This would make the capacity of the brake  $(2)(366) = 732 \text{ N} \cdot \text{m}$  instead of the present  $528 \text{ N} \cdot \text{m}$ , a 30 percent improvement. In addition, some of the friction material at the heel could be eliminated without seriously affecting the capacity, because of the low pressure in this area. This change might actually improve the overall design because the additional rim exposure would improve the heat-dissipation capacity.

### 16-3 External Contracting Rim Clutches and Brakes

The patented clutch-brake of Fig. 16-10 has external contracting friction elements, but the actuating mechanism is pneumatic. Here we shall study only pivoted external shoe brakes and clutches, though the methods presented can easily be adapted to the clutch-brake of Fig. 16-10.

Operating mechanisms can be classified as:

- 1 Solenoids
- 2 Levers, linkages, or toggle devices
- 3 Linkages with spring loading
- 4 Hydraulic and pneumatic devices

The static analysis required for these devices has already been covered in Sec. 3-1. The methods there apply to any mechanism system, including all those used in brakes and clutches. It is not necessary to repeat the material in Chap. 3 that applies directly to such mechanisms. Omitting the operating mechanisms from consideration allows us to concentrate on brake and clutch performance without the extraneous influences introduced by the need to analyze the statics of the control mechanisms.

The notation for external contracting shoes is shown in Fig. 16-11. The moments of the frictional and normal forces about the hinge pin are the same as for the internal

**Figure 16-10**

An external contracting clutch-brake that is engaged by expanding the flexible tube with compressed air. (Courtesy of Twin Disc Clutch Company.)

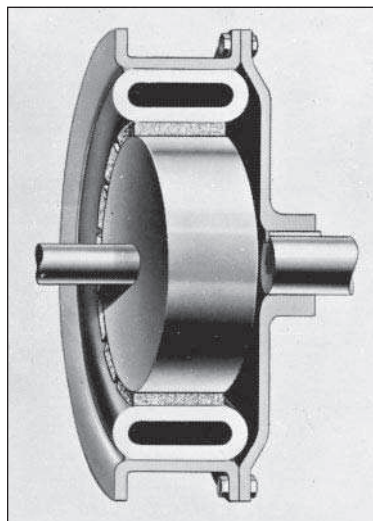
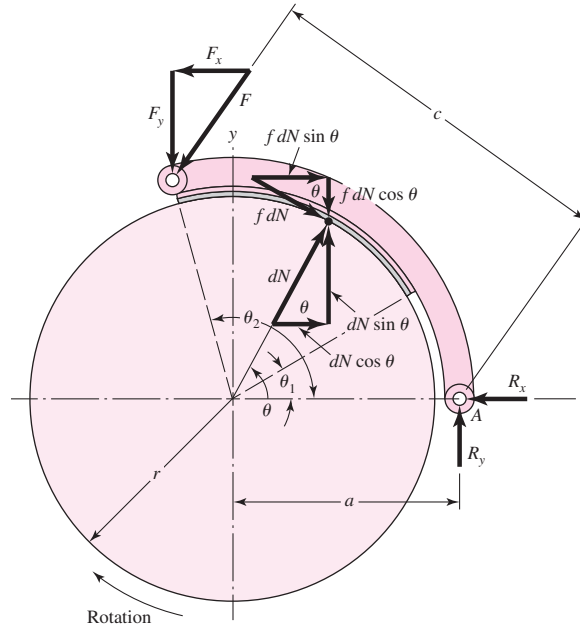


**Figure 16-11**

Notation of external  
contacting shoes.



expanding shoes. Equations (16-2) and (16-3) apply and are repeated here for convenience:

$$M_f = \frac{f p_a b r}{\sin \theta_a} \int_{\theta_1}^{\theta_2} \sin \theta (r - a \cos \theta) d\theta \quad (16-2)$$

$$M_N = \frac{p_a b r a}{\sin \theta_a} \int_{\theta_1}^{\theta_2} \sin^2 \theta d\theta \quad (16-3)$$

Both these equations give positive values for clockwise moments (Fig. 16-11) when used for external contracting shoes. The actuating force must be large enough to balance both moments:

$$F = \frac{M_N + M_f}{c} \quad (16-11)$$

The horizontal and vertical reactions at the hinge pin are found in the same manner as for internal expanding shoes. They are

$$R_x = \int dN \cos \theta + \int f dN \sin \theta - F_x \quad (a)$$

$$R_y = \int f dN \cos \theta - \int dN \sin \theta + F_y \quad (b)$$

By using Eq. (16-8) and Eq. (c) from Sec. 16-2, we have

$$\begin{aligned} R_x &= \frac{p_a b r}{\sin \theta_a} (A + f B) - F_x \\ R_y &= \frac{p_a b r}{\sin \theta_a} (f A - B) + F_y \end{aligned} \quad (16-12)$$

If the rotation is counterclockwise, the sign of the frictional term in each equation is reversed. Thus Eq. (16–11) for the actuating force becomes

$$F = \frac{M_N - M_f}{c} \quad (16-13)$$

and self-energization exists for counterclockwise rotation. The horizontal and vertical reactions are found, in the same manner as before, to be

$$R_x = \frac{p_a b r}{\sin \theta_a} (A - f B) - F_x$$

$$R_y = \frac{p_a b r}{\sin \theta_a} (-f A - B) + F_y \quad (16-14)$$

It should be noted that, when external contracting designs are used as clutches, the effect of centrifugal force is to decrease the normal force. Thus, as the speed increases, a larger value of the actuating force  $F$  is required.

A special case arises when the pivot is symmetrically located and also placed so that the moment of the friction forces about the pivot is zero. The geometry of such a brake will be similar to that of Fig. 16–12a. To get a pressure-distribution relation, we note that lining wear is such as to retain the cylindrical shape, much as a milling machine cutter feeding in the  $x$  direction would do to the shoe held in a vise. See Fig. 16–12b. This means the abscissa component of wear is  $w_0$  for all positions  $\theta$ . If wear in the radial direction is expressed as  $w(\theta)$ , then

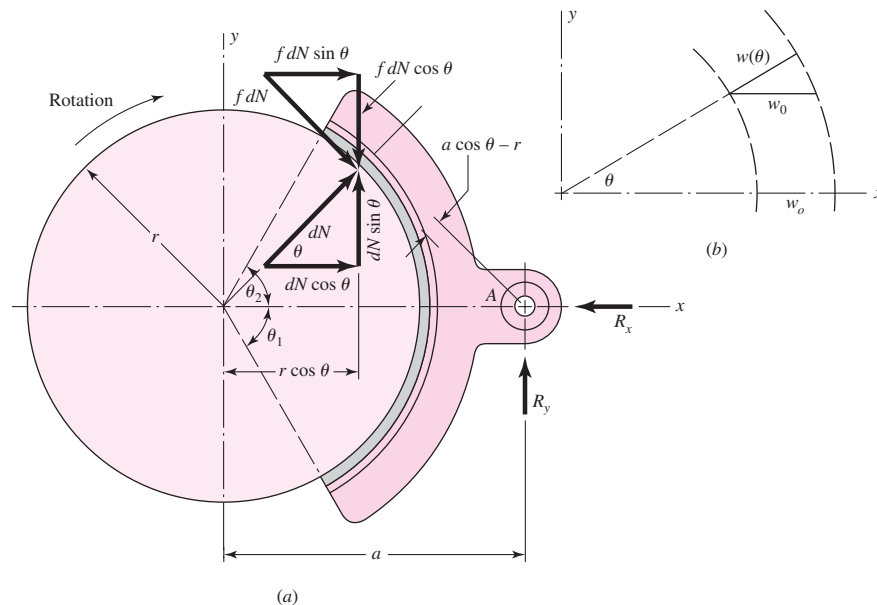
$$w(\theta) = w_0 \cos \theta$$

Using Eq. (12–26), p. 642, to express radial wear  $w(\theta)$  as

$$w(\theta) = K P V t$$

**Figure 16-12**

(a) Brake with symmetrical pivoted shoe; (b) wear of brake lining.



where  $K$  is a material constant,  $P$  is pressure,  $V$  is rim velocity, and  $t$  is time. Then, denoting  $P$  as  $p(\theta)$  above and solving for  $p(\theta)$  gives

$$p(\theta) = \frac{w(\theta)}{K V t} = \frac{w_0 \cos \theta}{K V t}$$

Since all elemental surface areas of the friction material see the same rubbing speed for the same duration,  $w_0/(K V t)$  is a constant and

$$p(\theta) = (\text{constant}) \cos \theta = p_a \cos \theta \quad (c)$$

where  $p_a$  is the maximum value of  $p(\theta)$ .

Proceeding to the force analysis, we observe from Fig. 16–12a that

$$dN = p b r d\theta \quad (d)$$

or

$$dN = p_a b r \cos \theta d\theta \quad (e)$$

The distance  $a$  to the pivot is chosen by finding where the moment of the frictional forces  $M_f$  is zero. First, this ensures that reaction  $R_y$  is at the correct location to establish symmetrical wear. Second, a cosinusoidal pressure distribution is sustained, preserving our predictive ability. Symmetry means  $\theta_1 = \theta_2$ , so

$$M_f = 2 \int_0^{\theta_2} (f dN)(a \cos \theta - r) = 0$$

Substituting Eq. (e) gives

$$2 f p_a b r \int_0^{\theta_2} (a \cos^2 \theta - r \cos \theta) d\theta = 0$$

from which

$$a = \frac{4r \sin \theta_2}{2\theta_2 + \sin 2\theta_2} \quad (16-15)$$

The distance  $a$  depends on the pressure distribution. Mislocating the pivot makes  $M_f$  zero about a different location, so the brake lining adjusts its local contact pressure, through wear, to compensate. The result is unsymmetrical wear, retiring the shoe lining, hence the shoe, sooner.

With the pivot located according to Eq. (16–15), the moment about the pin is zero, and the horizontal and vertical reactions are

$$R_x = 2 \int_0^{\theta_2} dN \cos \theta = \frac{p_a b r}{2} (2\theta_2 + \sin 2\theta_2) \quad (16-16)$$

where, because of symmetry,

$$\int f dN \sin \theta = 0$$

Also,

$$R_y = 2 \int_0^{\theta_2} f dN \sin \theta = \frac{p_a b r f}{2} (2\theta_2 + \sin 2\theta_2) \quad (16-17)$$

where

$$\int dN \sin \theta = 0$$

also because of symmetry. Note, too, that  $R_x = -N$  and  $R_y = -fN$ , as might be expected for the particular choice of the dimension  $a$ . Therefore the torque is

$$T = afN \quad (16-18)$$

## 16-4 Band-Type Clutches and Brakes

Flexible clutch and brake bands are used in power excavators and in hoisting and other machinery. The analysis follows the notation of Fig. 16-13.

Because of friction and the rotation of the drum, the actuating force  $P_2$  is less than the pin reaction  $P_1$ . Any element of the band, of angular length  $d\theta$ , will be in equilibrium under the action of the forces shown in the figure. Summing these forces in the vertical direction, we have

$$(P + dP) \sin \frac{d\theta}{2} + P \sin \frac{d\theta}{2} - dN = 0 \quad (a)$$

$$dN = Pd\theta \quad (b)$$

since for small angles  $\sin d\theta/2 = d\theta/2$ . Summing the forces in the horizontal direction gives

$$(P + dP) \cos \frac{d\theta}{2} - P \cos \frac{d\theta}{2} - f dN = 0 \quad (c)$$

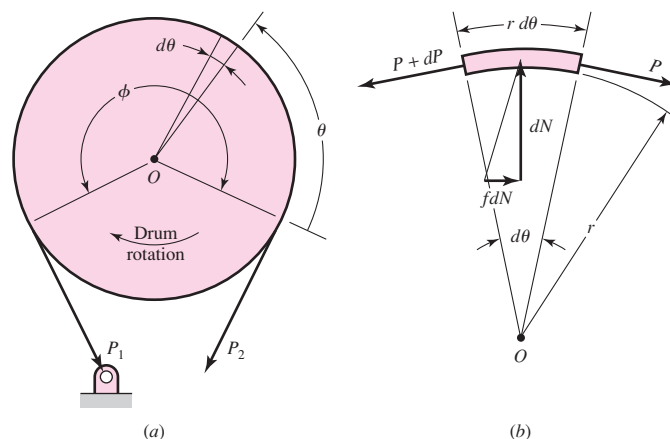
$$dP - f dN = 0 \quad (d)$$

since for small angles,  $\cos(d\theta/2) \doteq 1$ . Substituting the value of  $dN$  from Eq. (b) in (d) and integrating give

$$\int_{P_2}^{P_1} \frac{dP}{P} = f \int_0^\phi d\theta \quad \text{or} \quad \ln \frac{P_1}{P_2} = f\phi$$

**Figure 16-13**

Forces on a brake band.





and

$$\frac{P_1}{P_2} = e^{f\phi} \quad (16-19)$$

The torque may be obtained from the equation

$$T = (P_1 - P_2) \frac{D}{2} \quad (16-20)$$

The normal force  $dN$  acting on an element of area of width  $b$  and length  $r d\theta$  is

$$dN = pbr d\theta \quad (e)$$

where  $p$  is the pressure. Substitution of the value of  $dN$  from Eq. (b) gives

$$P d\theta = pbr d\theta$$

Therefore

$$p = \frac{P}{br} = \frac{2P}{bD} \quad (16-21)$$

The pressure is therefore proportional to the tension in the band. The maximum pressure  $p_a$  will occur at the toe and has the value

$$p_a = \frac{2P_1}{bD} \quad (16-22)$$

## 16-5 Frictional-Contact Axial Clutches

An axial clutch is one in which the mating frictional members are moved in a direction parallel to the shaft. One of the earliest of these is the cone clutch, which is simple in construction and quite powerful. However, except for relatively simple installations, it has been largely displaced by the disk clutch employing one or more disks as the operating members. Advantages of the disk clutch include the freedom from centrifugal effects, the large frictional area that can be installed in a small space, the more effective heat-dissipation surfaces, and the favorable pressure distribution. Figure 16-14 shows a

**Figure 16-14**

Cross-sectional view of a single-plate clutch; A, driver; B, driven plate (keyed to driven shaft); C, actuator.

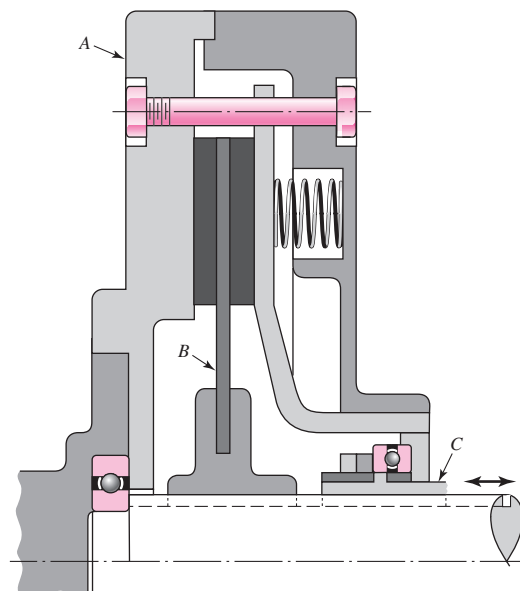


**Figure 16-15**

An oil-actuated multiple-disk clutch-brake for operation in an oil bath or spray. It is especially useful for rapid cycling. (Courtesy of Twin Disc Clutch Company.)

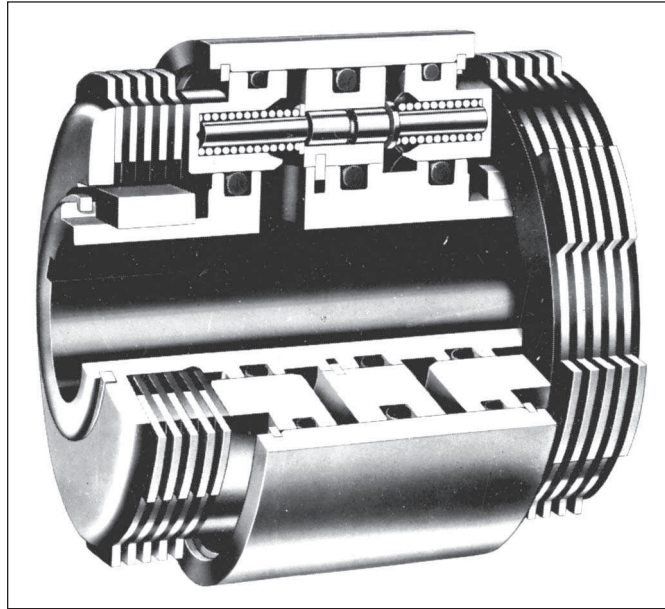
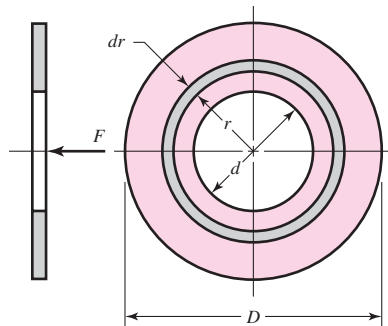


**Figure 16-16**

Disk friction member.



single-plate disk clutch; a multiple-disk clutch-brake is shown in Fig. 16-15. Let us now determine the capacity of such a clutch or brake in terms of the material and geometry.

Figure 16-16 shows a friction disk having an outside diameter  $D$  and an inside diameter  $d$ . We are interested in obtaining the axial force  $F$  necessary to produce a certain torque  $T$  and pressure  $p$ . Two methods of solving the problem, depending upon the construction of the clutch, are in general use. If the disks are rigid, then the greatest amount of wear will at first occur in the outer areas, since the work of friction is greater in those areas. After a certain amount of wear has taken place, the pressure distribution will change so as to permit the wear to be uniform. This is the basis of the first method of solution.

Another method of construction employs springs to obtain a uniform pressure over the area. It is this assumption of uniform pressure that is used in the second method of solution.

### Uniform Wear

After initial wear has taken place and the disks have worn down to a point where uniform wear is established, the axial wear can be expressed by Eq. (12-27), p. 643, as

$$w = f_1 f_2 K P V t$$

in which only  $P$  and  $V$  vary from place to place in the rubbing surfaces. By definition uniform wear is constant from place to place; therefore,

$$\begin{aligned} PV &= (\text{constant}) = C_1 \\ pr\omega &= C_2 \\ pr &= C_3 = p_{\max} r_i = p_a r_i = p_a \frac{d}{2} \end{aligned} \quad (a)$$

We can take an expression from Eq. (a), which is the condition for having the same amount of work done at radius  $r$  as is done at radius  $d/2$ . Referring to Fig. 16–16, we have an element of area of radius  $r$  and thickness  $dr$ . The area of this element is  $2\pi r dr$ , so that the normal force acting upon this element is  $dF = 2\pi pr dr$ . We can find the total normal force by letting  $r$  vary from  $d/2$  to  $D/2$  and integrating. Thus, with  $pr$  constant,

$$F = \int_{d/2}^{D/2} 2\pi pr dr = \pi p_a d \int_{d/2}^{D/2} dr = \frac{\pi p_a d}{2} (D - d) \quad (16-23)$$

The torque is found by integrating the product of the frictional force and the radius:

$$T = \int_{d/2}^{D/2} 2\pi f pr^2 dr = \pi f p_a d \int_{d/2}^{D/2} r dr = \frac{\pi f p_a d}{8} (D^2 - d^2) \quad (16-24)$$

By substituting the value of  $F$  from Eq. (16–23) we may obtain a more convenient expression for the torque. Thus

$$T = \frac{Ff}{4} (D + d) \quad (16-25)$$

In use, Eq. (16–23) gives the actuating force for the selected maximum pressure  $p_a$ . This equation holds for any number of friction pairs or surfaces. Equation (16–25), however, gives the torque capacity for only a single friction surface.

### Uniform Pressure

When uniform pressure can be assumed over the area of the disk, the actuating force  $F$  is simply the product of the pressure and the area. This gives

$$F = \frac{\pi p_a}{4} (D^2 - d^2) \quad (16-26)$$

As before, the torque is found by integrating the product of the frictional force and the radius:

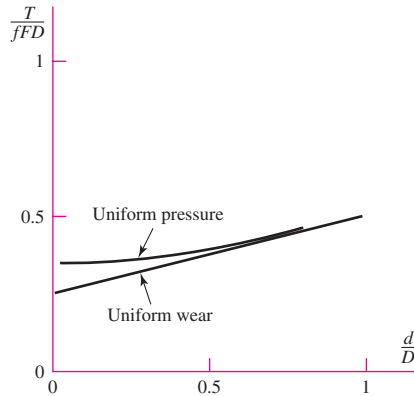
$$T = 2\pi f p \int_{d/2}^{D/2} r^2 dr = \frac{\pi f p}{12} (D^3 - d^3) \quad (16-27)$$

Since  $p = p_a$ , from Eq. (16–26) we can rewrite Eq. (16–27) as

$$T = \frac{Ff}{3} \frac{D^3 - d^3}{D^2 - d^2} \quad (16-28)$$

It should be noted for both equations that the torque is for a single pair of mating surfaces. This value must therefore be multiplied by the number of pairs of surfaces in contact.

**Figure 16-17**

 Dimensionless plot of Eqs. (b)  
 and (c).


Let us express Eq. (16-25) for torque during uniform wear as

$$\frac{T}{fFD} = \frac{1 + d/D}{4} \quad (b)$$

and Eq. (16-28) for torque during uniform pressure (new clutch) as

$$\frac{T}{fFD} = \frac{1}{3} \frac{1 - (d/D)^3}{1 - (d/D)^2} \quad (c)$$

and plot these in Fig. 16-17. What we see is a dimensionless presentation of Eqs. (b) and (c) which reduces the number of variables from five ( $T$ ,  $f$ ,  $F$ ,  $D$ , and  $d$ ) to three ( $T/FD$ ,  $f$ , and  $d/D$ ) which are dimensionless. This is the method of Buckingham. The dimensionless groups (called pi terms) are

$$\pi_1 = \frac{T}{FD} \quad \pi_2 = f \quad \pi_3 = \frac{d}{D}$$

This allows a five-dimensional space to be reduced to a three-dimensional space. Further, because of the “multiplicative” relation between  $f$  and  $T$  in Eqs. (b) and (c), it is possible to plot  $\pi_1/\pi_2$  versus  $\pi_3$  in a two-dimensional space (the plane of a sheet of paper) to view all cases over the domain of existence of Eqs. (b) and (c) and to compare, without risk of oversight! By examining Fig. 16-17 we can conclude that a new clutch, Eq. (b), always transmits more torque than an old clutch, Eq. (c). Furthermore, since clutches of this type are proportioned to make the diameter ratio  $d/D$  fall in the range  $0.6 \leq d/D \leq 1$ , the largest discrepancy between Eq. (b) and Eq. (c) will be

$$\frac{T}{fFD} = \frac{1 + 0.6}{4} = 0.400 \quad (\text{old clutch, uniform wear})$$

$$\frac{T}{fFD} = \frac{1}{3} \frac{1 - 0.6^3}{1 - 0.6^2} = 0.4083 \quad (\text{new clutch, uniform pressure})$$

so the proportional error is  $(0.4083 - 0.400)/0.400 = 0.021$ , or about 2 percent. Given the uncertainties in the actual coefficient of friction and the certainty that new clutches get old, there is little reason to use anything but Eqs. (16-23), (16-24), and (16-25).

## 16-6 Disk Brakes

As indicated in Fig. 16-16, there is no fundamental difference between a disk clutch and a disk brake. The analysis of the preceding section applies to disk brakes too.

We have seen that rim or drum brakes can be designed for self-energization. While this feature is important in reducing the braking effort required, it also has a disadvantage. When drum brakes are used as vehicle brakes, only a slight change in the coefficient of friction will cause a large change in the pedal force required for braking. A not unusual 30 percent reduction in the coefficient of friction due to a temperature change or moisture, for example, can result in a 50 percent change in the pedal force required to obtain the same braking torque obtainable prior to the change. The disk brake has no self-energization, and hence is not so susceptible to changes in the coefficient of friction.

Another type of disk brake is the *floating caliper brake*, shown in Fig. 16-18. The caliper supports a single floating piston actuated by hydraulic pressure. The action is much like that of a screw clamp, with the piston replacing the function of the screw. The floating action also compensates for wear and ensures a fairly constant pressure over the area of the friction pads. The seal and boot of Fig. 16-18 are designed to obtain clearance by backing off from the piston when the piston is released.

Caliper brakes (named for the nature of the actuating linkage) and disk brakes (named for the shape of the unlined surface) press friction material against the face(s)

**Figure 16-18**

An automotive disk brake.  
(Courtesy DaimlerChrysler  
Corporation.)

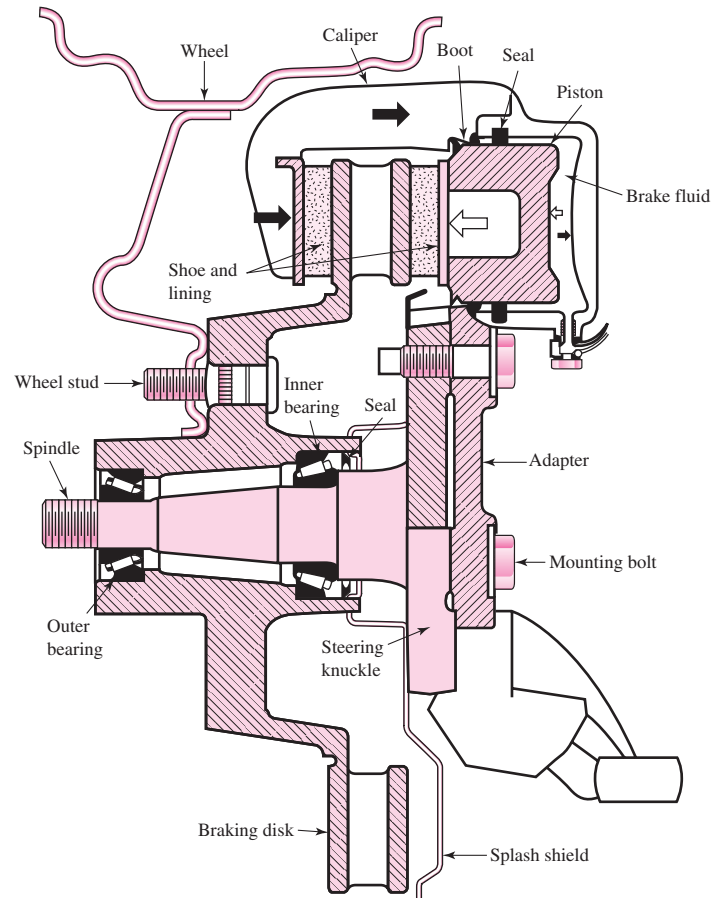
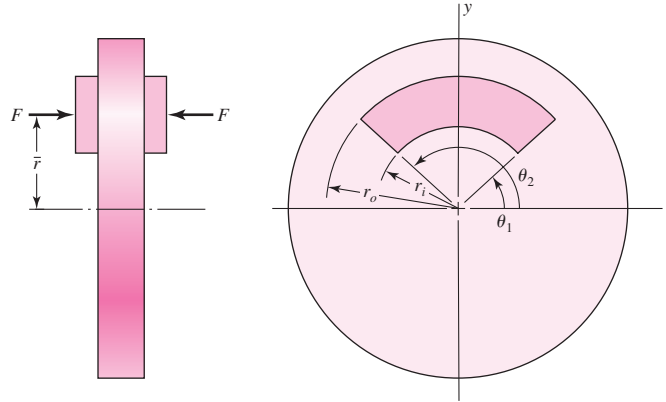


**Figure 16-19**

Geometry of contact area of an annular-pad segment of a caliper brake.



of a rotating disk. Depicted in Fig. 16–19 is the geometry of an annular-pad brake contact area. The governing axial wear equation is Eq. (12–27), p. 643,

$$w = f_1 f_2 K P V t$$

The coordinate  $\bar{r}$  locates the line of action of force  $F$  that intersects the  $y$  axis. Of interest also is the effective radius  $r_e$ , which is the radius of an equivalent shoe of infinitesimal radial thickness. If  $p$  is the local contact pressure, the actuating force  $F$  and the friction torque  $T$  are given by

$$F = \int_{\theta_1}^{\theta_2} \int_{r_i}^{r_o} p r dr d\theta = (\theta_2 - \theta_1) \int_{r_i}^{r_o} p r dr \quad (16-29)$$

$$T = \int_{\theta_1}^{\theta_2} \int_{r_i}^{r_o} f p r^2 dr d\theta = (\theta_2 - \theta_1) f \int_{r_i}^{r_o} p r^2 dr \quad (16-30)$$

The equivalent radius  $r_e$  can be found from  $f F r_e = T$ , or

$$r_e = \frac{T}{f F} = \frac{\int_{r_i}^{r_o} p r^2 dr}{\int_{r_i}^{r_o} p r dr} \quad (16-31)$$

The locating coordinate  $\bar{r}$  of the activating force is found by taking moments about the  $x$  axis:

$$M_x = F \bar{r} = \int_{\theta_1}^{\theta_2} \int_{r_i}^{r_o} p r (r \sin \theta) dr d\theta = (\cos \theta_1 - \cos \theta_2) \int_{r_i}^{r_o} p r^2 dr$$

$$\bar{r} = \frac{M_x}{F} = \frac{(\cos \theta_1 - \cos \theta_2)}{\theta_2 - \theta_1} r_e \quad (16-32)$$

### Uniform Wear

It is clear from Eq. (12–27) that for the axial wear to be the same everywhere, the product  $PV$  must be a constant. From Eq. (a), Sec. 16–5, the pressure  $p$  can be expressed in terms of the largest allowable pressure  $p_a$  (which occurs at the inner radius  $r_i$ ) as

$p = p_a r_i / r$ . Equation (16–29) becomes

$$F = (\theta_2 - \theta_1) p_a r_i (r_o - r_i) \quad (16-33)$$

Equation (16–30) becomes

$$T = (\theta_2 - \theta_1) f p_a r_i \int_{r_i}^{r_o} r dr = \frac{1}{2} (\theta_2 - \theta_1) f p_a r_i (r_o^2 - r_i^2) \quad (16-34)$$

Equation (16–31) becomes

$$r_e = \frac{p_a r_i \int_{r_i}^{r_o} r dr}{p_a r_i \int_{r_i}^{r_o} dr} = \frac{r_o^2 - r_i^2}{2} \frac{1}{r_o - r_i} = \frac{r_o + r_i}{2} \quad (16-35)$$

Equation (16–32) becomes

$$\bar{r} = \frac{\cos \theta_1 - \cos \theta_2}{\theta_2 - \theta_1} \frac{r_o + r_i}{2} \quad (16-36)$$

### Uniform Pressure

In this situation, approximated by a new brake,  $p = p_a$ . Equation (16–29) becomes

$$F = (\theta_2 - \theta_1) p_a \int_{r_i}^{r_o} r dr = \frac{1}{2} (\theta_2 - \theta_1) p_a (r_o^2 - r_i^2) \quad (16-37)$$

Equation (16–30) becomes

$$T = (\theta_2 - \theta_1) f p_a \int_{r_i}^{r_o} r^2 dr = \frac{1}{3} (\theta_2 - \theta_1) f p_a (r_o^3 - r_i^3) \quad (16-38)$$

Equation (16–31) becomes

$$r_e = \frac{p_a \int_{r_i}^{r_o} r^2 dr}{p_a \int_{r_i}^{r_o} r dr} = \frac{r_o^3 - r_i^3}{3} \frac{2}{r_o^2 - r_i^2} = \frac{2}{3} \frac{r_o^3 - r_i^3}{r_o^2 - r_i^2} \quad (16-39)$$

Equation (16–32) becomes

$$\bar{r} = \frac{\cos \theta_1 - \cos \theta_2}{\theta_2 - \theta_1} \frac{2}{3} \frac{r_o^3 - r_i^3}{r_o^2 - r_i^2} = \frac{2}{3} \frac{r_o^3 - r_i^3}{r_o^2 - r_i^2} \frac{\cos \theta_1 - \cos \theta_2}{\theta_2 - \theta_1} \quad (16-40)$$

### EXAMPLE 16-3

Two annular pads,  $r_i = 3.875$  in,  $r_o = 5.50$  in, subtend an angle of  $108^\circ$ , have a coefficient of friction of 0.37, and are actuated by a pair of hydraulic cylinders 1.5 in in diameter. The torque requirement is 13 000 lbf · in. For uniform wear

- Find the largest normal pressure  $p_a$ .
- Estimate the actuating force  $F$ .
- Find the equivalent radius  $r_e$  and force location  $\bar{r}$ .
- Estimate the required hydraulic pressure.

832 Mechanical Engineering Design

**Solution** (a) From Eq. (16–34), with  $T = 13\,000/2 = 6500$  lbf · in for each pad,

**Answer**

$$p_a = \frac{2T}{(\theta_2 - \theta_1)fr_i(r_o^2 - r_i^2)}$$

$$= \frac{2(6500)}{(144^\circ - 36^\circ)(\pi/180)0.37(3.875)(5.5^2 - 3.875^2)} = 315.8 \text{ psi}$$

(b) From Eq. (16–33),

**Answer**

$$F = (\theta_2 - \theta_1)p_ar_i(r_o - r_i) = (144^\circ - 36^\circ)(\pi/180)315.8(3.875)(5.5 - 3.875)$$

$$= 3748 \text{ lbf}$$

(c) From Eq. (16–35),

**Answer**

$$r_e = \frac{r_o + r_i}{2} = \frac{5.50 + 3.875}{2} = 4.688 \text{ in}$$

From Eq. (16–36),

**Answer**

$$\bar{r} = \frac{\cos \theta_1 - \cos \theta_2}{\theta_2 - \theta_1} \frac{r_o + r_i}{2} = \frac{\cos 36^\circ - \cos 144^\circ}{(144^\circ - 36^\circ)(\pi/180)} \frac{5.50 + 3.875}{2}$$

$$= 4.024 \text{ in}$$

(d) Each cylinder supplies the actuating force, 3748 lbf.

**Answer**

$$p_{\text{hydraulic}} = \frac{F}{A_p} = \frac{3748}{\pi(1.5^2/4)} = 2121 \text{ psi}$$

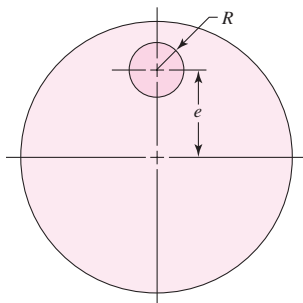


**Figure 16–20**

Geometry of circular pad of a caliper brake.

**Circular (Button or Puck) Pad Caliper Brake**

Figure 16–20 displays the pad geometry. Numerical integration is necessary to analyze this brake since the boundaries are difficult to handle in closed form. Table 16–1 gives the parameters for this brake as determined by Fazekas. The effective radius is given by

$$r_e = \delta e \quad (16-41)$$

The actuating force is given by

$$F = \pi R^2 p_{\text{av}} \quad (16-42)$$

and the torque is given by

$$T = fFr_e \quad (16-43)$$



**Table 16-1**

Parameters for a  
Circular-Pad Caliper  
Brake

Source: G. A. Fazekas, "On  
Circular Spot Brakes," *Trans.  
ASME, J. Engineering for  
Industry*, vol. 94, Series B,  
No. 3, August 1972,  
pp. 859–863.

$\frac{R}{e}$	$\delta = \frac{r_e}{e}$	$\frac{p_{\max}}{p_{\text{av}}}$
0.0	1.000	1.000
0.1	0.983	1.093
0.2	0.969	1.212
0.3	0.957	1.367
0.4	0.947	1.578
0.5	0.938	1.875

**EXAMPLE 16-4**

A button-pad disk brake uses dry sintered metal pads. The pad radius is  $\frac{1}{2}$  in, and its center is 2 in from the axis of rotation of the  $3\frac{1}{2}$ -in-diameter disk. Using half of the largest allowable pressure,  $p_{\max} = 350$  psi, find the actuating force and the brake torque. The coefficient of friction is 0.31.

**Solution**

Since the pad radius  $R = 0.5$  in and eccentricity  $e = 2$  in,

$$\frac{R}{e} = \frac{0.5}{2} = 0.25$$

From Table 16-1, by interpolation,  $\delta = 0.963$  and  $p_{\max}/p_{\text{av}} = 1.290$ . It follows that the effective radius  $e$  is found from Eq. (16-41):

$$r_e = \delta e = 0.963(2) = 1.926 \text{ in}$$

and the average pressure is

$$p_{\text{av}} = \frac{p_{\max}/2}{1.290} = \frac{350/2}{1.290} = 135.7 \text{ psi}$$

The actuating force  $F$  is found from Eq. (16-42) to be

$$\text{Answer} \quad F = \pi R^2 p_{\text{av}} = \pi (0.5)^2 135.7 = 106.6 \text{ lbf} \quad (\text{one side})$$

The brake torque  $T$  is

$$\text{Answer} \quad T = f F r_e = 0.31(106.6)1.926 = 63.65 \text{ lbf} \cdot \text{in} \quad (\text{one side})$$

## 16-7 Cone Clutches and Brakes

The drawing of a *cone clutch* in Fig. 16-21 shows that it consists of a *cup* keyed or splined to one of the shafts, a *cone* that must slide axially on splines or keys on the mating shaft, and a helical *spring* to hold the clutch in engagement. The clutch is disengaged by means of a fork that fits into the shifting groove on the friction cone. The *cone angle*  $\alpha$  and the diameter and face width of the cone are the important geometric design parameters. If the

**Figure 16-21**

Cross section of a cone clutch.

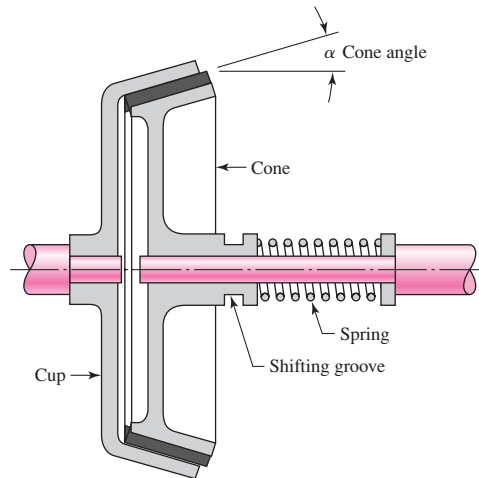
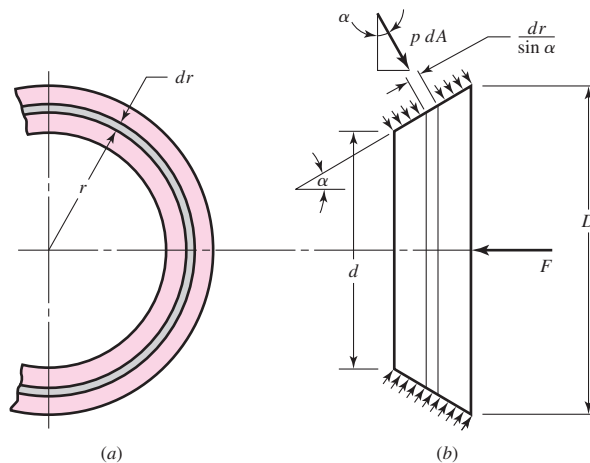


**Figure 16-22**

Contact area of a cone clutch.



cone angle is too small, say, less than about  $8^\circ$ , then the force required to disengage the clutch may be quite large. And the wedging effect lessens rapidly when larger cone angles are used. Depending upon the characteristics of the friction materials, a good compromise can usually be found using cone angles between  $10$  and  $15^\circ$ .

To find a relation between the operating force  $F$  and the torque transmitted, designate the dimensions of the friction cone as shown in Figure 16-22. As in the case of the axial clutch, we can obtain one set of relations for a uniform-wear and another set for a uniform-pressure assumption.

### Uniform Wear

The pressure relation is the same as for the axial clutch:

$$p = p_a \frac{d}{2r} \quad (a)$$

Next, referring to Fig. 16-22, we see that we have an element of area  $dA$  of radius  $r$  and width  $dr/\sin \alpha$ . Thus  $dA = (2\pi r dr)/\sin \alpha$ . As shown in Fig. 16-22, the operating

force will be the integral of the axial component of the differential force  $p \, dA$ . Thus

$$\begin{aligned} F &= \int p \, dA \sin \alpha = \int_{d/2}^{D/2} \left( p_a \frac{d}{2r} \right) \left( \frac{2\pi r \, dr}{\sin \alpha} \right) (\sin \alpha) \\ &= \pi p_a d \int_{d/2}^{D/2} dr = \frac{\pi p_a d}{2} (D - d) \end{aligned} \quad (16-44)$$

which is the same result as in Eq. (16-23).

The differential friction force is  $f p \, dA$ , and the torque is the integral of the product of this force with the radius. Thus

$$\begin{aligned} T &= \int r f p \, dA = \int_{d/2}^{D/2} (r f) \left( p_a \frac{d}{2r} \right) \left( \frac{2\pi r \, dr}{\sin \alpha} \right) \\ &= \frac{\pi f p_a d}{\sin \alpha} \int_{d/2}^{D/2} r \, dr = \frac{\pi f p_a d}{8 \sin \alpha} (D^2 - d^2) \end{aligned} \quad (16-45)$$

Note that Eq. (16-24) is a special case of Eq. (16-45), with  $\alpha = 90^\circ$ . Using Eq. (16-44), we find that the torque can also be written

$$T = \frac{F f}{4 \sin \alpha} (D + d) \quad (16-46)$$

### Uniform Pressure

Using  $p = p_a$ , the actuating force is found to be

$$F = \int p_a \, dA \sin \alpha = \int_{d/2}^{D/2} (p_a) \left( \frac{2\pi r \, dr}{\sin \alpha} \right) (\sin \alpha) = \frac{\pi p_a}{4} (D^2 - d^2) \quad (16-47)$$

The torque is

$$T = \int r f p_a \, dA = \int_{d/2}^{D/2} (r f p_a) \left( \frac{2\pi r \, dr}{\sin \alpha} \right) = \frac{\pi f p_a}{12 \sin \alpha} (D^3 - d^3) \quad (16-48)$$

Using Eq. (16-47) in Eq. (16-48) gives

$$T = \frac{F f}{3 \sin \alpha} \frac{D^3 - d^3}{D^2 - d^2} \quad (16-49)$$

As in the case of the axial clutch, we can write Eq. (16-46) dimensionlessly as

$$\frac{T \sin \alpha}{f F d} = \frac{1 + d/D}{4} \quad (b)$$

and write Eq. (16-49) as

$$\frac{T \sin \alpha}{f F d} = \frac{1}{3} \frac{1 - (d/D)^3}{1 - (d/D)^2} \quad (c)$$

This time there are six ( $T$ ,  $\alpha$ ,  $f$ ,  $F$ ,  $D$ , and  $d$ ) parameters and four pi terms:

$$\pi_1 = \frac{T}{F D} \quad \pi_2 = f \quad \pi_3 = \sin \alpha \quad \pi_4 = \frac{d}{D}$$

As in Fig. 16-17, we plot  $T \sin \alpha / (f F D)$  as ordinate and  $d/D$  as abscissa. The plots and conclusions are the same. There is little reason for using equations other than Eqs. (16-44), (16-45), and (16-46).

## 16–8 Energy Considerations

When the rotating members of a machine are caused to stop by means of a brake, the kinetic energy of rotation must be absorbed by the brake. This energy appears in the brake in the form of heat. In the same way, when the members of a machine that are initially at rest are brought up to speed, slipping must occur in the clutch until the driven members have the same speed as the driver. Kinetic energy is absorbed during slippage of either a clutch or a brake, and this energy appears as heat.

We have seen how the torque capacity of a clutch or brake depends upon the coefficient of friction of the material and upon a safe normal pressure. However, the character of the load may be such that, if this torque value is permitted, the clutch or brake may be destroyed by its own generated heat. The capacity of a clutch is therefore limited by two factors, the characteristics of the material and the ability of the clutch to dissipate heat. In this section we shall consider the amount of heat generated by a clutching or braking operation. If the heat is generated faster than it is dissipated, we have a temperature-rise problem; that is the subject of the next section.

To get a clear picture of what happens during a simple clutching or braking operation, refer to Fig. 16–1*a*, which is a mathematical model of a two-inertia system connected by a clutch. As shown, inertias  $I_1$  and  $I_2$  have initial angular velocities of  $\omega_1$  and  $\omega_2$ , respectively. During the clutch operation both angular velocities change and eventually become equal. We assume that the two shafts are rigid and that the clutch torque is constant.

Writing the equation of motion for inertia 1 gives

$$I_1 \ddot{\theta}_1 = -T \quad (a)$$

where  $\ddot{\theta}_1$  is the angular acceleration of  $I_1$  and  $T$  is the clutch torque. A similar equation for  $I_2$  is

$$I_2 \ddot{\theta}_2 = T \quad (b)$$

We can determine the instantaneous angular velocities  $\dot{\theta}_1$  and  $\dot{\theta}_2$  of  $I_1$  and  $I_2$  after any period of time  $t$  has elapsed by integrating Eqs. (a) and (b). The results are

$$\dot{\theta}_1 = -\frac{T}{I_1}t + \omega_1 \quad (c)$$

$$\dot{\theta}_2 = \frac{T}{I_2}t + \omega_2 \quad (d)$$

where  $\dot{\theta}_1 = \omega_1$  and  $\dot{\theta}_2 = \omega_2$  at  $t = 0$ . The difference in the velocities, sometimes called the relative velocity, is

$$\begin{aligned} \dot{\theta} &= \dot{\theta}_1 - \dot{\theta}_2 = -\frac{T}{I_1}t + \omega_1 - \left(\frac{T}{I_2}t + \omega_2\right) \\ &= \omega_1 - \omega_2 - T \left(\frac{I_1 + I_2}{I_1 I_2}\right)t \end{aligned} \quad (16-50)$$

The clutching operation is completed at the instant in which the two angular velocities  $\dot{\theta}_1$  and  $\dot{\theta}_2$  become equal. Let the time required for the entire operation be  $t_1$ . Then  $\dot{\theta} = 0$  when  $\dot{\theta}_1 = \dot{\theta}_2$ , and so Eq. (16–50) gives the time as

$$t_1 = \frac{I_1 I_2 (\omega_1 - \omega_2)}{T (I_1 + I_2)} \quad (16-51)$$

This equation shows that the time required for the engagement operation is directly proportional to the velocity difference and inversely proportional to the torque.

We have assumed the clutch torque to be constant. Therefore, using Eq. (16–50), we find the rate of energy-dissipation during the clutching operation to be

$$u = T\dot{\theta} = T \left[ \omega_1 - \omega_2 - T \left( \frac{I_1 + I_2}{I_1 I_2} \right) t \right] \quad (e)$$

This equation shows that the energy-dissipation rate is greatest at the start, when  $t = 0$ .

The total energy dissipated during the clutching operation or braking cycle is obtained by integrating Eq. (e) from  $t = 0$  to  $t = t_1$ . The result is found to be

$$\begin{aligned} E &= \int_0^{t_1} u \, dt = T \int_0^{t_1} \left[ \omega_1 - \omega_2 - T \left( \frac{I_1 + I_2}{I_1 I_2} \right) t \right] dt \\ &= \frac{I_1 I_2 (\omega_1 - \omega_2)^2}{2(I_1 + I_2)} \end{aligned} \quad (16-52)$$

where Eq. (16–51) was employed. Note that the energy dissipated is proportional to the velocity difference squared and is independent of the clutch torque.

Note that  $E$  in Eq. (16–52) is the energy lost or dissipated; this is the energy that is absorbed by the clutch or brake. If the inertias are expressed in U.S. customary units ( $\text{lbf} \cdot \text{in} \cdot \text{s}^2$ ), then the energy absorbed by the clutch assembly is in  $\text{in} \cdot \text{lbf}$ . Using these units, the heat generated in Btu is

$$H = \frac{E}{9336} \quad (16-53)$$

In SI, the inertias are expressed in kilogram-meter<sup>2</sup> units, and the energy dissipated is expressed in joules.

## 16-9 Temperature Rise

The temperature rise of the clutch or brake assembly can be approximated by the classic expression

$$\Delta T = \frac{H}{C_p W} \quad (16-54)$$

where  $\Delta T$  = temperature rise, °F

$C_p$  = specific heat capacity, Btu/(lb<sub>m</sub> · °F); use 0.12 for steel or cast iron

$W$  = mass of clutch or brake parts, lbm

A similar equation can be written for SI units. It is

$$\Delta T = \frac{E}{C_p m} \quad (16-55)$$

where  $\Delta T$  = temperature rise, °C

$C_p$  = specific heat capacity; use 500 J/kg · °C for steel or cast iron

$m$  = mass of clutch or brake parts, kg

The temperature-rise equations above can be used to explain what happens when a clutch or brake is operated. However, there are so many variables involved that it would

be most unlikely that such an analysis would even approximate experimental results. For this reason such analyses are most useful, for repetitive cycling, in pinpointing those design parameters that have the greatest effect on performance.

If an object is at initial temperature  $T_1$  in an environment of temperature  $T_\infty$ , then Newton's cooling model is expressed as

$$\frac{T - T_\infty}{T_1 - T_\infty} = \exp\left(-\frac{\hbar_{CR} A}{WC_p} t\right) \quad (16-56)$$

where  $T$  = temperature at time  $t$ , °F

$T_1$  = initial temperature, °F

$T_\infty$  = environmental temperature, °F

$\hbar_{CR}$  = overall coefficient of heat transfer, Btu/(in<sup>2</sup> · s · °F)

$A$  = lateral surface area, in<sup>2</sup>

$W$  = mass of the object, lbm

$C_p$  = specific heat capacity of the object, Btu/(lbm · °F)

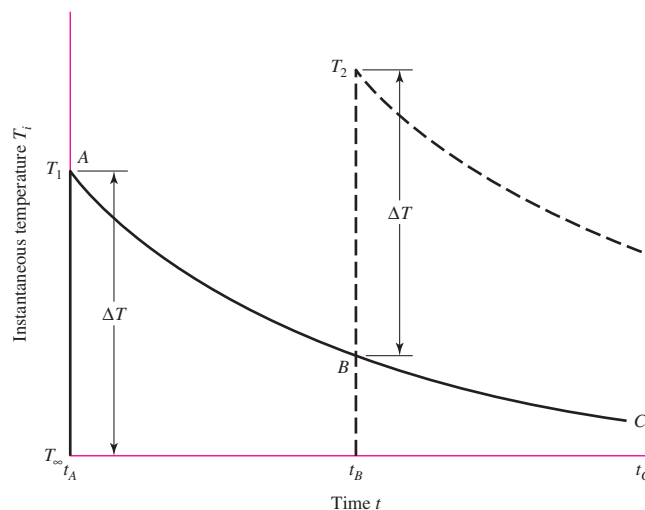
Figure 16–23 shows an application of Eq. (16–56). The curve  $ABC$  is the exponential decline of temperature given by Eq. (16–56). At time  $t_B$  a second application of the brake occurs. The temperature quickly rises to temperature  $T_2$ , and a new cooling curve is started. For repetitive brake applications, subsequent temperature peaks  $T_3, T_4, \dots$ , occur until the brake is able to dissipate by cooling between operations an amount of heat equal to the energy absorbed in the application. If this is a production situation with brake applications every  $t_1$  seconds, then a steady state develops in which all the peaks  $T_{\max}$  and all the valleys  $T_{\min}$  are repetitive.

The heat-dissipation capacity of disk brakes has to be planned to avoid reaching the temperatures of disk and pad that are detrimental to the parts. When a disk brake has a rhythm such as discussed above, then the rate of heat transfer is described by another Newtonian equation:

$$H_{\text{loss}} = \hbar_{CR} A(T - T_\infty) = (h_r + f_v h_c) A(T - T_\infty) \quad (16-57)$$

**Figure 16–23**

The effect of clutching or braking operations on temperature.  $T_\infty$  is the ambient temperature. Note that the temperature rise  $\Delta T$  may be different for each operation.



where  $H_{\text{loss}}$  = rate of energy loss, Btu/s

$\dot{h}_{\text{CR}}$  = overall coefficient of heat transfer, Btu/(in<sup>2</sup> · s · °F)

$h_r$  = radiation component of  $\dot{h}_{\text{CR}}$ , Btu/(in<sup>2</sup> · s · °F), Fig. 16–24a

$h_c$  = convective component of  $\dot{h}_{\text{CR}}$ , Btu/(in<sup>2</sup> · s · °F), Fig. 16–24a

$f_v$  = ventilation factor, Fig. 16–24b

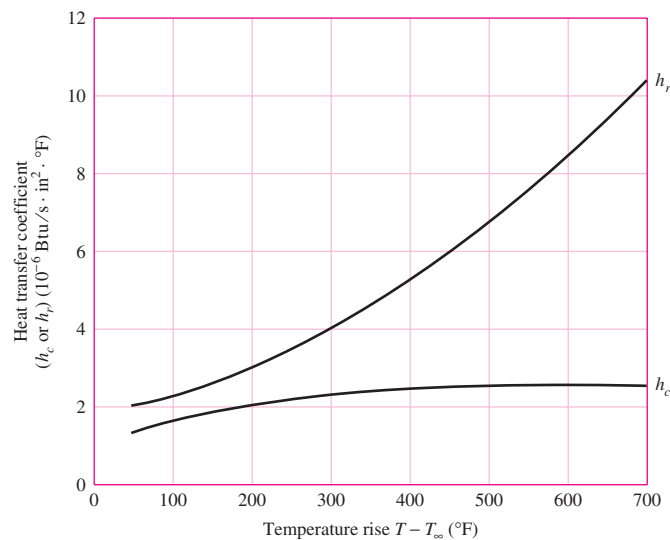
$T$  = disk temperature, °F

$T_\infty$  = ambient temperature, °F

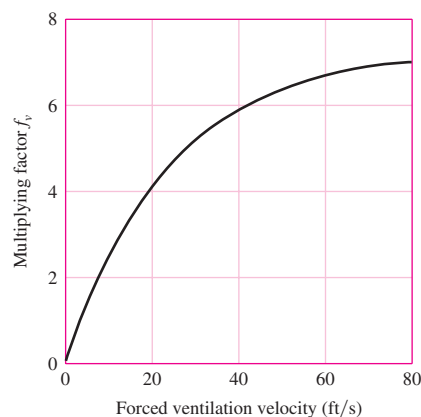
The energy  $E$  absorbed by the brake stopping an equivalent rotary inertia  $I$  in terms of original and final angular velocities  $\omega_o$  and  $\omega_f$  is given by Eq. (16–53) with  $I_1 = I$

**Figure 16–24**

(a) Heat-transfer coefficient in still air. (b) Ventilation factors.  
(Courtesy of Tolo-o-matic.)



(a)



(b)

and  $I_2 = 0$ ,

$$E = \frac{1}{2} \frac{I}{9336} (\omega_o^2 - \omega_f^2) \quad (16-58)$$

in Btu. The temperature rise  $\Delta T$  due to a single stop is

$$\Delta T = \frac{E}{WC} \quad (16-59)$$

$T_{\max}$  has to be high enough to transfer  $E$  Btu in  $t_1$  seconds. For steady state, rearrange Eq. (16-56) as

$$\frac{T_{\min} - T_{\infty}}{T_{\max} - T_{\infty}} = \exp(-\beta t_1)$$

where  $\beta = \hbar_{\text{CR}} A / (WC_p)$ . Cross-multiply, add  $T_{\max}$  to both sides, set  $T_{\max} - T_{\min} = \Delta T$ , and rearrange, obtaining

$$T_{\max} = T_{\infty} + \frac{\Delta T}{1 - \exp(-\beta t_1)} \quad (16-60)$$

### EXAMPLE 16-5

A caliper brake is used 24 times per hour to arrest a machine shaft from a speed of 250 rev/min to rest. The ventilation of the brake provides a mean air speed of 25 ft/s. The equivalent rotary inertia of the machine as seen from the brake shaft is 289 lbm · in · s. The disk is steel with a density  $\gamma = 0.282$  lbm/in<sup>3</sup>, a specific heat capacity of 0.108 Btu/(lbm · °F), a diameter of 6 in, a thickness of  $\frac{1}{4}$  in. The pads are dry sintered metal. The lateral area of the brake surface is 50 in<sup>2</sup>. Find  $T_{\max}$  and  $T_{\min}$  for the steady-state operation.

#### Solution

$$t_1 = 60^2 / 24 = 150 \text{ s}$$

Assuming a temperature rise of  $T_{\max} - T_{\infty} = 200^\circ\text{F}$ , from Fig. 16-24a,

$$h_r = 3.0(10^{-6}) \text{ Btu}/(\text{in}^2 \cdot \text{s} \cdot ^\circ\text{F})$$

$$h_c = 2.0(10^{-6}) \text{ Btu}/(\text{in}^2 \cdot \text{s} \cdot ^\circ\text{F})$$

Fig. 16-24b:

$$f_v = 4.8$$

$$\hbar_{\text{CR}} = h_r + f_v h_c = 3.0(10^{-6}) + 4.8(2.0)10^{-6} = 12.6(10^{-6}) \text{ Btu}/(\text{in}^2 \cdot \text{s} \cdot ^\circ\text{F})$$

The mass of the disk is

$$W = \frac{\pi \gamma D^2 h}{4} = \frac{\pi (0.282) 6^2 (0.25)}{4} = 1.99 \text{ lbm}$$

$$\text{Eq. (16-58): } E = \frac{1}{2} \frac{I}{9336} (\omega_o^2 - \omega_f^2) = \frac{289}{2(9336)} \left( \frac{2\pi}{60} 250 \right)^2 = 10.6 \text{ Btu}$$

$$\beta = \frac{\hbar_{\text{CR}} A}{WC_p} = \frac{12.6(10^{-6}) 50}{1.99(0.108)} = 2.93(10^{-3}) \text{ s}^{-1}$$



$$\text{Eq. (16-59):} \quad \Delta T = \frac{E}{WC_p} = \frac{10.6}{1.99(0.108)} = 49.3^\circ\text{F}$$

$$\text{Answer Eq. (16-60):} \quad T_{\max} = 70 + \frac{49.3}{1 - \exp[-2.93(10^{-3})150]} = 209^\circ\text{F}$$

$$\text{Answer} \quad T_{\min} = 209 - 49.3 = 160^\circ\text{F}$$

The predicted temperature rise here is  $T_{\max} - T_{\infty} = 139^\circ\text{F}$ . Iterating with revised values of  $h_r$  and  $h_c$  from Fig. 16-24a, we can make the solution converge to  $T_{\max} = 220^\circ\text{F}$  and  $T_{\min} = 171^\circ\text{F}$ .

Table 16-3 for dry sintered metal pads gives a continuous operating maximum temperature of 570–660°F. There is no danger of overheating.

## 16-10 Friction Materials

A brake or friction clutch should have the following lining material characteristics to a degree that is dependent on the severity of service:

- High and reproducible coefficient of friction
- Imperviousness to environmental conditions, such as moisture
- The ability to withstand high temperatures, together with good thermal conductivity and diffusivity, as well as high specific heat capacity
- Good resiliency
- High resistance to wear, scoring, and galling
- Compatible with the environment
- Flexibility

Table 16-2 gives area of friction surface required for several braking powers. Table 16-3 gives important characteristics of some friction materials for brakes and clutches.

**Table 16-2**

Area of Friction Material Required for a Given Average Braking Power Sources: M. J. Neale, *The Tribology Handbook*, Butterworth, London, 1973; *Friction Materials for Engineers*, Ferodo Ltd., Chapelen-le-frith, England, 1968.

Duty Cycle	Typical Applications	Ratio of Area to Average Braking Power, in <sup>2</sup> /(Btu/s)		
		Band and Drum Brakes	Plate Disk Brakes	Caliper Disk Brakes
Infrequent	Emergency brakes	0.85	2.8	0.28
Intermittent	Elevators, cranes, and winches	2.8	7.1	0.70
Heavy-duty	Excavators, presses	5.6–6.9	13.6	1.41

**Table 16-3**

Characteristics of Friction Materials for Brakes and Clutches Sources: Ferodo Ltd., Chapel-en-le-frith, England; Scan-pac, Mequon, Wisc.; Raybestos, New York, N.Y. and Stratford, Conn.; Gafke Corp., Chicago, Ill.; General Metals Powder Co., Akron, Ohio; D. A. B. Industries, Troy, Mich.; Friction Products Co., Medina, Ohio.

Material	Friction Coefficient $f$	Maximum Pressure $P_{\max}$ , psi	Maximum Temperature Instantaneous, °F	Continuous, °F	Maximum Velocity $V_{\max}$ , ft/min	Applications
Cermet	0.32	150	1500	750		Brakes and clutches
Sintered metal (dry)	0.29–0.33	300–400	930–1020	570–660	3600	Clutches and caliper disk brakes
Sintered metal (wet)	0.06–0.08	500	930	570	3600	Clutches
Rigid molded asbestos (dry)	0.35–0.41	100	660–750	350	3600	Drum brakes and clutches
Rigid molded asbestos (wet)	0.06	300	660	350	3600	Industrial clutches
Rigid molded asbestos pads	0.31–0.49	750	930–1380	440–660	4800	Disk brakes
Rigid molded nonasbestos	0.33–0.63	100–150		500–750	4800–7500	Clutches and brakes
Semirigid molded asbestos	0.37–0.41	100	660	300	3600	Clutches and brakes
Flexible molded asbestos	0.39–0.45	100	660–750	300–350	3600	Clutches and brakes
Wound asbestos yarn and wire	0.38	100	660	300	3600	Vehicle clutches
Woven asbestos yarn and wire	0.38	100	500	260	3600	Industrial clutches and brakes
Woven cotton	0.47	100	230	170	3600	Industrial clutches and brakes
Resilient paper (wet)	0.09–0.15	400	300		$PV < 500\,000$ psi · ft/min	Clutches and transmission bands

The manufacture of friction materials is a highly specialized process, and it is advisable to consult manufacturers' catalogs and handbooks, as well as manufacturers directly, in selecting friction materials for specific applications. Selection involves a consideration of the many characteristics as well as the standard sizes available.

The *woven-cotton lining* is produced as a fabric belt that is impregnated with resins and polymerized. It is used mostly in heavy machinery and is usually supplied in rolls up to 50 ft in length. Thicknesses available range from  $\frac{1}{8}$  to 1 in, in widths up to about 12 in.

A *woven-asbestos lining* is made in a similar manner to the cotton lining and may also contain metal particles. It is not quite as flexible as the cotton lining and comes in a smaller range of sizes. Along with the cotton lining, the asbestos lining was widely used as a brake material in heavy machinery.

*Molded-asbestos linings* contain asbestos fiber and friction modifiers; a thermoset polymer is used, with heat, to form a rigid or semirigid molding. The principal use was in drum brakes.

*Molded-asbestos pads* are similar to molded linings but have no flexibility; they were used for both clutches and brakes.

*Sintered-metal pads* are made of a mixture of copper and/or iron particles with friction modifiers, molded under high pressure and then heated to a high temperature to fuse the material. These pads are used in both brakes and clutches for heavy-duty applications.

*Cermet pads* are similar to the sintered-metal pads and have a substantial ceramic content.

Table 16–4 lists properties of typical brake linings. The linings may consist of a mixture of fibers to provide strength and ability to withstand high temperatures, various friction particles to obtain a degree of wear resistance as well as a higher coefficient of friction, and bonding materials.

Table 16–5 includes a wider variety of clutch friction materials, together with some of their properties. Some of these materials may be run wet by allowing them to dip in oil or to be sprayed by oil. This reduces the coefficient of friction somewhat but carries away more heat and permits higher pressures to be used.

**Table 16–4**

Some Properties  
of Brake Linings

	<b>Woven Lining</b>	<b>Molded Lining</b>	<b>Rigid Block</b>
Compressive strength, kpsi	10–15	10–18	10–15
Compressive strength, MPa	70–100	70–125	70–100
Tensile strength, kpsi	2.5–3	4–5	3–4
Tensile strength, MPa	17–21	27–35	21–27
Max. temperature, °F	400–500	500	750
Max. temperature, °C	200–260	260	400
Max. speed, ft/min	7500	5000	7500
Max. speed, m/s	38	25	38
Max. pressure, psi	50–100	100	150
Max. pressure, kPa	340–690	690	1000
Frictional coefficient, mean	0.45	0.47	0.40–45

**Table 16-5**

Friction Materials for Clutches

Material	Friction Coefficient		Max. Temperature		Max. Pressure	
	Wet	Dry	°F	°C	psi	kPa
Cast iron on cast iron	0.05	0.15–0.20	600	320	150–250	1000–1750
Powdered metal* on cast iron	0.05–0.1	0.1–0.4	1000	540	150	1000
Powdered metal* on hard steel	0.05–0.1	0.1–0.3	1000	540	300	2100
Wood on steel or cast iron	0.16	0.2–0.35	300	150	60–90	400–620
Leather on steel or cast iron	0.12	0.3–0.5	200	100	10–40	70–280
Cork on steel or cast iron	0.15–0.25	0.3–0.5	200	100	8–14	50–100
Felt on steel or cast iron	0.18	0.22	280	140	5–10	35–70
Woven asbestos* on steel or cast iron	0.1–0.2	0.3–0.6	350–500	175–260	50–100	350–700
Molded asbestos* on steel or cast iron	0.08–0.12	0.2–0.5	500	260	50–150	350–1000
Impregnated asbestos* on steel or cast iron	0.12	0.32	500–750	260–400	150	1000
Carbon graphite on steel	0.05–0.1	0.25	700–1000	370–540	300	2100

\*The friction coefficient can be maintained with  $\pm 5$  percent for specific materials in this group.

## 16-11 Miscellaneous Clutches and Couplings

The square-jaw clutch shown in Fig. 16-25a is one form of positive-contact clutch. These clutches have the following characteristics:

- 1 They do not slip.
- 2 No heat is generated.
- 3 They cannot be engaged at high speeds.
- 4 Sometimes they cannot be engaged when both shafts are at rest.
- 5 Engagement at any speed is accompanied by shock.

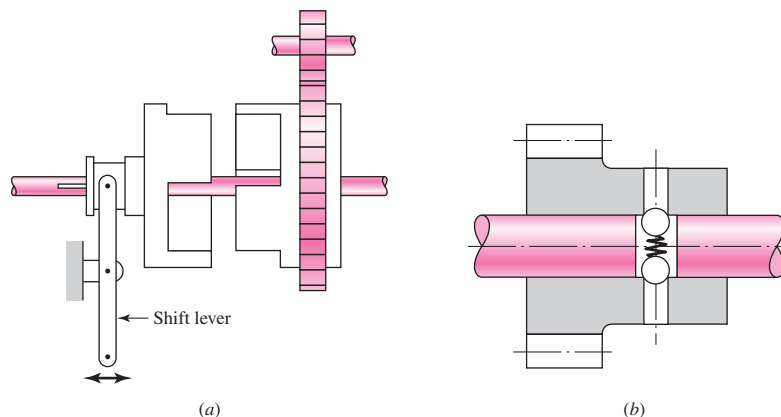
The greatest differences among the various types of positive clutches are concerned with the design of the jaws. To provide a longer period of time for shift action during engagement, the jaws may be ratchet-shaped, spiral-shaped, or gear-tooth-shaped. Sometimes a great many teeth or jaws are used, and they may be cut either circumferentially, so that they engage by cylindrical mating, or on the faces of the mating elements.

Although positive clutches are not used to the extent of the frictional-contact types, they do have important applications where synchronous operation is required, as, for example, in power presses or rolling-mill screw-downs.

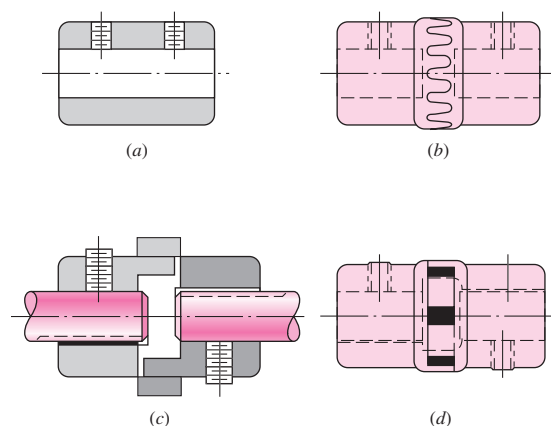
Devices such as linear drives or motor-operated screwdrivers must run to a definite limit and then come to a stop. An overload-release type of clutch is required for these applications. Figure 16-25b is a schematic drawing illustrating the principle of operation of such a clutch. These clutches are usually spring-loaded so as to release at a

**Figure 16-25**

(a) Square-jaw clutch;  
(b) overload release clutch  
using a detent.

**Figure 16-26**

Shaft couplings. (a) Plain.  
(b) Light-duty toothed coupling.  
(c) BOST-FLEX® through-bore  
design having elastomer  
insert to transmit torque by  
compression; insert permits  $1^\circ$   
misalignment. (d) Three-jaw  
coupling available with  
bronze, rubber, or  
polyurethane insert to minimize  
vibration. (Reproduced by  
permission, Boston Gear  
Division, Colfax Corp.)



predetermined torque. The clicking sound which is heard when the overload point is reached is considered to be a desirable signal.

Both fatigue and shock loads must be considered in obtaining the stresses and deflections of the various portions of positive clutches. In addition, wear must generally be considered. The application of the fundamentals discussed in Parts 1 and 2 is usually sufficient for the complete design of these devices.

An overrunning clutch or coupling permits the driven member of a machine to “freewheel” or “overrun” because the driver is stopped or because another source of power increases the speed of the driven mechanism. The construction uses rollers or balls mounted between an outer sleeve and an inner member having cam flats machined around the periphery. Driving action is obtained by wedging the rollers between the sleeve and the cam flats. This clutch is therefore equivalent to a pawl and ratchet with an infinite number of teeth.

There are many varieties of overrunning clutches available, and they are built in capacities up to hundreds of horsepower. Since no slippage is involved, the only power loss is that due to bearing friction and windage.

The shaft couplings shown in Fig. 16-26 are representative of the selection available in catalogs.

## 16–12 Flywheels

The equation of motion for the flywheel represented in Fig. 16–1b is

$$\sum M = T_i(\theta_i, \dot{\theta}_i) - T_o(\theta_o, \dot{\theta}_o) - I\ddot{\theta} = 0$$

or

$$I\ddot{\theta} = T_i(\theta_i, \omega_i) - T_o(\theta_o, \omega_o) \quad (a)$$

where  $T_i$  is considered positive and  $T_o$  negative, and where  $\dot{\theta}$  and  $\ddot{\theta}$  are the first and second time derivatives of  $\theta$ , respectively. Note that both  $T_i$  and  $T_o$  may depend for their values on the angular displacements  $\theta_i$  and  $\theta_o$  as well as their angular velocities  $\omega_i$  and  $\omega_o$ . In many cases the torque characteristic depends upon only one of these. Thus, the torque delivered by an induction motor depends upon the speed of the motor. In fact, motor manufacturers publish charts detailing the torque-speed characteristics of their various motors.

When the input and output torque functions are given, Eq. (a) can be solved for the motion of the flywheel using well-known techniques for solving linear and nonlinear differential equations. We can dispense with this here by assuming a rigid shaft, giving  $\theta_i = \theta = \theta_o$  and  $\omega_i = \omega = \omega_o$ . Thus, Eq. (a) becomes

$$I\ddot{\theta} = T_i(\theta, \omega) - T_o(\theta, \omega) \quad (b)$$

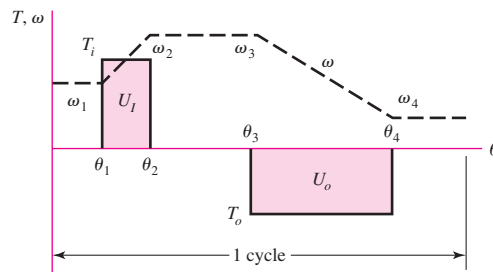
When the two torque functions are known and the starting values of the displacement  $\theta$  and velocity  $\omega$  are given, Eq. (b) can be solved for  $\theta$ ,  $\omega$ , and  $\ddot{\theta}$  as functions of time. However, we are not really interested in the instantaneous values of these terms at all. Primarily we want to know the overall performance of the flywheel. What should its moment of inertia be? How do we match the power source to the load? And what are the resulting performance characteristics of the system that we have selected?

To gain insight into the problem, a hypothetical situation is diagrammed in Fig. 16–27. An input power source subjects a flywheel to a constant torque  $T_i$  while the shaft rotates from  $\theta_1$  to  $\theta_2$ . This is a positive torque and is plotted upward. Equation (b) indicates that a positive acceleration  $\ddot{\theta}$  will be the result, and so the shaft velocity increases from  $\omega_1$  to  $\omega_2$ . As shown, the shaft now rotates from  $\theta_2$  to  $\theta_3$  with zero torque and hence, from Eq. (b), with zero acceleration. Therefore  $\omega_3 = \omega_2$ . From  $\theta_3$  to  $\theta_4$  a load, or output torque, of constant magnitude is applied, causing the shaft to slow down from  $\omega_3$  to  $\omega_4$ . Note that the output torque is plotted in the negative direction in accordance with Eq. (b).

The work input to the flywheel is the area of the rectangle between  $\theta_1$  and  $\theta_2$ , or

$$U_i = T_i(\theta_2 - \theta_1) \quad (c)$$

Figure 16–27



The work output of the flywheel is the area of the rectangle from  $\theta_3$  to  $\theta_4$ , or

$$U_o = T_o(\theta_4 - \theta_3) \quad (d)$$

If  $U_o$  is greater than  $U_i$ , the load uses more energy than has been delivered to the flywheel and so  $\omega_4$  will be less than  $\omega_1$ . If  $U_o = U_i$ ,  $\omega_4$  will be equal to  $\omega_1$  because the gains and losses are equal; we are assuming no friction losses. And finally,  $\omega_4$  will be greater than  $\omega_1$  if  $U_i > U_o$ .

We can also write these relations in terms of kinetic energy. At  $\theta = \theta_1$  the flywheel has a velocity of  $\omega_1$  rad/s, and so its kinetic energy is

$$E_1 = \frac{1}{2} I \omega_1^2 \quad (e)$$

At  $\theta = \theta_2$  the velocity is  $\omega_2$ , and so

$$E_2 = \frac{1}{2} I \omega_2^2 \quad (f)$$

Thus the change in kinetic energy is

$$E_2 - E_1 = \frac{1}{2} I (\omega_2^2 - \omega_1^2) \quad (16-61)$$

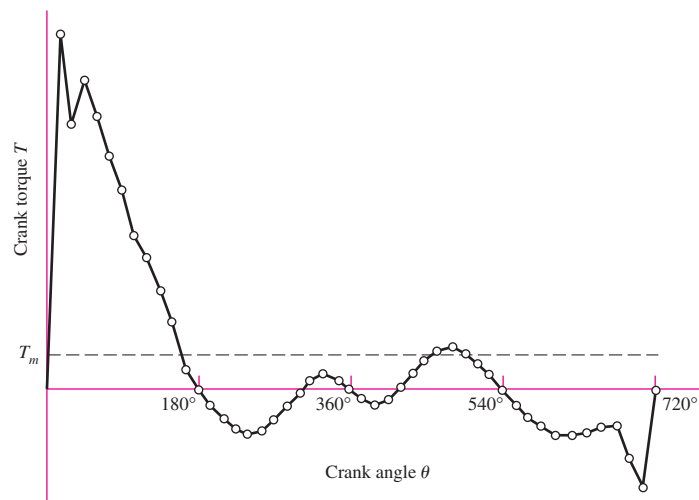
Many of the torque displacement functions encountered in practical engineering situations are so complicated that they must be integrated by numerical methods. Figure 16-28, for example, is a typical plot of the engine torque for one cycle of motion of a single-cylinder internal combustion engine. Since a part of the torque curve is negative, the flywheel must return part of the energy back to the engine. Integrating this curve from  $\theta = 0$  to  $4\pi$  and dividing the result by  $4\pi$  yields the mean torque  $T_m$  available to drive a load during the cycle.

It is convenient to define a *coefficient of speed fluctuation* as

$$C_s = \frac{\omega_2 - \omega_1}{\omega} \quad (16-62)$$

**Figure 16-28**

Relation between torque and crank angle for a one-cylinder, four-stroke-cycle internal combustion engine.



where  $\omega$  is the nominal angular velocity, given by

$$\omega = \frac{\omega_2 + \omega_1}{2} \quad (16-63)$$

Equation (16-61) can be factored to give

$$E_2 - E_1 = \frac{I}{2}(\omega_2 - \omega_1)(\omega_2 + \omega_1)$$

Since  $\omega_2 - \omega_1 = C_s \omega$  and  $\omega_2 + \omega_1 = 2\omega$ , we have

$$E_2 - E_1 = C_s I \omega^2 \quad (16-64)$$

Equation (16-64) can be used to obtain an appropriate flywheel inertia corresponding to the energy change  $E_2 - E_1$ .

### EXAMPLE 16-6

Table 16-6 lists values of the torque used to plot Fig. 16-28. The nominal speed of the engine is to be 250 rad/s.

(a) Integrate the torque-displacement function for one cycle and find the energy that can be delivered to a load during the cycle.

(b) Determine the mean torque  $T_m$  (see Fig. 16-28).

(c) The greatest energy fluctuation is approximately between  $\theta = 15^\circ$  and  $\theta = 150^\circ$  on the torque diagram; see Fig. 16-28 and note that  $T_o = -T_m$ . Using a coefficient of speed fluctuation  $C_s = 0.1$ , find a suitable value for the flywheel inertia.

(d) Find  $\omega_2$  and  $\omega_1$ .

### Solution

(a) Using  $n = 48$  intervals of  $\Delta\theta = 4\pi/48$ , numerical integration of the data of Table 16-6 yields  $E = 3368 \text{ in} \cdot \text{lbf}$ . This is the energy that can be delivered to the load.

**Table 16-6**

Plotting Data for  
Fig. 16-29

$\theta$ , deg	$T$ , lbf · in	$\theta$ , deg	$T$ , lbf · in	$\theta$ , deg	$T$ , lbf · in	$\theta$ , deg	$T$ , lbf · in
0	0	195	-107	375	-85	555	-107
15	2800	210	-206	390	-125	570	-206
30	2090	225	-260	405	-89	585	-292
45	2430	240	-323	420	8	600	-355
60	2160	255	-310	435	126	615	-371
75	1840	270	-242	450	242	630	-362
90	1590	285	-126	465	310	645	-312
105	1210	300	-8	480	323	660	-272
120	1066	315	89	495	280	675	-274
135	803	330	125	510	206	690	-548
150	532	345	85	525	107	705	-760
165	184	360	0	540	0	720	0
180	0						



**Answer** (b)

$$T_m = \frac{3368}{4\pi} = 268 \text{ lbf} \cdot \text{in}$$

(c) The largest positive loop on the torque-displacement diagram occurs between  $\theta = 0^\circ$  and  $\theta = 180^\circ$ . We select this loop as yielding the largest speed change. Subtracting  $268 \text{ lbf} \cdot \text{in}$  from the values in Table 16–6 for this loop gives, respectively,  $-268, 2532, 1822, 2162, 1892, 1572, 1322, 942, 798, 535, 264, -84$ , and  $-268 \text{ lbf} \cdot \text{in}$ . Numerically integrating  $T - T_m$  with respect to  $\theta$  yields  $E_2 - E_1 = 3531 \text{ lbf} \cdot \text{in}$ . We now solve Eq. (16–64) for  $I$ . This gives

**Answer**

$$I = \frac{E_2 - E_1}{C_s \omega^2} = \frac{3531}{0.1(250)^2} = 0.565 \text{ lbf} \cdot \text{s}^2 \text{ in}$$

(d) Equations (16–62) and (16–63) can be solved simultaneously for  $\omega_2$  and  $\omega_1$ . Substituting appropriate values in these two equations yields

**Answer**

$$\omega_2 = \frac{\omega}{2}(2 + C_s) = \frac{250}{2}(2 + 0.1) = 262.5 \text{ rad/s}$$

**Answer**

$$\omega_1 = 2\omega - \omega_2 = 2(250) - 262.5 = 237.5 \text{ rad/s}$$

These two speeds occur at  $\theta = 180^\circ$  and  $\theta = 0^\circ$ , respectively.

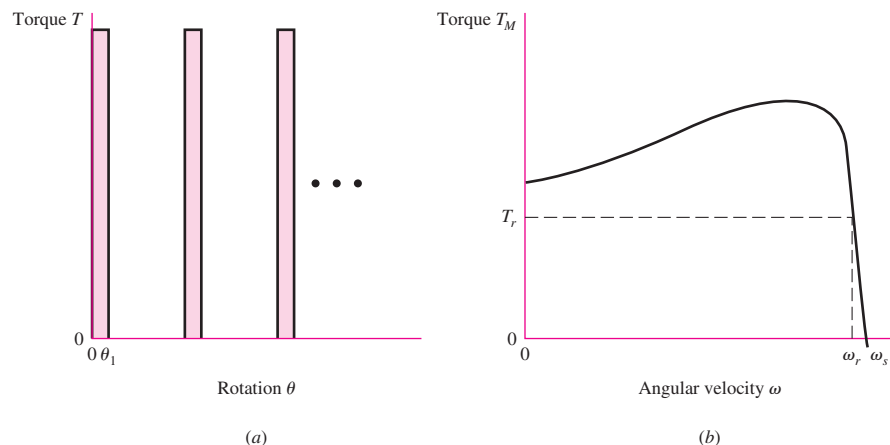
Punch-press torque demand often takes the form of a severe impulse and the running friction of the drive train. The motor overcomes the minor task of overcoming friction while attending to the major task of restoring the flywheel's angular speed. The situation can be idealized as shown in Fig. 16–29. Neglecting the running friction, Euler's equation can be written as

$$T(\theta_1 - 0) = \frac{1}{2}I(\omega_1^2 - \omega_2^2) = E_2 - E_1$$

where the only significant inertia is that of the flywheel. Punch presses can have the motor and flywheel on one shaft, then, through a gear reduction, drive a slider-crank mechanism that carries the punching tool. The motor can be connected to the punch

**Figure 16–29**

(a) Punch-press torque demand during punching. (b) Squirrel-cage electric motor torque-speed characteristic.



continuously, creating a punching rhythm, or it can be connected on command through a clutch that allows one punch and a disconnect. The motor and flywheel must be sized for the most demanding service, which is steady punching. The work done is given by

$$W = \int_{\theta_1}^{\theta_2} [T(\theta) - T] d\theta = \frac{1}{2} I (\omega_{\max}^2 - \omega_{\min}^2)$$

This equation can be arranged to include the coefficient of speed fluctuation  $C_s$  as follows:

$$\begin{aligned} W &= \frac{1}{2} I (\omega_{\max}^2 - \omega_{\min}^2) = \frac{I}{2} (\omega_{\max} - \omega_{\min}) (\omega_{\max} + \omega_{\min}) \\ &= \frac{I}{2} (C_s \bar{\omega}) (2\omega_0) = I C_s \bar{\omega} \omega_0 \end{aligned}$$

When the speed fluctuation is low,  $\omega_0 \doteq \bar{\omega}$ , and

$$I = \frac{W}{C_s \bar{\omega}^2}$$

An induction motor has a linear torque characteristic  $T = a\omega + b$  in the range of operation. The constants  $a$  and  $b$  can be found from the nameplate speed  $\omega_r$  and the synchronous speed  $\omega_s$ :

$$\begin{aligned} a &= \frac{T_r - T_s}{\omega_r - \omega_s} = \frac{T_r}{\omega_r - \omega_s} = -\frac{T_r}{\omega_s - \omega_r} \\ b &= \frac{T_r \omega_s - T_s \omega_r}{\omega_s - \omega_r} = \frac{T_r \omega_s}{\omega_s - \omega_r} \end{aligned} \quad (16-65)$$

For example, a 3-hp three-phase squirrel-cage ac motor rated at 1125 rev/min has a torque of  $63\,025(3)/1125 = 168.1$  lbf · in. The rated angular velocity is  $\omega_r = 2\pi n_r/60 = 2\pi(1125)/60 = 117.81$  rad/s, and the synchronous angular velocity  $\omega_s = 2\pi(1200)/60 = 125.66$  rad/s. Thus  $a = -21.41$  lbf · in · s/rad, and  $b = 2690.9$  lbf · in, and we can express  $T(\omega)$  as  $a\omega + b$ . During the interval from  $t_1$  to  $t_2$  the motor accelerates the flywheel according to  $I\ddot{\theta} = T_M$  (i.e.,  $Td\omega/dt = T_M$ ). Separating the equation  $T_M = I d\omega/dt$  we have

$$\int_{t_1}^{t_2} dt = \int_{\omega_r}^{\omega_2} \frac{I d\omega}{T_M} = I \int_{\omega_r}^{\omega_2} \frac{d\omega}{a\omega + b} = \frac{I}{a} \ln \frac{a\omega_2 + b}{a\omega_r + b} = \frac{I}{a} \ln \frac{T_2}{T_r}$$

or

$$t_2 - t_1 = \frac{I}{a} \ln \frac{T_2}{T_r} \quad (16-66)$$

For the deceleration interval when the motor and flywheel feel the punch torque on the shaft as  $T_L$ ,  $(T_M - T_L) = I d\omega/dt$ , or

$$\int_0^{t_1} dt = I \int_{\omega_2}^{\omega_r} \frac{d\omega}{T_M - T_L} = I \int_{\omega_2}^{\omega_r} \frac{d\omega}{a\omega + b - T_L} = \frac{I}{a} \ln \frac{a\omega_r + b - T_L}{a\omega_2 + b - T_L}$$

or

$$t_1 = \frac{I}{a} \ln \frac{T_r - T_L}{T_2 - T_L} \quad (16-67)$$

We can divide Eq. (16–66) by Eq. (16–67) to obtain

$$\frac{T_2}{T_r} = \left( \frac{T_L - T_r}{T_L - T_2} \right)^{(t_2 - t_1)/t_1} \quad (16-68)$$

Equation (16–68) can be solved for  $T_2$  numerically. Having  $T_2$  the flywheel inertia is, from Eq. (16–66),

$$I = \frac{a(t_2 - t_1)}{\ln(T_2/T_r)} \quad (16-69)$$

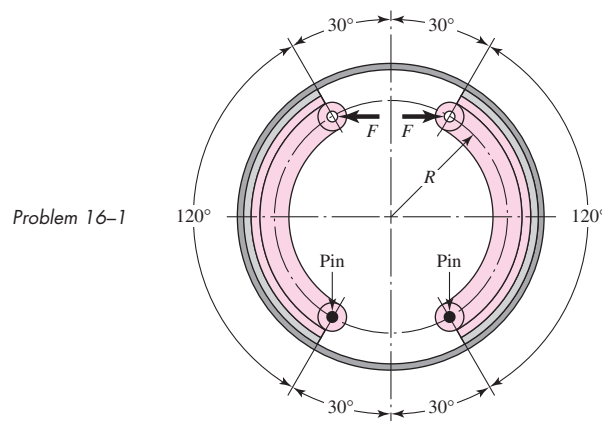
It is important that  $a$  be in units of  $\text{lbf} \cdot \text{in} \cdot \text{s/rad}$  so that  $I$  has proper units. The constant  $a$  should not be in  $\text{lbf} \cdot \text{in}$  per rev/min or  $\text{lbf} \cdot \text{in}$  per rev/s.

## PROBLEMS

### 16-1

The figure shows an internal rim-type brake having an inside rim diameter of 12 in and a dimension  $R = 5$  in. The shoes have a face width of  $1\frac{1}{2}$  in and are both actuated by a force of 500 lbf. The mean coefficient of friction is 0.28.

- Find the maximum pressure and indicate the shoe on which it occurs.
- Estimate the braking torque effected by each shoe, and find the total braking torque.
- Estimate the resulting hinge-pin reactions.



### 16-2

For the brake in Prob. 16–1, consider the pin and actuator locations to be the same. However, instead of  $120^\circ$ , let the friction surface of the brake shoes be  $90^\circ$  and centrally located. Find the maximum pressure and the total braking torque.

### 16-3

In the figure for Prob. 16–1, the inside rim diameter is 280 mm and the dimension  $R$  is 90 mm. The shoes have a face width of 30 mm. Find the braking torque and the maximum pressure for each shoe if the actuating force is 1000 N, the drum rotation is counterclockwise, and  $f = 0.30$ .

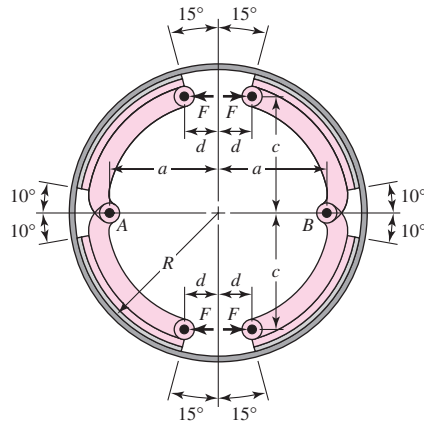
### 16-4

The figure shows a 400-mm-diameter brake drum with four internally expanding shoes. Each of the hinge pins  $A$  and  $B$  supports a pair of shoes. The actuating mechanism is to be arranged to produce the same force  $F$  on each shoe. The face width of the shoes is 75 mm. The material used permits a coefficient of friction of 0.24 and a maximum pressure of 1000 kPa.

- Determine the actuating force.

**Problem 16–4**

The dimensions in millimeters are  
 $a = 150$ ,  $c = 165$ ,  $R = 200$ ,  
and  $d = 50$ .

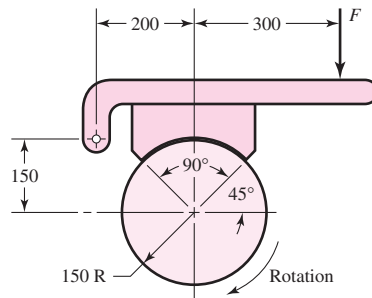


(b) Estimate the brake capacity.

(c) Noting that rotation may be in either direction, estimate the hinge-pin reactions.

**16–5**

The block-type hand brake shown in the figure has a face width of 30 mm and a mean coefficient of friction of 0.25. For an estimated actuating force of 400 N, find the maximum pressure on the shoe and find the braking torque.



**Problem 16–5**

Dimensions in millimeters.

**16–6**

Suppose the standard deviation of the coefficient of friction in Prob. 16–5 is  $\hat{\sigma}_f = 0.025$ , where the deviation from the mean is due entirely to environmental conditions. Find the brake torques corresponding to  $\pm 3\hat{\sigma}_f$ .

**16–7**

The brake shown in the figure has a coefficient of friction of 0.30, a face width of 2 in, and a limiting shoe lining pressure of 150 psi. Find the limiting actuating force  $F$  and the torque capacity.

**16–8**

Refer to the symmetrical pivoted external brake shoe of Fig. 16–12 and Eq. (16–15). Suppose the pressure distribution was uniform, that is, the pressure  $p$  is independent of  $\theta$ . What would the pivot distance  $a'$  be? If  $\theta_1 = \theta_2 = 60^\circ$ , compare  $a$  with  $a'$ .

**16–9**

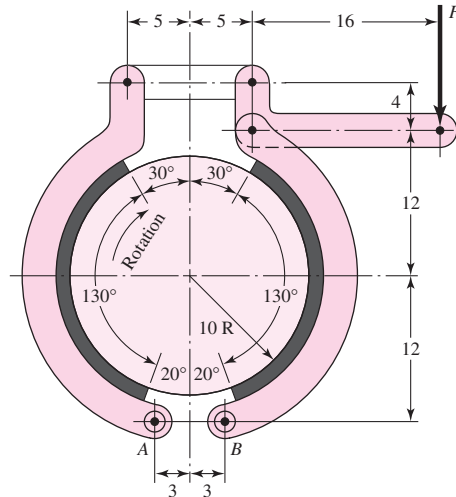
The shoes on the brake depicted in the figure subtend a  $90^\circ$  arc on the drum of this external pivoted-shoe brake. The actuation force  $P$  is applied to the lever. The rotation direction of the drum is counterclockwise, and the coefficient of friction is 0.30.

(a) What should the dimension  $e$  be?

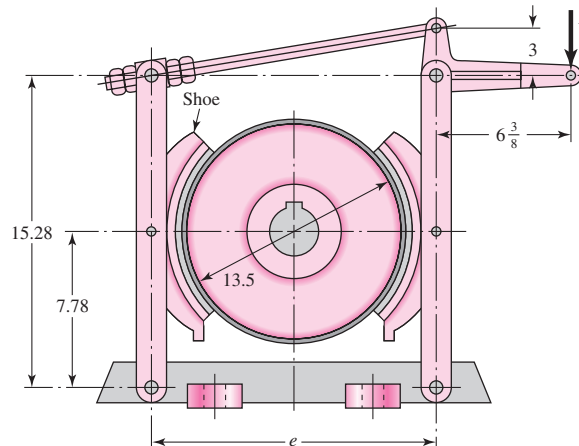
(b) Draw the free-body diagrams of the handle lever and both shoe levers, with forces expressed in terms of the actuation force  $P$ .

(c) Does the direction of rotation of the drum affect the braking torque?

Problem 16–7  
Dimensions in inches.



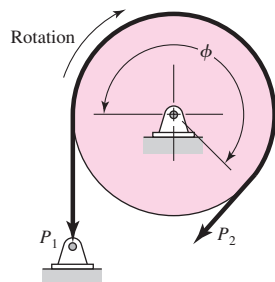
Problem 16–9  
Dimensions in inches.



**16-10** Problem 16–9 is preliminary to analyzing the brake. A molded lining is used dry in the brake of Prob. 16–9 on a cast iron drum. The shoes are 7.5 in wide and subtend a  $90^\circ$  arc. Find the actuation force and the braking torque.

**16-11** The maximum band interface pressure on the brake shown in the figure is 90 psi. Use a 14-in-diameter drum, a band width of 4 in, a coefficient of friction of 0.25, and an angle-of-wrap of  $270^\circ$ . Find the band tensions and the torque capacity.

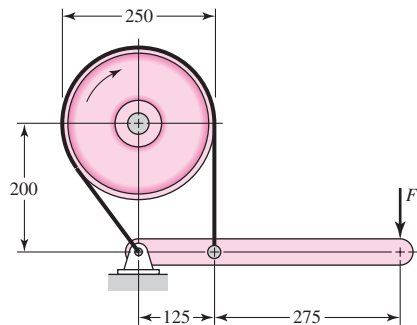
Problem 16–11



**16-12** The drum for the band brake in Prob. 16-11 is 300 mm in diameter. The band selected has a mean coefficient of friction of 0.28 and a width of 80 mm. It can safely support a tension of 7.6 kN. If the angle of wrap is  $270^\circ$ , find the lining pressure and the torque capacity.

**16-13** The brake shown in the figure has a coefficient of friction of 0.30 and is to operate using a maximum force  $F$  of 400 N. If the band width is 50 mm, find the band tensions and the braking torque.

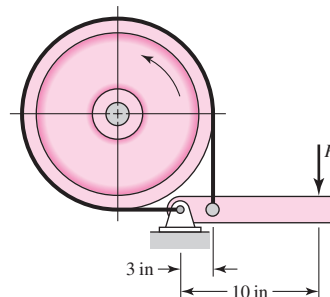
Problem 16-13  
Dimensions in millimeters.



**16-14** The figure depicts a band brake whose drum rotates counterclockwise at 200 rev/min. The drum diameter is 16 in and the band lining 3 in wide. The coefficient of friction is 0.20. The maximum lining interface pressure is 70 psi.

- Find the brake torque, necessary force  $P$ , and steady-state power.
- Complete the free-body diagram of the drum. Find the bearing radial load that a pair of straddle-mounted bearings would have to carry.
- What is the lining pressure  $p$  at both ends of the contact arc?

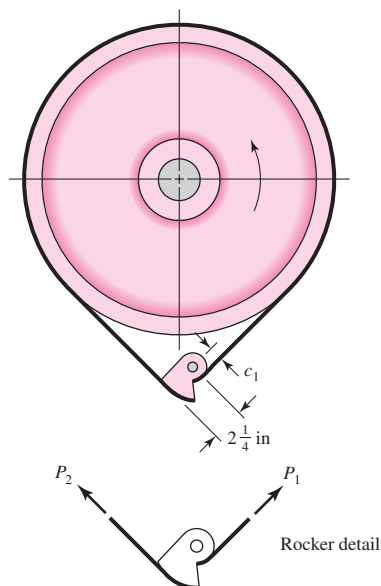
Problem 16-14



**16-15** The figure shows a band brake designed to prevent “backward” rotation of the shaft. The angle of wrap is  $270^\circ$ , the band width is  $2\frac{1}{8}$  in, and the coefficient of friction is 0.20. The torque to be resisted by the brake is 150 lbf · ft. The diameter of the pulley is  $8\frac{1}{4}$  in.

- What dimension  $c_1$  will just prevent backward motion?
- If the rocker was designed with  $c_1 = 1$  in, what is the maximum pressure between the band and drum at 150 lbf · ft back torque?
- If the back-torque demand is 100 lbf · in, what is the largest pressure between the band and drum?

Problem 16–15



- 16–16** A plate clutch has a single pair of mating friction surfaces 300 mm OD by 225 mm ID. The mean value of the coefficient of friction is 0.25, and the actuating force is 5 kN.
- Find the maximum pressure and the torque capacity using the uniform-wear model.
  - Find the maximum pressure and the torque capacity using the uniform-pressure model.

- 16–17** A hydraulically operated multidisk plate clutch has an effective disk outer diameter of 6.5 in and an inner diameter of 4 in. The coefficient of friction is 0.24, and the limiting pressure is 120 psi. There are six planes of sliding present.
- Using the uniform wear model, estimate the axial force  $F$  and the torque  $T$ .
  - Let the inner diameter of the friction pairs  $d$  be a variable. Complete the following table:

$d$ , in	2	3	4	5	6
$T$ , lbf · in					

- What does the table show?

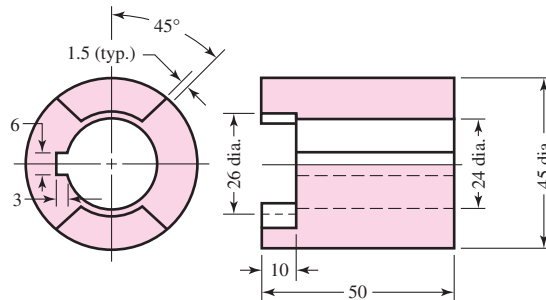
- 16–18** Look again at Prob. 16–17.
- Show how the optimal diameter  $d^*$  is related to the outside diameter  $D$ .
  - What is the optimal inner diameter?
  - What does the tabulation show about maxima?
  - Common proportions for such plate clutches lie in the range  $0.45 \leq d/D \leq 0.80$ . Is the result in part *a* useful?

- 16–19** A cone clutch has  $D = 330$  mm,  $d = 306$  mm, a cone length of 60 mm, and a coefficient of friction of 0.26. A torque of 200 N · m is to be transmitted. For this requirement, estimate the actuating force and pressure by both models.

- 16–20** Show that for the caliper brake the  $T/(fFD)$  versus  $d/D$  plots are the same as Eqs. (b) and (c) of Sec. 16–5.

- 16–21** A two-jaw clutch has the dimensions shown in the figure and is made of ductile steel. The clutch has been designed to transmit 2 kW at 500 rev/min. Find the bearing and shear stresses in the key and the jaws.

**Problem 16–21**  
Dimensions in millimeters.



**16–22** A brake has a normal braking torque of  $320 \text{ N} \cdot \text{m}$  and heat-dissipating surfaces whose mass is  $18 \text{ kg}$ . Suppose a load is brought to rest in  $8.3 \text{ s}$  from an initial angular speed of  $1800 \text{ rev/min}$  using the normal braking torque; estimate the temperature rise of the heat-dissipating surfaces.

**16–23** A cast-iron flywheel has a rim whose OD is  $60 \text{ in}$  and whose ID is  $56 \text{ in}$ . The flywheel weight is to be such that an energy fluctuation of  $5000 \text{ ft} \cdot \text{lbf}$  will cause the angular speed to vary no more than  $240$  to  $260 \text{ rev/min}$ . Estimate the coefficient of speed fluctuation. If the weight of the spokes is neglected, what should be the width of the rim?

**16–24** A single-geared blanking press has a stroke of  $8 \text{ in}$  and a rated capacity of  $35 \text{ tons}$ . A cam-driven ram is assumed to be capable of delivering the full press load at constant force during the last  $15 \text{ percent}$  of a constant-velocity stroke. The camshaft has an average speed of  $90 \text{ rev/min}$  and is geared to the flywheel shaft at a  $6:1$  ratio. The total work done is to include an allowance of  $16 \text{ percent}$  for friction.

- Estimate the maximum energy fluctuation.
- Find the rim weight for an effective diameter of  $48 \text{ in}$  and a coefficient of speed fluctuation of  $0.10$ .

**16–25** Using the data of Table 16–6, find the mean output torque and flywheel inertia required for a three-cylinder in-line engine corresponding to a nominal speed of  $2400 \text{ rev/min}$ . Use  $C_s = 0.30$ .

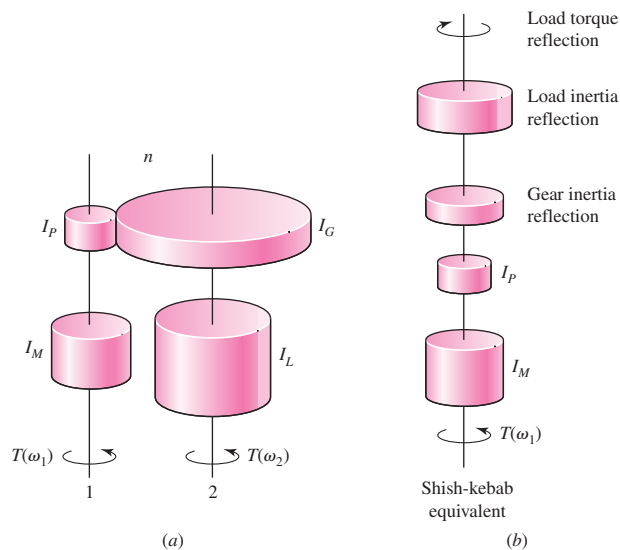
**16–26** When a motor armature inertia, a pinion inertia, and a motor torque reside on a motor shaft, and a gear inertia, a load inertia, and a load torque exist on a second shaft, it is useful to reflect all the torques and inertias to one shaft, say, the armature shaft. We need some rules to make such reflection easy. Consider the pinion and gear as disks of pitch radius.

- A torque on a second shaft is reflected to the motor shaft as the load torque divided by the negative of the stepdown ratio.
- An inertia on a second shaft is reflected to the motor shaft as its inertia divided by the stepdown ratio squared.
- The inertia of a disk gear on a second shaft in mesh with a disk pinion on the motor shaft is reflected to the pinion shaft as the *pinion* inertia multiplied by the stepdown ratio squared.

- Verify the three rules.
- Using the rules, reduce the two-shaft system in the figure to a motor-shaft shish-kebab equivalent. Correctly done, the dynamic response of the shish kebab and the real system are identical.
- For a stepdown ratio of  $n = 10$  compare the shish-kebab inertias.



Problem 16–26  
Dimensions in millimeters.



### 16–27

Apply the rules of Prob. 16–26 to the three-shaft system shown in the figure to create a motor shaft shish kebab.

(a) Show that the equivalent inertia  $I_e$  is given by

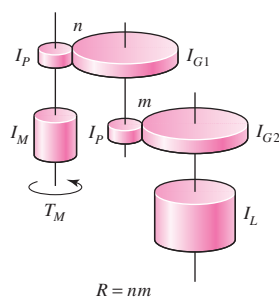
$$I_e = I_M + I_P + n^2 I_P + \frac{I_P}{n^2} + \frac{m^2 I_P}{n^2} + \frac{I_L}{m^2 n^2}$$

(b) If the overall gear reduction  $R$  is a constant  $nm$ , show that the equivalent inertia becomes

$$I_e = I_M + I_P + n^2 I_P + \frac{I_P}{n^2} + \frac{R^2 I_P}{n^4} + \frac{I_L}{R^2}$$

(c) If the problem is to minimize the gear-train inertia, find the ratios  $n$  and  $m$  for the values of  $I_P = 1$ ,  $I_M = 10$ ,  $I_L = 100$ , and  $R = 10$ .

Problem 16–27



### 16–28

For the conditions of Prob. 16–27, make a plot of the equivalent inertia  $I_e$  as ordinate and the stepdown ratio  $n$  as abscissa in the range  $1 \leq n \leq 10$ . How does the minimum inertia compare to the single-step inertia?

### 16–29

A punch-press geared 10:1 is to make six punches per minute under circumstances where the torque on the crankshaft is 1300 lbf · ft for  $\frac{1}{2}$  s. The motor's nameplate reads 3 bhp at 1125 rev/min for continuous duty. Design a satisfactory flywheel for use on the motor shaft to the extent of specifying material and rim inside and outside diameters as well as its width. As you prepare your

specifications, note  $\omega_{\max}$ ,  $\omega_{\min}$ , the coefficient of speed fluctuation  $C_s$ , energy transfer, and peak power that the flywheel transmits to the punch-press. Note power and shock conditions imposed on the gear train because the flywheel is on the motor shaft.

**16–30** The punch-press of Prob. 16–29 needs a flywheel for service on the crankshaft of the punch-press. Design a satisfactory flywheel to the extent of specifying material, rim inside and outside diameters, and width. Note  $\omega_{\max}$ ,  $\omega_{\min}$ ,  $C_s$ , energy transfer, and peak power the flywheel transmits to the punch. What is the peak power seen in the gear train? What power and shock conditions must the gear-train transmit?

**16–31** Compare the designs resulting from the tasks assigned in Probs. 16–29 and 16–30. What have you learned? What recommendations do you have?

# 17

## Flexible Mechanical Elements

### Chapter Outline

<b>17-1</b>	Belts <b>860</b>
<b>17-2</b>	Flat- and Round-Belt Drives <b>863</b>
<b>17-3</b>	V Belts <b>878</b>
<b>17-4</b>	Timing Belts <b>886</b>
<b>17-5</b>	Roller Chain <b>887</b>
<b>17-6</b>	Wire Rope <b>896</b>
<b>17-7</b>	Flexible Shafts <b>904</b>

Belts, ropes, chains, and other similar elastic or flexible machine elements are used in conveying systems and in the transmission of power over comparatively long distances. It often happens that these elements can be used as a replacement for gears, shafts, bearings, and other relatively rigid power-transmission devices. In many cases their use simplifies the design of a machine and substantially reduces the cost.

In addition, since these elements are elastic and usually quite long, they play an important part in absorbing shock loads and in damping out and isolating the effects of vibration. This is an important advantage as far as machine life is concerned.

Most flexible elements do not have an infinite life. When they are used, it is important to establish an inspection schedule to guard against wear, aging, and loss of elasticity. The elements should be replaced at the first sign of deterioration.

## 17-1 Belts

The four principal types of belts are shown, with some of their characteristics, in Table 17-1. *Crowned pulleys* are used for flat belts, and *grooved pulleys*, or *sheaves*, for round and V belts. Timing belts require *toothed wheels*, or *sprockets*. In all cases, the pulley axes must be separated by a certain minimum distance, depending upon the belt type and size, to operate properly. Other characteristics of belts are:

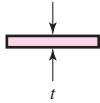
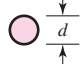
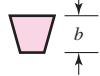
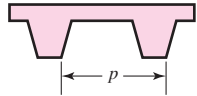
- They may be used for long center distances.
- Except for timing belts, there is some slip and creep, and so the angular-velocity ratio between the driving and driven shafts is neither constant nor exactly equal to the ratio of the pulley diameters.
- In some cases an idler or tension pulley can be used to avoid adjustments in center distance that are ordinarily necessitated by age or the installation of new belts.

Figure 17-1 illustrates the geometry of open and closed flat-belt drives. For a flat belt with this drive the belt tension is such that the sag or droop is visible in Fig. 17-2a, when the belt is running. Although the top is preferred for the loose side of the belt, for other belt types either the top or the bottom may be used, because their installed tension is usually greater.

Two types of reversing drives are shown in Fig. 17-2. Notice that both sides of the belt contact the pulleys in Figs. 17-2b and 17-2c, and so these drives cannot be used with V belts or timing belts.

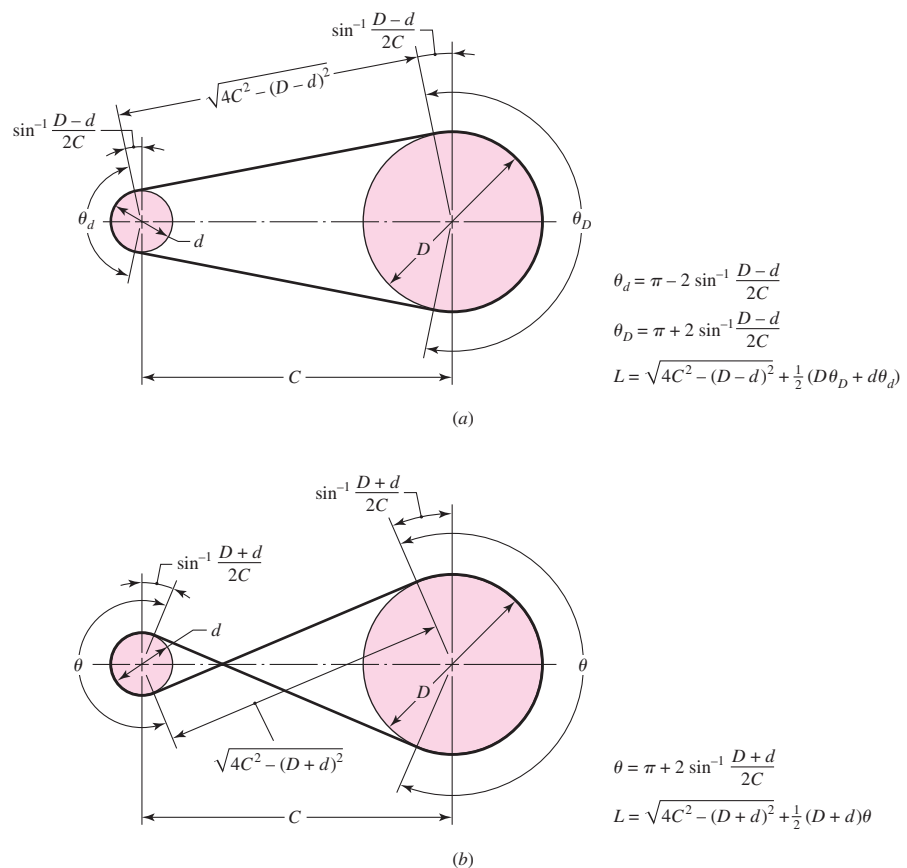
**Table 17-1**

Characteristics of Some  
 Common Belt Types.  
 Figures are Cross  
 Sections except for the  
 Timing Belt, which is a  
 Side View

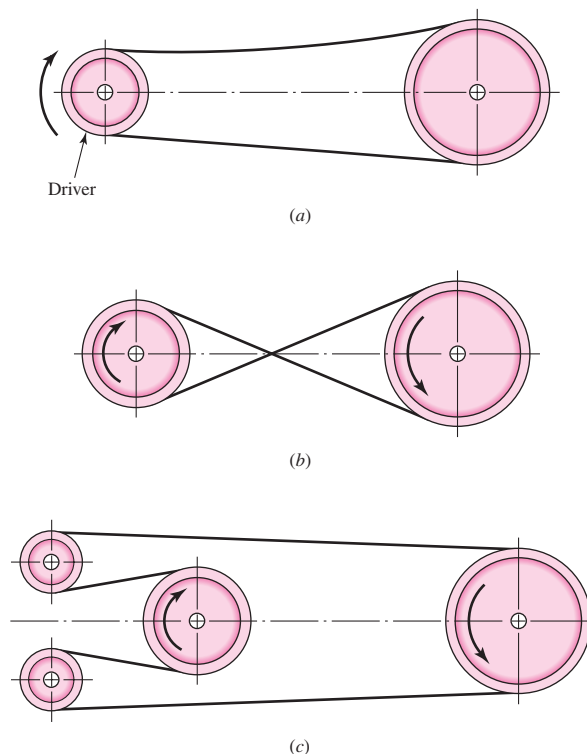
Belt Type	Figure	Joint	Size Range	Center Distance
Flat		Yes	$t = \begin{cases} 0.03 \text{ to } 0.20 \text{ in} \\ 0.75 \text{ to } 5 \text{ mm} \end{cases}$	No upper limit
Round		Yes	$d = \frac{1}{8} \text{ to } \frac{3}{4} \text{ in}$	No upper limit
V		None	$b = \begin{cases} 0.31 \text{ to } 0.91 \text{ in} \\ 8 \text{ to } 19 \text{ mm} \end{cases}$	Limited
Timing		None	$p = 2 \text{ mm and up}$	Limited

**Figure 17-1**

Flat-belt geometry. (a) Open belt. (b) Crossed belt.

**Figure 17-2**

Nonreversing and reversing belt drives. (a) Nonreversing open belt. (b) Reversing crossed belt. Crossed belts must be separated to prevent rubbing if high-friction materials are used. (c) Reversing open-belt drive.



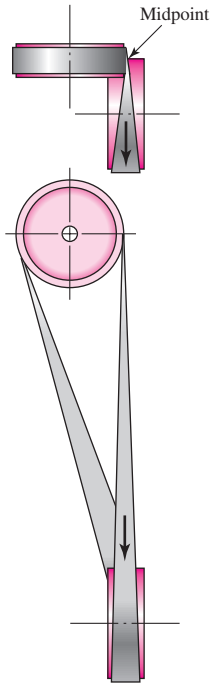


**Figure 17-3**

Quarter-twist belt drive; an idler guide pulley must be used if motion is to be in both directions.

Figure 17-3 shows a flat-belt drive with out-of-plane pulleys. The shafts need not be at right angles as in this case. Note the top view of the drive in Fig. 17-3. The pulleys must be positioned so that the belt leaves each pulley in the midplane of the other pulley face. Other arrangements may require guide pulleys to achieve this condition.

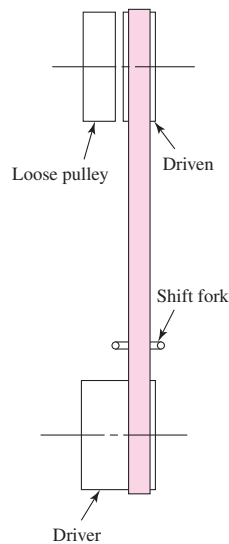
Another advantage of flat belts is shown in Fig. 17-4, where clutching action is obtained by shifting the belt from a loose to a tight or driven pulley.

Figure 17-5 shows two variable-speed drives. The drive in Fig. 17-5a is commonly used only for flat belts. The drive of Fig. 17-5b can also be used for V belts and round belts by using grooved sheaves.

Flat belts are made of urethane and also of rubber-impregnated fabric reinforced with steel wire or nylon cords to take the tension load. One or both surfaces may have a friction surface coating. Flat belts are quiet, they are efficient at high speeds, and they can transmit large amounts of power over long center distances. Usually, flat belting is purchased by the roll and cut and the ends are joined by using special kits furnished by the manufacturer. Two or more flat belts running side by side, instead of a single wide belt, are often used to form a conveying system.

A V belt is made of fabric and cord, usually cotton, rayon, or nylon, and impregnated with rubber. In contrast with flat belts, V belts are used with similar sheaves and at shorter center distances. V belts are slightly less efficient than flat belts, but a number of them can be used on a single sheave, thus making a multiple drive. V belts are made only in certain lengths and have no joints.

Timing belts are made of rubberized fabric and steel wire and have teeth that fit into grooves cut on the periphery of the sprockets. The timing belt does not stretch or slip and consequently transmits power at a constant angular-velocity ratio. The fact that the belt is toothed provides several advantages over ordinary belting. One of these is that no initial tension is necessary, so that fixed-center drives may be used. Another is



**Figure 17-4**

This drive eliminates the need for a clutch. Flat belt can be shifted left or right by use of a fork.

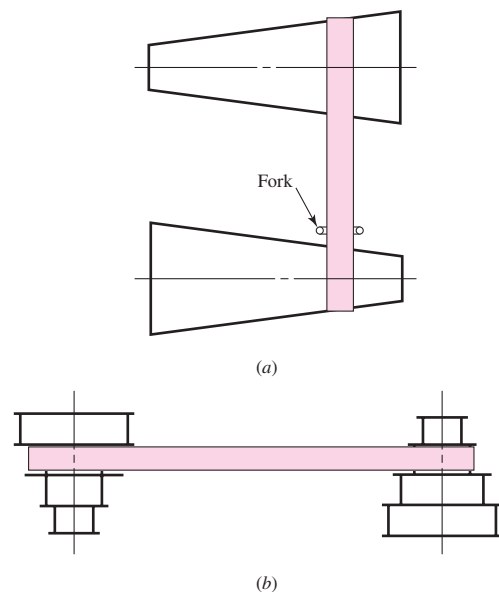


**Figure 17-5**

Variable-speed belt drives.

the elimination of the restriction on speeds; the teeth make it possible to run at nearly any speed, slow or fast. Disadvantages are the first cost of the belt, the necessity of grooving the sprockets, and the attendant dynamic fluctuations caused at the belt-tooth meshing frequency.

## 17-2 Flat- and Round-Belt Drives

Modern flat-belt drives consist of a strong elastic core surrounded by an elastomer; these drives have distinct advantages over gear drives or V-belt drives. A flat-belt drive has an efficiency of about 98 percent, which is about the same as for a gear drive. On the other hand, the efficiency of a V-belt drive ranges from about 70 to 96 percent.<sup>1</sup> Flat-belt drives produce very little noise and absorb more torsional vibration from the system than either V-belt or gear drives.

When an open-belt drive (Fig. 17-1a) is used, the contact angles are found to be

$$\begin{aligned}\theta_d &= \pi - 2 \sin^{-1} \frac{D-d}{2C} \\ \theta_D &= \pi + 2 \sin^{-1} \frac{D-d}{2C}\end{aligned}\tag{17-1}$$

where  $D$  = diameter of large pulley

$d$  = diameter of small pulley

$C$  = center distance

$\theta$  = angle of contact

The length of the belt is found by summing the two arc lengths with twice the distance between the beginning and end of contact. The result is

$$L = [4C^2 - (D-d)^2]^{1/2} + \frac{1}{2}(D\theta_D + d\theta_d)\tag{17-2}$$

A similar set of equations can be derived for the crossed belt of Fig. 17-2b. For this belt, the angle of wrap is the same for both pulleys and is

$$\theta = \pi + 2 \sin^{-1} \frac{D+d}{2C}\tag{17-3}$$

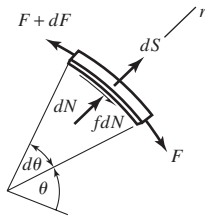
The belt length for crossed belts is found to be

$$L = [4C^2 - (D+d)^2]^{1/2} + \frac{1}{2}(D+d)\theta\tag{17-4}$$

Firbank<sup>2</sup> explains flat-belt-drive theory in the following way. A change in belt tension due to friction forces between the belt and pulley will cause the belt to elongate or contract and move relative to the surface of the pulley. This motion is caused by *elastic creep* and is associated with sliding friction as opposed to static friction. The action at the driving pulley, through that portion of the angle of contact that is actually transmitting power, is such that the belt moves more slowly than the surface speed of the pulley because of the elastic creep. The angle of contact is made up of the *effective arc*,

<sup>1</sup>A. W. Wallin, "Efficiency of Synchronous Belts and V-Belts," *Proc. Nat. Conf. Power Transmission*, vol. 5, Illinois Institute of Technology, Chicago, Nov. 7-9, 1978, pp. 265-271.

<sup>2</sup>T. C. Firbank, *Mechanics of the Flat Belt Drive*, ASME paper no. 72-PTG-21.


**Figure 17-6**

Free body of an infinitesimal element of a flat belt in contact with a pulley.

through which power is transmitted, and the *idle arc*. For the driving pulley the belt first contacts the pulley with a *tight-side tension*  $F_1$  and a velocity  $V_1$ , which is the same as the surface velocity of the pulley. The belt then passes through the idle arc with no change in  $F_1$  or  $V_1$ . Then creep or sliding contact begins, and the belt tension changes in accordance with the friction forces. At the end of the effective arc the belt leaves the pulley with a *loose-side tension*  $F_2$  and a reduced speed  $V_2$ .

Firbank has used this theory to express the mechanics of flat-belt drives in mathematical form and has verified the results by experiment. His observations include the finding that substantially more power is transmitted by static friction than sliding friction. He also found that the coefficient of friction for a belt having a nylon core and leather surface was typically 0.7, but that it could be raised to 0.9 by employing special surface finishes.

Our model will assume that the friction force on the belt is proportional to the normal pressure along the arc of contact. We seek first a relationship between the tight side tension and slack side tension, similar to that of band brakes but incorporating the consequences of movement, that is, centrifugal tension in the belt. In Fig. 17-6 we see a free body of a small segment of the belt. The differential force  $dS$  is due to centrifugal force,  $dN$  is the normal force between the belt and pulley, and  $f dN$  is the shearing traction due to friction at the point of slip. The belt width is  $b$  and the thickness is  $t$ . The belt mass per unit length is  $m$ . The centrifugal force  $dS$  can be expressed as

$$dS = (mr d\theta)r\omega^2 = mr^2\omega^2 d\theta = mV^2 d\theta = F_c d\theta \quad (a)$$

where  $V$  is the belt speed. Summing forces radially gives

$$\sum F_r = -(F + dF)\frac{d\theta}{2} - F\frac{d\theta}{2} + dN + dS = 0$$

Ignoring the higher-order term, we have

$$dN = F d\theta - dS \quad (b)$$

Summing forces tangentially gives

$$\sum F_t = -f dN - F + (F + dF) = 0$$

from which, incorporating Eqs. (a) and (b), we obtain

$$dF = f dN = f F d\theta - f dS = f F d\theta - f mr^2\omega^2 d\theta$$

or

$$\frac{dF}{d\theta} - fF = -fmr^2\omega^2 \quad (c)$$

The solution to this nonhomogeneous first-order linear differential equation is

$$F = A \exp(f\theta) + mr^2\omega^2 \quad (d)$$

where  $A$  is an arbitrary constant. Assuming  $\theta$  starts at the loose side, the boundary condition that  $F$  at  $\theta = 0$  equals  $F_2$  gives  $A = F_2 - mr^2\omega^2$ . The solution is

$$F = (F_2 - mr^2\omega^2) \exp(f\theta) + mr^2\omega^2 \quad (17-5)$$

At the end of the angle of wrap  $\phi$ , the tight side,

$$F|_{\theta=\phi} = F_1 = (F_2 - mr^2\omega^2) \exp(f\phi) + mr^2\omega^2 \quad (17-6)$$



Now we can write

$$\frac{F_1 - mr^2\omega^2}{F_2 - mr^2\omega^2} = \frac{F_1 - F_c}{F_2 - F_c} = \exp(f\phi) \quad (17-7)$$

where, from Eq. (a),  $F_c = mr^2\omega^2$ . It is also useful that Eq. (17-7) can be written as

$$F_1 - F_2 = (F_1 - F_c) \frac{\exp(f\phi) - 1}{\exp(f\phi)} \quad (17-8)$$

Now  $F_c$  is found as follows: with  $n$  being the rotational speed, in rev/min, of the pulley of diameter  $d$ , the belt speed is

$$V = \pi dn/12 \quad \text{ft/min}$$

The weight  $w$  of a foot of belt is given in terms of the weight density  $\gamma$  in lbf/in<sup>3</sup> as  $w = 12\gamma bt$  lbf/ft where  $b$  and  $t$  are in inches.  $F_c$  is written as

$$F_c = \frac{w}{g} \left( \frac{V}{60} \right)^2 = \frac{w}{32.17} \left( \frac{V}{60} \right)^2 \quad (e)$$

Figure 17-7 shows a free body of a pulley and part of the belt. The tight side tension  $F_1$  and the loose side tension  $F_2$  have the following additive components:

$$F_1 = F_i + F_c + \Delta F' = F_i + F_c + T/D \quad (f)$$

$$F_2 = F_i + F_c - \Delta F' = F_i + F_c - T/D \quad (g)$$

where  $F_i$  = initial tension

$F_c$  = hoop tension due to centrifugal force

$\Delta F'$  = tension due to the transmitted torque  $T$

$D$  = diameter of the pulley

The difference between  $F_1$  and  $F_2$  is related to the pulley torque. Subtracting Eq. (g) from Eq. (f) gives

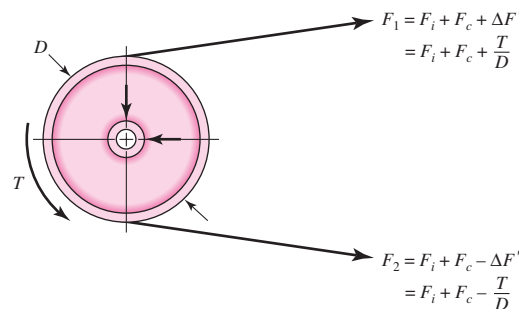
$$F_1 - F_2 = \frac{2T}{D} = \frac{T}{D/2} \quad (h)$$

Adding Eqs. (f) and (g) gives

$$F_1 + F_2 = 2F_i + 2F_c$$

**Figure 17-7**

Forces and torques on a pulley.



from which

$$F_i = \frac{F_1 + F_2}{2} - F_c \quad (i)$$

Dividing Eq. (i) by Eq. (h), manipulating, and using Eq. (17–7) gives

$$\begin{aligned} \frac{F_i}{T/D} &= \frac{(F_1 + F_2)/2 - F_c}{(F_1 - F_2)/2} = \frac{F_1 + F_2 - 2F_c}{F_1 - F_2} = \frac{(F_1 - F_c) + (F_2 - F_c)}{(F_1 - F_c) - (F_2 - F_c)} \\ &= \frac{(F_1 - F_c)/(F_2 - F_c) + 1}{(F_1 - F_c)/(F_2 - F_c) - 1} = \frac{\exp(f\phi) + 1}{\exp(f\phi) - 1} \end{aligned}$$

from which

$$F_i = \frac{T}{D} \frac{\exp(f\phi) + 1}{\exp(f\phi) - 1} \quad (17-9)$$

Equation (17–9) give us a fundamental insight into flat belting. If  $F_i$  equals zero, then  $T$  equals zero: no initial tension, no torque transmitted. The torque is in proportion to the initial tension. This means that if there is to be a satisfactory flat-belt drive, the initial tension must be (1) provided, (2) sustained, (3) in the proper amount, and (4) maintained by routine inspection.

From Eq. (f), incorporating Eq. (17–9) gives

$$\begin{aligned} F_1 &= F_i + F_c + \frac{T}{D} = F_c + F_i + F_i \frac{\exp(f\phi) - 1}{\exp(f\phi) + 1} \\ &= F_c + \frac{F_i[\exp(f\phi) + 1] + F_i[\exp(f\phi) - 1]}{\exp(f\phi) + 1} \\ F_1 &= F_c + F_i \frac{2 \exp(f\phi)}{\exp(f\phi) + 1} \quad (17-10) \end{aligned}$$

From Eq. (g), incorporating Eq. (17–9) gives

$$\begin{aligned} F_2 &= F_i + F_c - \frac{T}{D} = F_c + F_i - F_i \frac{\exp(f\phi) - 1}{\exp(f\phi) + 1} \\ &= F_c + \frac{F_i[\exp(f\phi) + 1] - F_i[\exp(f\phi) - 1]}{\exp(f\phi) + 1} \\ F_2 &= F_c + F_i \frac{2}{\exp(f\phi) + 1} \quad (17-11) \end{aligned}$$

Equation (17-7) is called the *belting equation*, but Eqs. (17-9), (17-10), and (17-11) reveal how belting works. We plot Eqs. (17-10) and (17-11) as shown in Fig. 17-8 against  $F_i$  as abscissa. The initial tension needs to be sufficient so that the difference between the  $F_1$  and  $F_2$  curve is  $2T/D$ . With no torque transmitted, the least possible belt tension is  $F_1 = F_2 = F_c$ .

The transmitted horsepower is given by

$$H = \frac{(F_1 - F_2)V}{33\,000} \quad (j)$$

Manufacturers provide specifications for their belts that include allowable tension  $F_a$  (or stress  $\sigma_{\text{all}}$ ), the tension being expressed in units of force per unit width. Belt life is usually several years. The severity of flexing at the pulley and its effect on life is reflected in a pulley correction factor  $C_p$ . Speed in excess of 600 ft/min and its effect on life is reflected in a velocity correction factor  $C_v$ . For polyamide and urethane belts use  $C_v = 1$ . For leather belts see Fig. 17-9. A service factor  $K_s$  is used for excursions of load from nominal, applied to the nominal power as  $H_d = H_{\text{nom}} K_s n_d$ , where  $n_d$  is the

**Figure 17-8**

Plot of initial tension  $F_i$  against belt tension  $F_1$  or  $F_2$ , showing the intercept  $F_c$ , the equations of the curves, and where  $2T/D$  is to be found.

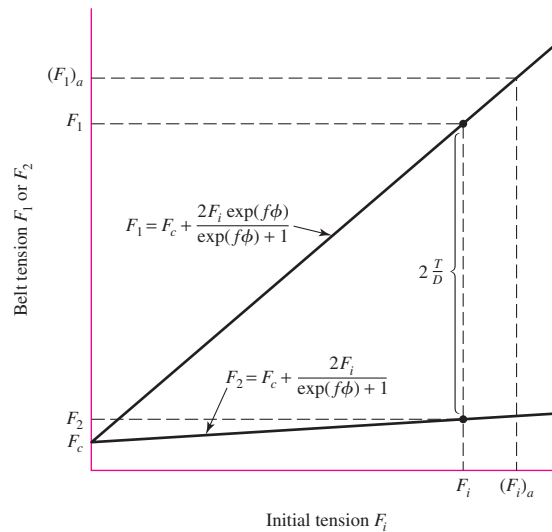
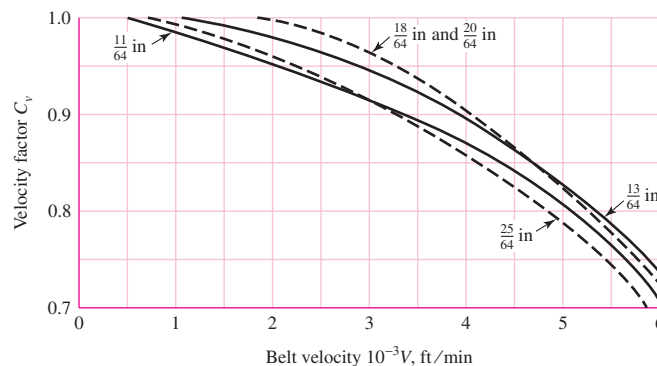


**Figure 17-9**

Velocity correction factor  $C_v$  for leather belts for various thicknesses. (Data source: Machinery's Handbook, 20th ed., Industrial Press, New York, 1976, p. 1047.)



design factor for exigencies. These effects are incorporated as follows:

$$(F_1)_a = bF_aC_pC_v \quad (17-12)$$

where  $(F_1)_a$  = allowable largest tension, lbf

$b$  = belt width, in

$F_a$  = manufacturer's allowed tension, lbf/in

$C_p$  = pulley correction factor (Table 17-4)

$C_v$  = velocity correction factor

The steps in analyzing a flat-belt drive can include

- 1 Find  $\exp(f\phi)$  from belt-drive geometry and friction
- 2 From belt geometry and speed find  $F_c$
- 3 From  $T = 63\,025H_{\text{nom}}K_s n_d/n$  find necessary torque
- 4 From torque  $T$  find the necessary  $(F_1)_a - F_2 = 2T/D$
- 5 Find  $F_2$  from  $(F_1)_a - [(F_1)_a - F_2]$
- 6 From Eq. (i) find the necessary initial tension  $F_i$
- 7 Check the friction development,  $f' < f$ . Use Eq. (17-7) solved for  $f'$ :

$$f' = \frac{1}{\phi} \ln \frac{(F_1)_a - F_c}{F_2 - F_c}$$

- 8 Find the factor of safety from  $n_{fs} = H_a/(H_{\text{nom}}K_s)$

It is unfortunate that many of the available data on belting are from sources in which they are presented in a very simplistic manner. These sources use a variety of charts, nomographs, and tables to enable someone who knows nothing about belting to apply them. Little, if any, computation is needed for such a person to obtain valid results. Since a basic understanding of the process, in many cases, is lacking, there is no way this person can vary the steps in the process to obtain a better design.

Incorporating the available belt-drive data into a form that provides a good understanding of belt mechanics involves certain adjustments in the data. Because of this, the results from the analysis presented here will not correspond exactly with those of the sources from which they were obtained.

A moderate variety of belt materials, with some of their properties, are listed in Table 17-2. These are sufficient for solving a large variety of design and analysis problems. The design equation to be used is Eq. (j).

The values given in Table 17-2 for the allowable belt tension are based on a belt speed of 600 ft/min. For higher speeds, use Fig. 17-9 to obtain  $C_v$  values for leather belts. For polyamide and urethane belts, use  $C_v = 1.0$ .

The service factors  $K_s$  for V-belt drives, given in Table 17-15 in Sec. 17-3, are also recommended here for flat- and round-belt drives.

Minimum pulley sizes for the various belts are listed in Tables 17-2 and 17-3. The pulley correction factor accounts for the amount of bending or flexing of the belt and how this affects the life of the belt. For this reason it is dependent on the size and material of the belt used. See Table 17-4. Use  $C_p = 1.0$  for urethane belts.

Flat-belt pulleys should be crowned to keep belts from running off the pulleys. If only one pulley is crowned, it should be the larger one. Both pulleys must be crowned whenever the pulley axes are not in a horizontal position. Use Table 17-5 for the crown height.

**Table 17-2**Properties of Some Flat- and Round-Belt Materials. (Diameter =  $d$ , thickness =  $t$ , width =  $w$ )

Material	Specification	Size, in	Minimum Pulley Diameter, in	Allowable Tension per Unit Width at 600 ft/min, lbf/in	Specific Weight, lbf/in <sup>3</sup>	Coefficient of Friction
Leather	1 ply	$t = \frac{11}{64}$	3	30	0.035–0.045	0.4
		$t = \frac{13}{64}$	$3\frac{1}{2}$	33	0.035–0.045	0.4
	2 ply	$t = \frac{18}{64}$	$4\frac{1}{2}$	41	0.035–0.045	0.4
		$t = \frac{20}{64}$	6 <sup>a</sup>	50	0.035–0.045	0.4
		$t = \frac{23}{64}$	9 <sup>a</sup>	60	0.035–0.045	0.4
Polyamide <sup>b</sup>	F-0 <sup>c</sup>	$t = 0.03$	0.60	10	0.035	0.5
	F-1 <sup>c</sup>	$t = 0.05$	1.0	35	0.035	0.5
	F-2 <sup>c</sup>	$t = 0.07$	2.4	60	0.051	0.5
	A-2 <sup>c</sup>	$t = 0.11$	2.4	60	0.037	0.8
	A-3 <sup>c</sup>	$t = 0.13$	4.3	100	0.042	0.8
	A-4 <sup>c</sup>	$t = 0.20$	9.5	175	0.039	0.8
	A-5 <sup>c</sup>	$t = 0.25$	13.5	275	0.039	0.8
Urethane <sup>d</sup>	w = 0.50	$t = 0.062$	See	5.2 <sup>e</sup>	0.038–0.045	0.7
	w = 0.75	$t = 0.078$	Table	9.8 <sup>e</sup>	0.038–0.045	0.7
	w = 1.25	$t = 0.090$	17–3	18.9 <sup>e</sup>	0.038–0.045	0.7
	Round	$d = \frac{1}{4}$	See	8.3 <sup>e</sup>	0.038–0.045	0.7
		$d = \frac{3}{8}$	Table	18.6 <sup>e</sup>	0.038–0.045	0.7
		$d = \frac{1}{2}$	17–3	33.0 <sup>e</sup>	0.038–0.045	0.7
		$d = \frac{3}{4}$		74.3 <sup>e</sup>	0.038–0.045	0.7

<sup>a</sup>Add 2 in to pulley size for belts 8 in wide or more.<sup>b</sup>Source: *Habasit Engineering Manual*, Habasit Belting, Inc., Chamblee (Atlanta), Ga.<sup>c</sup>Friction cover of acrylonitrile-butadiene rubber on both sides.<sup>d</sup>Source: Eagle Belting Co., Des Plaines, Ill.<sup>e</sup>At 6% elongation; 12% is maximum allowable value.**Table 17-3**Minimum Pulley Sizes for  
Flat and Round Urethane  
Belts. (Listed are the  
Pulley Diameters in  
Inches)Source: Eagle Belting Co.,  
Des Plaines, Ill.

Belt Style	Belt Size, in	Ratio of Pulley Speed to Belt Length, rev/(ft · min)		
		Up to 250	250 to 499	500 to 1000
Flat	0.50 × 0.062	0.38	0.44	0.50
	0.75 × 0.078	0.50	0.63	0.75
	1.25 × 0.090	0.50	0.63	0.75
Round	$\frac{1}{4}$	1.50	1.75	2.00
	$\frac{3}{8}$	2.25	2.62	3.00
	$\frac{1}{2}$	3.00	3.50	4.00
	$\frac{3}{4}$	5.00	6.00	7.00

**Table 17-4**

Pulley Correction Factor  $C_p$  for Flat Belts\*

Material	Small-Pulley Diameter, in					
	1.6 to 4	4.5 to 8	9 to 12.5	14, 16	18 to 31.5	Over 31.5
Leather	0.5	0.6	0.7	0.8	0.9	1.0
Polyamide, F-0	0.95	1.0	1.0	1.0	1.0	1.0
F-1	0.70	0.92	0.95	1.0	1.0	1.0
F-2	0.73	0.86	0.96	1.0	1.0	1.0
A-2	0.73	0.86	0.96	1.0	1.0	1.0
A-3	—	0.70	0.87	0.94	0.96	1.0
A-4	—	—	0.71	0.80	0.85	0.92
A-5	—	—	—	0.72	0.77	0.91

\*Average values of  $C_p$  for the given ranges were approximated from curves in the *Habasit Engineering Manual*, Habasit Belting, Inc., Chamblee (Atlanta), Ga.

**Table 17-5**

Crown Height and ISO  
Pulley Diameters for Flat  
Belts\*

ISO Pulley Diameter, in	Crown Height, in	ISO Pulley Diameter, in	Crown Height, in	
			$w \leq 10$ in	$w > 10$ in
1.6, 2, 2.5	0.012	12.5, 14	0.03	0.03
2.8, 3.15	0.012	12.5, 14	0.04	0.04
3.55, 4, 4.5	0.012	22.4, 25, 28	0.05	0.05
5, 5.6	0.016	31.5, 35.5	0.05	0.06
6.3, 7.1	0.020	40	0.05	0.06
8, 9	0.024	45, 50, 56	0.06	0.08
10, 11.2	0.030	63, 71, 80	0.07	0.10

\*Crown should be rounded, not angled; maximum roughness is  $R_a = AA\ 63\ \mu\text{in}$ .

**EXAMPLE 17-1**

A polyamide A-3 flat belt 6 in wide is used to transmit 15 hp under light shock conditions where  $K_s = 1.25$ , and a factor of safety equal to or greater than 1.1 is appropriate. The pulley rotational axes are parallel and in the horizontal plane. The shafts are 8 ft apart. The 6-in driving pulley rotates at 1750 rev/min in such a way that the loose side is on top. The driven pulley is 18 in in diameter. See Fig. 17-10. The factor of safety is for unquantifiable exigencies.

- Estimate the centrifugal tension  $F_c$  and the torque  $T$ .
- Estimate the allowable  $F_1$ ,  $F_2$ ,  $F_i$  and allowable power  $H_a$ .
- Estimate the factor of safety. Is it satisfactory?

**Figure 17-10**

The flat-belt drive of Ex. 17-1.



**Solution** (a) Eq. (17-1):  $\phi = \theta_d = \pi - 2 \sin^{-1} \left[ \frac{18 - 6}{2(8)12} \right] = 3.0165 \text{ rad}$

$$\exp(f\phi) = \exp[0.8(3.0165)] = 11.17$$

$$V = \pi(6)1750/12 = 2749 \text{ ft/min}$$

Table 17-2:  $w = 12\gamma bt = 12(0.042)6(0.130) = 0.393 \text{ lbf/ft}$

**Answer** Eq. (e):  $F_c = \frac{w}{g} \left( \frac{V}{60} \right)^2 = \frac{0.393}{32.17} \left( \frac{2749}{60} \right)^2 = 25.6 \text{ lbf}$

$$T = \frac{63\,025 H_{\text{nom}} K_s n_d}{n} = \frac{63\,025(15)1.25(1.1)}{1750}$$

**Answer**  $= 742.8 \text{ lbf} \cdot \text{in}$

(b) The necessary  $(F_1)_a - F_2$  to transmit the torque  $T$ , from Eq. (h), is

$$(F_1)_a - F_2 = \frac{2T}{d} = \frac{2(742.8)}{6} = 247.6 \text{ lbf}$$

From Table 17-2  $F_a = 100 \text{ lbf}$ . For polyamide belts  $C_v = 1$ , and from Table 17-4  $C_p = 0.70$ . From Eq. (17-12) the allowable largest belt tension  $(F_1)_a$  is

**Answer**  $(F_1)_a = b F_a C_p C_v = 6(100)0.70(1) = 420 \text{ lbf}$

then

**Answer**  $F_2 = (F_1)_a - [(F_1)_a - F_2] = 420 - 247.6 = 172.4 \text{ lbf}$

and from Eq. (i)

$$F_i = \frac{(F_1)_a + F_2}{2} - F_c = \frac{420 + 172.4}{2} - 25.6 = 270.6 \text{ lbf}$$

**Answer** The combination  $(F_1)_a$ ,  $F_2$ , and  $F_i$  will transmit the design power of  $15(1.25)(1.1) = 20.6 \text{ hp}$  and protect the belt. We check the friction development by solving Eq. (17-7) for  $f'$ :

$$f' = \frac{1}{\phi} \ln \frac{(F_1)_a - F_c}{F_2 - F_c} = \frac{1}{3.0165} \ln \frac{420 - 25.6}{172.4 - 25.6} = 0.328$$

From Table 17-2,  $f = 0.8$ . Since  $f' < f$ , that is,  $0.328 < 0.80$ , there is no danger of slipping.

(c)

**Answer**  $n_{fs} = \frac{H}{H_{\text{nom}} K_s} = \frac{20.6}{15(1.25)} = 1.1 \quad (\text{as expected})$

**Answer** The belt is satisfactory and the maximum allowable belt tension exists. If the initial tension is maintained, the capacity is the design power of 20.6 hp.

Initial tension is the key to the functioning of the flat belt as intended. There are ways of controlling initial tension. One way is to place the motor and drive pulley on a pivoted mounting plate so that the weight of the motor, pulley, and mounting plate and a share of the belt weight induces the correct initial tension and maintains it. A second way is use of a spring-loaded idler pulley, adjusted to the same task. Both of these methods accommodate to temporary or permanent belt stretch. See Fig. 17–11.

Because flat belts were used for long center-to-center distances, the weight of the belt itself can provide the initial tension. The static belt deflects to an approximate catenary curve, and the dip from a straight belt can be measured against a stretched music wire. This provides a way of measuring and adjusting the dip. From catenary theory the dip is related to the initial tension by

$$d = \frac{12L^2w}{8F_i} = \frac{3L^2w}{2F_i} \quad (17-13)$$

where  $d = \text{dip, in}$

$L = \text{center-to-center distance, ft}$

$w = \text{weight per foot of the belt, lbf/ft}$

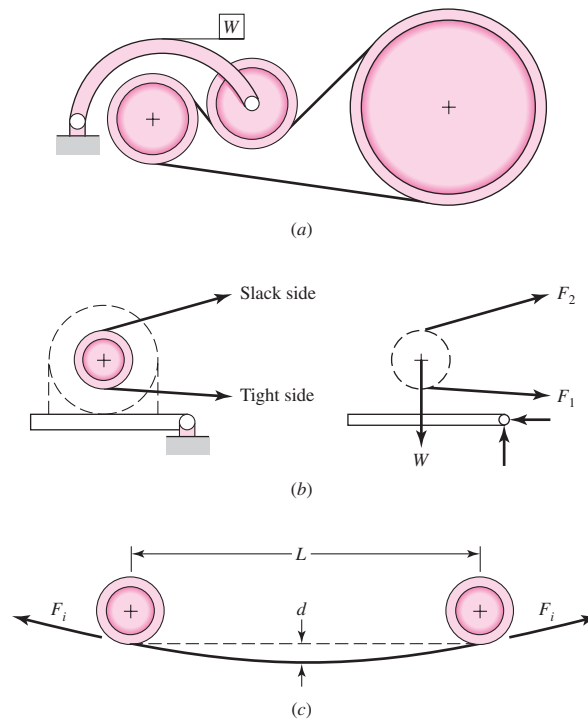
$F_i = \text{initial tension, lbf}$

In Ex. 17–1 the dip corresponding to a 270.6-lb initial tension is

$$d = \frac{3(8^2)0.393}{2(270.6)} = 0.14 \text{ in}$$

**Figure 17–11**

Belt-tensioning schemes.  
(a) Weighted idler pulley.  
(b) Pivoted motor mount.  
(c) Catenary-induced tension.





A decision set for a flat belt can be

- Function: power, speed, durability, reduction, service factor,  $C$
- Design factor:  $n_d$
- Initial tension maintenance
- Belt material
- Drive geometry,  $d, D$
- Belt thickness:  $t$
- Belt width:  $b$

Depending on the problem, some or all of the last four could be design variables. Belt cross-sectional area is really the design decision, but available belt thicknesses and widths are discrete choices. Available dimensions are found in suppliers' catalogs.

### EXAMPLE 17-2

Design a flat-belt drive to connect horizontal shafts on 16-ft centers. The velocity ratio is to be 2.25:1. The angular speed of the small driving pulley is 860 rev/min, and the nominal power transmission is to be 60 hp under very light shock.

#### Solution

- Function:  $H_{\text{nom}} = 60$  hp, 860 rev/min, 2.25:1 ratio,  $K_s = 1.15$ ,  $C = 16$  ft
- Design factor:  $n_d = 1.05$
- Initial tension maintenance: catenary
- Belt material: polyamide
- Drive geometry,  $d, D$
- Belt thickness:  $t$
- Belt width:  $b$

The last four could be design variables. Let's make a few more a priori decisions.

#### Decision

$d = 16$  in,  $D = 2.25d = 2.25(16) = 36$  in.

#### Decision

Use polyamide A-3 belt; therefore  $t = 0.13$  in and  $C_v = 1$ .  
Now there is one design decision remaining to be made, the belt width  $b$ .

Table 17-2:  $\gamma = 0.042$  lbf/in<sup>3</sup>       $f = 0.8$        $F_a = 100$  lbf/in at 600 rev/min

Table 17-4:  $C_p = 0.94$

Eq. (17-12):  $F_{1a} = b(100)0.94(1) = 94.0b$  lbf

(1)

$$H_d = H_{\text{nom}} K_s n_d = 60(1.15)1.05 = 72.5 \text{ hp}$$

$$T = \frac{63\,025 H_d}{n} = \frac{63\,025(72.5)}{860} = 5310 \text{ lbf} \cdot \text{in}$$

Estimate  $\exp(f\phi)$  for full friction development:

$$\text{Eq. (17-1):} \quad \phi = \theta_d = \pi - 2 \sin^{-1} \frac{36 - 16}{2(16)12} = 3.037 \text{ rad}$$

$$\exp(f\phi) = \exp[0.80(3.037)] = 11.35$$

Estimate centrifugal tension  $F_c$  in terms of belt width  $b$ :

$$w = 12\gamma bt = 12(0.042)b(0.13) = 0.0655b \text{ lbf/ft}$$

$$V = \pi dn/12 = \pi(16)860/12 = 3602 \text{ ft/min}$$

$$\text{Eq. (e): } F_c = \frac{w}{g} \left( \frac{V}{60} \right)^2 = \frac{0.0655b}{32.17} \left( \frac{3602}{60} \right)^2 = 7.34b \text{ lbf} \quad (2)$$

For design conditions, that is, at  $H_d$  power level, using Eq. (h) gives

$$(F_1)_a - F_2 = 2T/d = 2(5310)/16 = 664 \text{ lbf} \quad (3)$$

$$F_2 = (F_1)_a - [(F_1)_a - F_2] = 94.0b - 664 \text{ lbf} \quad (4)$$

Using Eq. (i) gives

$$F_i = \frac{(F_1)_a + F_2}{2} - F_c = \frac{94.0b + 94.0b - 664}{2} - 7.34b = 86.7b - 332 \text{ lbf} \quad (5)$$

Place friction development at its highest level, using Eq. (17-7):

$$f\phi = \ln \frac{(F_1)_a - F_c}{F_2 - F_c} = \ln \frac{94.0b - 7.34b}{94.0b - 664 - 7.34b} = \ln \frac{86.7b}{86.7b - 664}$$

Solving the preceding equation for belt width  $b$  at which friction is fully developed gives

$$b = \frac{664}{86.7} \frac{\exp(f\phi)}{\exp(f\phi) - 1} = \frac{664}{86.7} \frac{11.38}{11.38 - 1} = 8.40 \text{ in}$$

A belt width greater than 8.40 in will develop friction less than  $f = 0.80$ . The manufacturer's data indicate that the next available larger width is 10-in.

### Decision

Use 10-in-wide belt.

It follows that for a 10-in-wide belt

$$\text{Eq. (2): } F_c = 7.34(10) = 73.4 \text{ lbf}$$

$$\text{Eq. (1): } (F_1)_a = 94(10) = 940 \text{ lbf}$$

$$\text{Eq. (4): } F_2 = 94(10) - 664 = 276 \text{ lbf}$$

$$\text{Eq. (5): } F_i = 86.7(10) - 332 = 535 \text{ lbf}$$

The transmitted power, from Eq. (3), is

$$H_t = \frac{[(F_1)_a - F_2]V}{33\,000} = \frac{664(3602)}{33\,000} = 72.5 \text{ hp}$$

and the level of friction development  $f'$ , from Eq. (17-7) is

$$f' = \frac{1}{\phi} \ln \frac{(F_1)_a - F_c}{F_2 - F_c} = \frac{1}{3.037} \ln \frac{940 - 73.4}{276 - 73.4} = 0.479$$

which is less than  $f = 0.8$ , and thus is satisfactory. Had a 9-in belt width been available, the analysis would show  $(F_1)_a = 846$  lbf,  $F_2 = 182$  lbf,  $F_i = 448$  lbf, and  $f' = 0.63$ . With a figure of merit available reflecting cost, thicker belts (A-4 or A-5) could be examined to ascertain which of the satisfactory alternatives is best. From Eq. (17-13) the catenary dip is

$$d = \frac{3L^2w}{2F_i} = \frac{3(15^2)0.0655(10)}{2(535)} = 0.413 \text{ in}$$

**Figure 17-12**

Flat-belt tensions.

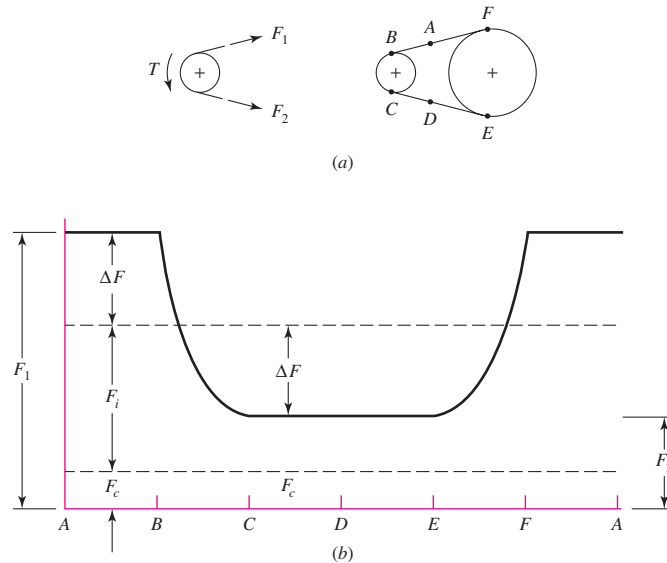


Figure 17-12 illustrates the variation of flexible flat-belt tensions at some cardinal points during a belt pass.

### Flat Metal Belts

Thin flat metal belts with their attendant strength and geometric stability could not be fabricated until laser welding and thin rolling technology made possible belts as thin as 0.002 in and as narrow as 0.026 in. The introduction of perforations allows no-slip applications. Thin metal belts exhibit

- High strength-to-weight ratio
- Dimensional stability
- Accurate timing
- Usefulness to temperatures up to 700°F
- Good electrical and thermal conduction properties

In addition, stainless steel alloys offer “inert,” nonabsorbent belts suitable to hostile (corrosive) environments, and can be made sterile for food and pharmaceutical applications.

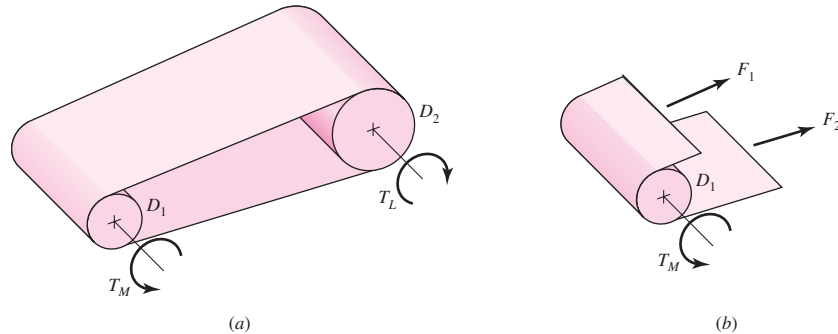
Thin metal belts can be classified as friction drives, timing or positioning drives, or tape drives. Among friction drives are plain, metal-coated, and perforated belts. Crowned pulleys are used to compensate for tracking errors.

Figure 17-13 shows a thin flat metal belt with the tight tension  $F_1$  and the slack side tension  $F_2$  revealed. The relationship between  $F_1$  and  $F_2$  and the driving torque  $T$  is the same as in Eq. (h). Equations (17-9), (17-10), and (17-11) also apply. The largest allowable tension, as in Eq. (17-12), is posed in terms of stress in metal belts. A bending stress is created by making the belt conform to the pulley, and its tensile magnitude  $\sigma_b$  is given by

$$\sigma_b = \frac{Et}{(1 - \nu^2)D} = \frac{E}{(1 - \nu^2)(D/t)} \quad (17-14)$$

**Figure 17-13**

Metal-belt tensions and  
torques.



where  $E$  = Young's modulus

$t$  = belt thickness

$\nu$  = Poisson's ratio

$D$  = pulley diameter

The tensile stresses  $(\sigma)_1$  and  $(\sigma)_2$  imposed by the belt tensions  $F_1$  and  $F_2$  are

$$(\sigma)_1 = F_1/(bt) \quad \text{and} \quad (\sigma)_2 = F_2/(bt)$$

The largest tensile stress is  $(\sigma_b)_1 + F_1/(bt)$  and the smallest is  $(\sigma_b)_2 + F_2/(bt)$ . During a belt pass both levels of stress appear.

Although the belts are of simple geometry, the method of Marin is not used because the condition of the butt weldment (to form the loop) is not accurately known, and the testing of coupons is difficult. The belts are run to failure on two equal-sized pulleys. Information concerning fatigue life, as shown in Table 17-6, is obtainable. Tables 17-7 and 17-8 give additional information.

Table 17-6 shows metal belt life expectancies for a stainless steel belt. From Eq. (17-14) with  $E = 28$  Mpsi and  $\nu = 0.29$ , the bending stresses corresponding to the four entries of the table are 48 914, 76 428, 91 805, and 152 855 psi. Using a natural log transformation on stress and passes shows that the regression line ( $r = -0.96$ ) is

$$\sigma = 14\,169\,982N_p^{-0.407} = 14.17(10^6)N_p^{-0.407} \quad (17-15)$$

where  $N_p$  is the number of belt passes.

**Table 17-6**

Belt Life for Stainless  
Steel Friction Drives\*

$\frac{D}{t}$	Belt Passes
625	$\geq 10^6$
400	$0.500 \cdot 10^6$
333	$0.165 \cdot 10^6$
200	$0.085 \cdot 10^6$

\*Data courtesy of Belt  
Technologies, Agawam, Mass.

**Table 17-7**Minimum Pulley  
Diameter\*

Belt Thickness, in	Minimum Pulley Diameter, in
0.002	1.2
0.003	1.8
0.005	3.0
0.008	5.0
0.010	6.0
0.015	10
0.020	12.5
0.040	25.0

\*Data courtesy of Belt Technologies, Agawam, Mass.

**Table 17-8**Typical Material  
Properties, Metal Belts\*

Alloy	Yield Strength, kpsi	Young's Modulus, Mpsi	Poisson's Ratio
301 or 302 stainless steel	175	28	0.285
BeCu	170	17	0.220
1075 or 1095 carbon steel	230	30	0.287
Titanium	150	15	—
Inconel	160	30	0.284

\*Data courtesy of Belt Technologies, Agawam, Mass.

The selection of a metal flat belt can consist of the following steps:

- 1 Find  $\exp(f\phi)$  from geometry and friction
- 2 Find endurance strength

$$S_f = 14.17(10^6)N_p^{-0.407} \quad \text{301, 302 stainless}$$

$$S_f = S_y/3 \quad \text{others}$$

- 3 Allowable tension

$$F_{1a} = \left[ S_f - \frac{Et}{(1 - \nu^2)D} \right] tb = ab$$

- 4  $\Delta F = 2T/D$

$$F_2 = F_{1a} - \Delta F = ab - \Delta F$$

$$F_i = \frac{F_{1a} + F_2}{2} = \frac{ab + ab - \Delta F}{2} = ab - \frac{\Delta F}{2}$$

$$b_{\min} = \frac{\Delta F}{a} \frac{\exp(f\phi)}{\exp(f\phi) - 1}$$

- 8 Choose  $b > b_{\min}$ ,  $F_1 = ab$ ,  $F_2 = ab - \Delta F$ ,  $F_i = ab - \Delta F/2$ ,  $T = \Delta F D/2$

9 Check frictional development  $f'$ :

$$f' = \frac{1}{\phi} \ln \frac{F_1}{F_2} \quad f' < f$$

### EXAMPLE 17-3

A friction-drive stainless steel metal belt runs over two 4-in metal pulleys ( $f = 0.35$ ). The belt thickness is to be 0.003 in. For a life exceeding  $10^6$  belt passes with smooth torque ( $K_s = 1$ ), (a) select the belt if the torque is to be 30 lbf · in, and (b) find the initial tension  $F_i$ .

**Solution** (a) From step 1,  $\phi = \theta_d = \pi$ , therefore  $\exp(0.35\pi) = 3.00$ . From step 2,

$$(S_f)_{10^6} = 14.17(10^6)(10^6)^{-0.407} = 51\,210 \text{ psi}$$

From steps 3, 4, 5, and 6,

$$F_{1a} = \left[ 51\,210 - \frac{28(10^6)0.003}{(1 - 0.285^2)4} \right] 0.003b = 85.1b \text{ lbf} \quad (1)$$

$$\Delta F = 2T/D = 2(30)/4 = 15 \text{ lbf}$$

$$F_2 = F_{1a} - \Delta F = 85.1b - 15 \text{ lbf} \quad (2)$$

$$F_i = \frac{F_{1a} + F_2}{2} = \frac{85.1b + 15}{2} \text{ lbf} \quad (3)$$

From step 7,

$$b_{\min} = \frac{\Delta F}{a} \frac{\exp(f\phi)}{\exp(f\phi) - 1} = \frac{15}{85.1} \frac{3.00}{3.00 - 1} = 0.264 \text{ in}$$

**Decision** Select an available 0.75-in-wide belt 0.003 in thick.

$$\text{Eq. (1):} \quad F_1 = 85.1(0.75) = 63.8 \text{ lbf}$$

$$\text{Eq. (2):} \quad F_2 = 85.1(0.75) - 15 = 48.8 \text{ lbf}$$

$$\text{Eq. (3):} \quad F_i = (63.8 + 48.8)/2 = 56.3 \text{ lbf}$$

$$f' = \frac{1}{\phi} \ln \frac{F_1}{F_2} = \frac{1}{\pi} \ln \frac{63.8}{48.8} = 0.0853$$

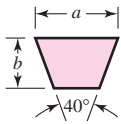
Note  $f' < f$ , that is,  $0.0853 < 0.35$ .

## 17-3 V Belts

The cross-sectional dimensions of V belts have been standardized by manufacturers, with each section designated by a letter of the alphabet for sizes in inch dimensions. Metric sizes are designated in numbers. Though these have not been included here, the procedure for analyzing and designing them is the same as presented here. Dimensions, minimum sheave diameters, and the horsepower range for each of the lettered sections are listed in Table 17-9.

**Table 17-9**

Standard V-Belt Sections



Belt Section	Width $a$ , in	Thickness $b$ , in	Minimum Sheave Diameter, in	hp Range, One or More Belts
A	$\frac{1}{2}$	$\frac{11}{32}$	3.0	$\frac{1}{4}$ –10
B	$\frac{21}{32}$	$\frac{7}{16}$	5.4	1–25
C	$\frac{7}{8}$	$\frac{17}{32}$	9.0	15–100
D	$1\frac{1}{4}$	$\frac{3}{4}$	13.0	50–250
E	$1\frac{1}{2}$	1	21.6	100 and up

**Table 17-10**Inside Circumferences of  
Standard V Belts

Section	Circumference, in
A	26, 31, 33, 35, 38, 42, 46, 48, 51, 53, 55, 57, 60, 62, 64, 66, 68, 71, 75, 78, 80, 85, 90, 96, 105, 112, 120, 128
B	35, 38, 42, 46, 48, 51, 53, 55, 57, 60, 62, 64, 65, 66, 68, 71, 75, 78, 79, 81, 83, 85, 90, 93, 97, 100, 103, 105, 112, 120, 128, 131, 136, 144, 158, 173, 180, 195, 210, 240, 270, 300
C	51, 60, 68, 75, 81, 85, 90, 96, 105, 112, 120, 128, 136, 144, 158, 162, 173, 180, 195, 210, 240, 270, 300, 330, 360, 390, 420
D	120, 128, 144, 158, 162, 173, 180, 195, 210, 240, 270, 300, 330, 360, 390, 420, 480, 540, 600, 660
E	180, 195, 210, 240, 270, 300, 330, 360, 390, 420, 480, 540, 600, 660

**Table 17-11**

Length Conversion Dimensions (Add the Listed Quantity to the Inside Circumference to Obtain the Pitch Length in Inches)

Belt section	A	B	C	D	E
Quantity to be added	1.3	1.8	2.9	3.3	4.5

To specify a V belt, give the belt-section letter, followed by the inside circumference in inches (standard circumferences are listed in Table 17-10). For example, B75 is a B-section belt having an inside circumference of 75 in.

Calculations involving the belt length are usually based on the pitch length. For any given belt section, the pitch length is obtained by adding a quantity to the inside circumference (Tables 17-10 and 17-11). For example, a B75 belt has a pitch length of 76.8 in. Similarly, calculations of the velocity ratios are made using the pitch diameters of the sheaves, and for this reason the stated diameters are usually understood to be the pitch diameters even though they are not always so specified.

The groove angle of a sheave is made somewhat smaller than the belt-section angle. This causes the belt to wedge itself into the groove, thus increasing friction. The exact value of this angle depends on the belt section, the sheave diameter, and the angle of contact. If it is made too much smaller than the belt, the force required to pull the belt out of the groove as the belt leaves the pulley will be excessive. Optimum values are given in the commercial literature.

The minimum sheave diameters have been listed in Table 17–9. For best results, a V belt should be run quite fast: 4000 ft/min is a good speed. Trouble may be encountered if the belt runs much faster than 5000 ft/min or much slower than 1000 ft/min.

The *pitch length*  $L_p$  and the center-to-center distance  $C$  are

$$L_p = 2C + \pi(D + d)/2 + (D - d)^2/(4C) \quad (17-16a)$$

$$C = 0.25 \left\{ \left[ L_p - \frac{\pi}{2}(D + d) \right] + \sqrt{\left[ L_p - \frac{\pi}{2}(D + d) \right]^2 - 2(D - d)^2} \right\} \quad (17-16b)$$

where  $D$  = pitch diameter of the large sheave and  $d$  = pitch diameter of the small sheave.

In the case of flat belts, there is virtually no limit to the center-to-center distance. Long center-to-center distances are not recommended for V belts because the excessive vibration of the slack side will shorten the belt life materially. In general, the center-to-center distance should be no greater than 3 times the sum of the sheave diameters and no less than the diameter of the larger sheave. Link-type V belts have less vibration, because of better balance, and hence may be used with longer center-to-center distances.

The basis for power ratings of V belts depends somewhat on the manufacturer; it is not often mentioned quantitatively in vendors' literature but is available from vendors. The basis may be a number of hours, 24 000, for example, or a life of  $10^8$  or  $10^9$  belt passes. Since the number of belts must be an integer, an undersized belt set that is augmented by one belt can be substantially oversized. Table 17–12 gives power ratings of standard V belts.

The rating, whether in terms of hours or belt passes, is for a belt running on equal-diameter sheaves ( $180^\circ$  of wrap), of moderate length, and transmitting a steady load. Deviations from these laboratory test conditions are acknowledged by multiplicative adjustments. If the tabulated power of a belt for a C-section belt is 9.46 hp for a 12-in-diameter sheave at a peripheral speed of 3000 ft/min (Table 17–12), then, when the belt is used under other conditions, the tabulated value  $H_{\text{tab}}$  is adjusted as follows:

$$H_a = K_1 K_2 H_{\text{tab}} \quad (17-17)$$

where  $H_a$  = allowable power, per belt, Table 17–12

$K_1$  = angle-of-wrap correction factor, Table 17–13

$K_2$  = belt length correction factor, Table 17–14

The allowable power can be near to  $H_{\text{tab}}$ , depending upon circumstances.

In a V belt the effective coefficient of friction  $f'$  is  $f/\sin(\phi/2)$ , which amounts to an augmentation by a factor of about 3 due to the grooves. The effective coefficient of friction  $f'$  is sometimes tabulated against *sheave* groove angles of  $30^\circ$ ,  $34^\circ$ , and  $38^\circ$ , the tabulated values being 0.50, 0.45, and 0.40, respectively, revealing a belt material-on-metal coefficient of friction of 0.13 for each case. The Gates Rubber Company declares its effective coefficient of friction to be 0.5123 for grooves. Thus

$$\frac{F_1 - F_c}{F_2 - F_c} = \exp(0.5123\phi) \quad (17-18)$$

The design power is given by

$$H_d = H_{\text{nom}} K_s n_d \quad (17-19)$$

where  $H_{\text{nom}}$  is the nominal power,  $K_s$  is the service factor given in Table 17–15, and  $n_d$  is the design factor. The number of belts,  $N_b$ , is usually the next higher integer to  $H_d/H_a$ .



**Table 17-12**Horsepower Ratings of  
Standard V Belts

Belt Section	Sheave Pitch Diameter, in	Belt Speed, ft/min				
		1000	2000	3000	4000	5000
A	2.6	0.47	0.62	0.53	0.15	
	3.0	0.66	1.01	1.12	0.93	0.38
	3.4	0.81	1.31	1.57	1.53	1.12
	3.8	0.93	1.55	1.92	2.00	1.71
	4.2	1.03	1.74	2.20	2.38	2.19
	4.6	1.11	1.89	2.44	2.69	2.58
	5.0 and up	1.17	2.03	2.64	2.96	2.89
B	4.2	1.07	1.58	1.68	1.26	0.22
	4.6	1.27	1.99	2.29	2.08	1.24
	5.0	1.44	2.33	2.80	2.76	2.10
	5.4	1.59	2.62	3.24	3.34	2.82
	5.8	1.72	2.87	3.61	3.85	3.45
	6.2	1.82	3.09	3.94	4.28	4.00
	6.6	1.92	3.29	4.23	4.67	4.48
C	7.0 and up	2.01	3.46	4.49	5.01	4.90
	6.0	1.84	2.66	2.72	1.87	
	7.0	2.48	3.94	4.64	4.44	3.12
	8.0	2.96	4.90	6.09	6.36	5.52
	9.0	3.34	5.65	7.21	7.86	7.39
	10.0	3.64	6.25	8.11	9.06	8.89
	11.0	3.88	6.74	8.84	10.0	10.1
D	12.0 and up	4.09	7.15	9.46	10.9	11.1
	10.0	4.14	6.13	6.55	5.09	1.35
	11.0	5.00	7.83	9.11	8.50	5.62
	12.0	5.71	9.26	11.2	11.4	9.18
	13.0	6.31	10.5	13.0	13.8	12.2
	14.0	6.82	11.5	14.6	15.8	14.8
	15.0	7.27	12.4	15.9	17.6	17.0
E	16.0	7.66	13.2	17.1	19.2	19.0
	17.0 and up	8.01	13.9	18.1	20.6	20.7
	16.0	8.68	14.0	17.5	18.1	15.3
	18.0	9.92	16.7	21.2	23.0	21.5
	20.0	10.9	18.7	24.2	26.9	26.4
	22.0	11.7	20.3	26.6	30.2	30.5
	24.0	12.4	21.6	28.6	32.9	33.8
	26.0	13.0	22.8	30.3	35.1	36.7
	28.0 and up	13.4	23.7	31.8	37.1	39.1

That is,

$$N_b \geq \frac{H_d}{H_a} \quad N_b = 1, 2, 3, \dots \quad (17-20)$$

Designers work on a per-belt basis.

The flat-belt tensions shown in Fig. 17-12 ignored the tension induced by bending the belt about the pulleys. This is more pronounced with V belts, as shown in Fig. 17-14.

The centrifugal tension  $F_c$  is given by

$$F_c = K_c \left( \frac{V}{1000} \right)^2 \quad (17-21)$$

where  $K_c$  is from Table 17-16.

**Table 17-13**

Angle of Contact  
Correction Factor  $K_1$  for  
VV\* and V-Flat Drives

$\frac{D-d}{C}$	$\theta$ , deg	VV	$K_1$ V Flat
0.00	180	1.00	0.75
0.10	174.3	0.99	0.76
0.20	166.5	0.97	0.78
0.30	162.7	0.96	0.79
0.40	156.9	0.94	0.80
0.50	151.0	0.93	0.81
0.60	145.1	0.91	0.83
0.70	139.0	0.89	0.84
0.80	132.8	0.87	0.85
0.90	126.5	0.85	0.85
1.00	120.0	0.82	0.82
1.10	113.3	0.80	0.80
1.20	106.3	0.77	0.77
1.30	98.9	0.73	0.73
1.40	91.1	0.70	0.70
1.50	82.8	0.65	0.65

\*A curvefit for the VV column in terms of  $\theta$  is  
 $K_1 = 0.143\,543 + 0.007\,46\,8\,\theta - 0.000\,015\,052\,\theta^2$   
in the range  $90^\circ \leq \theta \leq 180^\circ$ .

**Table 17-14**

Belt-Length Correction  
Factor  $K_2$ \*

Length Factor	Nominal Belt Length, in				
	A Belts	B Belts	C Belts	D Belts	E Belts
0.85	Up to 35	Up to 46	Up to 75	Up to 128	
0.90	38–46	48–60	81–96	144–162	Up to 195
0.95	48–55	62–75	105–120	173–210	210–240
1.00	60–75	78–97	128–158	240	270–300
1.05	78–90	105–120	162–195	270–330	330–390
1.10	96–112	128–144	210–240	360–420	420–480
1.15	120 and up	158–180	270–300	480	540–600
1.20		195 and up	330 and up	540 and up	660

\*Multiply the rated horsepower per belt by this factor to obtain the corrected horsepower.

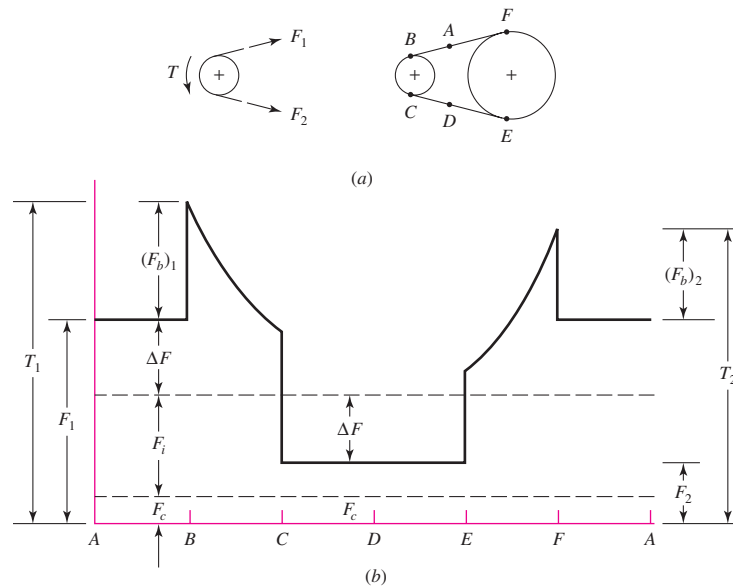
**Table 17-15**

Suggested Service  
Factors  $K_S$  for V-Belt  
Drives

Driven Machinery	Source of Power	
	Normal Torque Characteristic	High or Nonuniform Torque
Uniform	1.0 to 1.2	1.1 to 1.3
Light shock	1.1 to 1.3	1.2 to 1.4
Medium shock	1.2 to 1.4	1.4 to 1.6
Heavy shock	1.3 to 1.5	1.5 to 1.8

**Figure 17-14**

V-belt tensions.

**Table 17-16**

Some V-Belt Parameters\*

Belt Section	$K_b$	$K_c$
A	220	0.561
B	576	0.965
C	1 600	1.716
D	5 680	3.498
E	10 850	5.041
3V	230	0.425
5V	1098	1.217
8V	4830	3.288

\*Data courtesy of Gates Rubber Co., Denver, Colo.

The power that is transmitted per belt is based on  $\Delta F = F_1 - F_2$ , where

$$\Delta F = \frac{63\,025 H_d / N_b}{n(d/2)} \quad (17-22)$$

then from Eq. (17-8) the largest tension  $F_1$  is given by

$$F_1 = F_c + \frac{\Delta F \exp(f\phi)}{\exp(f\phi) - 1} \quad (17-23)$$

From the definition of  $\Delta F$ , the least tension  $F_2$  is

$$F_2 = F_1 - \Delta F \quad (17-24)$$

From Eq. (j) in Sec. 17-2

$$F_i = \frac{F_1 + F_2}{2} - F_c \quad (17-25)$$

The factor of safety is

$$n_{fs} = \frac{H_a N_b}{H_{\text{nom}} K_s} \quad (17-26)$$

Durability (life) correlations are complicated by the fact that the bending induces flexural stresses in the belt; the corresponding belt tension that induces the same maximum tensile stress is  $F_{b1}$  at the driving sheave and  $F_{b2}$  at the driven pulley. These equivalent tensions are added to  $F_1$  as

$$T_1 = F_1 + (F_b)_1 = F_1 + \frac{K_b}{d}$$

$$T_2 = F_1 + (F_b)_2 = F_1 + \frac{K_b}{D}$$

where  $K_b$  is given in Table 17–16. The equation for the tension versus pass trade-off used by the Gates Rubber Company is of the form

$$T^b N_P = K^b$$

where  $N_P$  is the number of passes and  $b$  is approximately 11. See Table 17–17. The Miner rule is used to sum damage incurred by the two tension peaks:

$$\frac{1}{N_P} = \left(\frac{K}{T_1}\right)^{-b} + \left(\frac{K}{T_2}\right)^{-b}$$

or

$$N_P = \left[ \left(\frac{K}{T_1}\right)^{-b} + \left(\frac{K}{T_2}\right)^{-b} \right]^{-1} \quad (17-27)$$

The lifetime  $t$  in hours is given by

$$t = \frac{N_P L_P}{720V} \quad (17-28)$$

**Table 17-17**

Durability Parameters for  
Some V-Belt Sections

Source: M. E. Spotts, *Design  
of Machine Elements*, 6th ed.  
Prentice Hall, Englewood  
Cliffs, N.J., 1985.

Belt Section	10 <sup>8</sup> to 10 <sup>9</sup> Force Peaks		10 <sup>9</sup> to 10 <sup>10</sup> Force Peaks		Minimum Sheave Diameter, in
	K	b	K	b	
A	674	11.089			3.0
B	1193	10.926			5.0
C	2038	11.173			8.5
D	4208	11.105			13.0
E	6061	11.100			21.6
3V	728	12.464	1062	10.153	2.65
5V	1654	12.593	2394	10.283	7.1
8V	3638	12.629	5253	10.319	12.5

The constants  $K$  and  $b$  have their ranges of validity. If  $N_P > 10^9$ , report that  $N_P = 10^9$  and  $t > N_P L_P / (720V)$  without placing confidence in numerical values beyond the validity interval. See the statement about  $N_P$  and  $t$  near the conclusion of Ex. 17-4.

The analysis of a V-belt drive can consist of the following steps:

- Find  $V$ ,  $L_P$ ,  $C$ ,  $\phi$ , and  $\exp(0.5123\phi)$
- Find  $H_d$ ,  $H_a$ , and  $N_b$  from  $H_d/H_a$  and round up
- Find  $F_c$ ,  $\Delta F$ ,  $F_1$ ,  $F_2$ , and  $F_i$ , and  $n_{fs}$
- Find belt life in number of passes, or hours, if possible

### EXAMPLE 17-4

A 10-hp split-phase motor running at 1750 rev/min is used to drive a rotary pump, which operates 24 hours per day. An engineer has specified a 7.4-in small sheave, an 11-in large sheave, and three B112 belts. The service factor of 1.2 was augmented by 0.1 because of the continuous-duty requirement. Analyze the drive and estimate the belt life in passes and hours.

#### Solution

The peripheral speed  $V$  of the belt is

$$V = \pi dn/12 = \pi(7.4)1750/12 = 3390 \text{ ft/min}$$

Table 17-11:  $L_P = L + L_c = 112 + 1.8 = 113.8 \text{ in}$

$$\begin{aligned} \text{Eq. (17-16b): } C &= 0.25 \left\{ \left[ 113.8 - \frac{\pi}{2}(11 + 7.4) \right] \right. \\ &\quad \left. + \sqrt{\left[ 113.8 - \frac{\pi}{2}(11 + 7.4) \right]^2 - 2(11 - 7.4)^2} \right\} \\ &= 42.4 \text{ in} \end{aligned}$$

$$\begin{aligned} \text{Eq. (17-1): } \phi = \theta_d &= \pi - 2 \sin^{-1}(11 - 7.4)/[2(42.4)] = 3.057 \text{ rad} \\ \exp[0.5123(3.057)] &= 4.788 \end{aligned}$$

Interpolating in Table 17-12 for  $V = 3390 \text{ ft/min}$  gives  $H_{\text{tab}} = 4.693 \text{ hp}$ . The wrap angle in degrees is  $3.057(180)/\pi = 175^\circ$ . From Table 17-13,  $K_1 = 0.99$ . From Table 17-14,  $K_2 = 1.05$ . Thus, from Eq. (17-17),

$$H_a = K_1 K_2 H_{\text{tab}} = 0.99(1.05)4.693 = 4.878 \text{ hp}$$

$$\text{Eq. (17-19): } H_d = H_{\text{nom}} K_s n_d = 10(1.2 + 0.1)(1) = 13 \text{ hp}$$

$$\text{Eq. (17-20): } N_b \geq H_d/H_a = 13/4.878 = 2.67 \rightarrow 3$$

From Table 17-16,  $K_c = 0.965$ . Thus, from Eq. (17-21),

$$F_c = 0.965(3390/1000)^2 = 11.1 \text{ lbf}$$

$$\text{Eq. (17-22): } \Delta F = \frac{63\,025(13)/3}{1750(7.4/2)} = 42.2 \text{ lbf}$$

$$\text{Eq. (17-23): } F_1 = 11.1 + \frac{42.2(4.788)}{4.788 - 1} = 64.4 \text{ lbf}$$

$$\text{Eq. (17-24):} \quad F_2 = F_1 - \Delta F = 64.4 - 42.2 = 22.2 \text{ lbf}$$

$$\text{Eq. (17-25):} \quad F_i = \frac{64.4 + 22.2}{2} - 11.1 = 32.2 \text{ lbf}$$

$$\text{Eq. (17-26):} \quad n_{fs} = \frac{H_a N_b}{H_{\text{nom}} K_s} = \frac{4.878(3)}{10(1.3)} = 1.13$$

Life: From Table 17-16,  $K_b = 576$ .

$$F_{b1} = \frac{K_b}{d} = \frac{576}{7.4} = 77.8 \text{ lbf}$$

$$F_{b2} = \frac{576}{11} = 52.4 \text{ lbf}$$

$$T_1 = F_1 + F_{b1} = 64.4 + 77.8 = 142.2 \text{ lbf}$$

$$T_2 = F_1 + F_{b2} = 64.4 + 52.4 = 116.8 \text{ lbf}$$

From Table 17-17,  $K = 1193$  and  $b = 10.926$ .

$$\text{Eq. (17-27):} \quad N_P = \left[ \left( \frac{1193}{142.2} \right)^{-10.926} + \left( \frac{1193}{116.8} \right)^{-10.926} \right]^{-1} = 11(10^9) \text{ passes}$$

**Answer** Since  $N_P$  is out of the validity range of Eq. (17-27), life is reported as greater than  $10^9$  passes. Then

$$\text{Answer Eq. (17-28):} \quad t > \frac{10^9(113.8)}{720(3390)} = 46\,600 \text{ h}$$

## 17-4 Timing Belts

A timing belt is made of a rubberized fabric coated with a nylon fabric, and has steel wire within to take the tension load. It has teeth that fit into grooves cut on the periphery of the pulleys (Fig. 17-15). A timing belt does not stretch appreciably or slip and consequently transmits power at a constant angular-velocity ratio. No initial tension is needed.

**Figure 17-15**

Timing-belt drive showing portions of the pulley and belt. Note that the pitch diameter of the pulley is greater than the diametral distance across the top lands of the teeth.

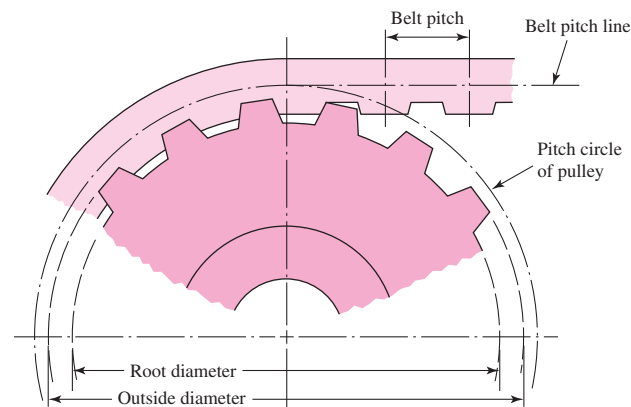


**Table 17-18**Standard Pitches  
of Timing Belts

Service	Designation	Pitch $p$ , in
Extra light	XL	$\frac{1}{5}$
Light	L	$\frac{3}{8}$
Heavy	H	$\frac{1}{2}$
Extra heavy	XH	$\frac{7}{8}$
Double extra heavy	XXH	$1\frac{1}{4}$

Such belts can operate over a very wide range of speeds, have efficiencies in the range of 97 to 99 percent, require no lubrication, and are quieter than chain drives. There is no chordal-speed variation, as in chain drives (see Sec. 17-5), and so they are an attractive solution for precision-drive requirements.

The steel wire, the tension member of a timing belt, is located at the belt pitch line (Fig. 17-15). Thus the pitch length is the same regardless of the thickness of the backing.

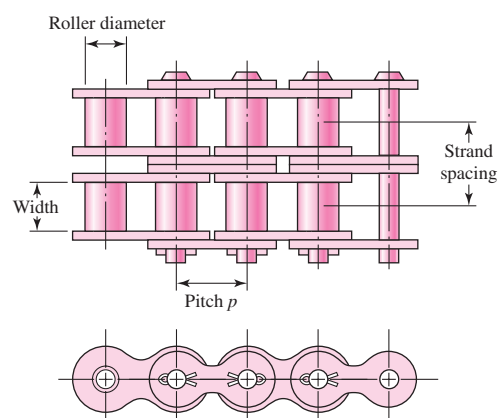
The five standard inch-series pitches available are listed in Table 17-18 with their letter designations. Standard pitch lengths are available in sizes from 6 to 180 in. Pulleys come in sizes from 0.60 in pitch diameter up to 35.8 in and with groove numbers from 10 to 120.

The design and selection process for timing belts is so similar to that for V belts that the process will not be presented here. As in the case of other belt drives, the manufacturers will provide an ample supply of information and details on sizes and strengths.

## 17-5 Roller Chain

Basic features of chain drives include a constant ratio, since no slippage or creep is involved; long life; and the ability to drive a number of shafts from a single source of power.

Roller chains have been standardized as to sizes by the ANSI. Figure 17-16 shows the nomenclature. The pitch is the linear distance between the centers of the rollers. The width is the space between the inner link plates. These chains are manufactured in single, double, triple, and quadruple strands. The dimensions of standard sizes are listed in Table 17-19.

**Figure 17-16**Portion of a double-strand  
roller chain.

**Table 17-19**

 Dimensions of American  
 Standard Roller  
 Chains—Single Strand

 Source: Compiled from ANSI  
 B29.1-1975.

ANSI Chain Number	Pitch, in (mm)	Width, in (mm)	Minimum Tensile Strength, lbf (N)	Average Weight, lbf/ft (N/m)	Roller Diameter, in (mm)	Multiple- Strand Spacing, in (mm)
25	0.250 (6.35)	0.125 (3.18)	780 (3 470)	0.09 (1.31)	0.130 (3.30)	0.252 (6.40)
35	0.375 (9.52)	0.188 (4.76)	1 760 (7 830)	0.21 (3.06)	0.200 (5.08)	0.399 (10.13)
41	0.500 (12.70)	0.25 (6.35)	1 500 (6 670)	0.25 (3.65)	0.306 (7.77)	— —
40	0.500 (12.70)	0.312 (7.94)	3 130 (13 920)	0.42 (6.13)	0.312 (7.92)	0.566 (14.38)
50	0.625 (15.88)	0.375 (9.52)	4 880 (21 700)	0.69 (10.1)	0.400 (10.16)	0.713 (18.11)
60	0.750 (19.05)	0.500 (12.7)	7 030 (31 300)	1.00 (14.6)	0.469 (11.91)	0.897 (22.78)
80	1.000 (25.40)	0.625 (15.88)	12 500 (55 600)	1.71 (25.0)	0.625 (15.87)	1.153 (29.29)
100	1.250 (31.75)	0.750 (19.05)	19 500 (86 700)	2.58 (37.7)	0.750 (19.05)	1.409 (35.76)
120	1.500 (38.10)	1.000 (25.40)	28 000 (124 500)	3.87 (56.5)	0.875 (22.22)	1.789 (45.44)
140	1.750 (44.45)	1.000 (25.40)	38 000 (169 000)	4.95 (72.2)	1.000 (25.40)	1.924 (48.87)
160	2.000 (50.80)	1.250 (31.75)	50 000 (222 000)	6.61 (96.5)	1.125 (28.57)	2.305 (58.55)
180	2.250 (57.15)	1.406 (35.71)	63 000 (280 000)	9.06 (132.2)	1.406 (35.71)	2.592 (65.84)
200	2.500 (63.50)	1.500 (38.10)	78 000 (347 000)	10.96 (159.9)	1.562 (39.67)	2.817 (71.55)
240	3.00 (76.70)	1.875 (47.63)	112 000 (498 000)	16.4 (239)	1.875 (47.62)	3.458 (87.83)

Figure 17-17 shows a sprocket driving a chain and rotating in a counterclockwise direction. Denoting the chain pitch by  $p$ , the pitch angle by  $\gamma$ , and the pitch diameter of the sprocket by  $D$ , from the trigonometry of the figure we see

$$\sin \frac{\gamma}{2} = \frac{p/2}{D/2} \quad \text{or} \quad D = \frac{p}{\sin(\gamma/2)} \quad (a)$$

Since  $\gamma = 360^\circ/N$ , where  $N$  is the number of sprocket teeth, Eq. (a) can be written

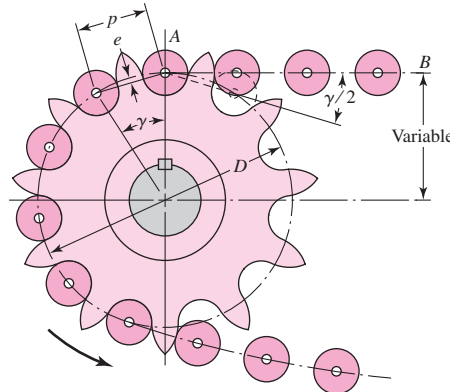
$$D = \frac{p}{\sin(180^\circ/N)} \quad (17-29)$$

The angle  $\gamma/2$ , through which the link swings as it enters contact, is called the *angle of articulation*. It can be seen that the magnitude of this angle is a function of the number of teeth. Rotation of the link through this angle causes impact between the



**Figure 17-17**

Engagement of a chain and sprocket.



rollers and the sprocket teeth and also wear in the chain joint. Since the life of a properly selected drive is a function of the wear and the surface fatigue strength of the rollers, it is important to reduce the angle of articulation as much as possible.

The number of sprocket teeth also affects the velocity ratio during the rotation through the pitch angle  $\gamma$ . At the position shown in Fig. 17-17, the chain  $AB$  is tangent to the pitch circle of the sprocket. However, when the sprocket has turned an angle of  $\gamma/2$ , the chain line  $AB$  moves closer to the center of rotation of the sprocket. This means that the chain line  $AB$  is moving up and down, and that the lever arm varies with rotation through the pitch angle, all resulting in an uneven chain exit velocity. You can think of the sprocket as a polygon in which the exit velocity of the chain depends upon whether the exit is from a corner, or from a flat of the polygon. Of course, the same effect occurs when the chain first enters into engagement with the sprocket.

The chain velocity  $V$  is defined as the number of feet coming off the sprocket per unit time. Thus the chain velocity in feet per minute is

$$V = \frac{Npn}{12} \quad (17-30)$$

where  $N$  = number of sprocket teeth

$p$  = chain pitch, in

$n$  = sprocket speed, rev/min

The maximum exit velocity of the chain is

$$v_{\max} = \frac{\pi Dn}{12} = \frac{\pi np}{12 \sin(\gamma/2)} \quad (b)$$

where Eq. (a) has been substituted for the pitch diameter  $D$ . The minimum exit velocity occurs at a diameter  $d$ , smaller than  $D$ . Using the geometry of Fig. 17-17, we find

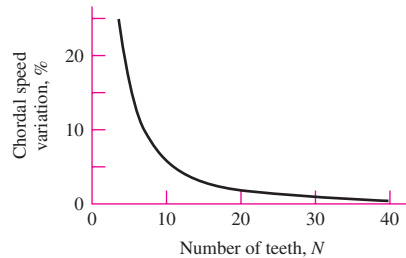
$$d = D \cos \frac{\gamma}{2} \quad (c)$$

Thus the minimum exit velocity is

$$v_{\min} = \frac{\pi dn}{12} = \frac{\pi np \cos(\gamma/2)}{12 \sin(\gamma/2)} \quad (d)$$

Now substituting  $\gamma/2 = 180^\circ/N$  and employing Eqs. (17-30), (b), and (d), we find the

| Figure 17-18



speed variation to be

$$\frac{\Delta V}{V} = \frac{v_{\max} - v_{\min}}{V} = \frac{\pi}{N} \left[ \frac{1}{\sin(180^\circ/N)} - \frac{1}{\tan(180^\circ/N)} \right] \quad (17-31)$$

This is called the *chordal speed variation* and is plotted in Fig. 17-18. When chain drives are used to synchronize precision components or processes, due consideration must be given to these variations. For example, if a chain drive synchronized the cutting of photographic film with the forward drive of the film, the lengths of the cut sheets of film might vary too much because of this chordal speed variation. Such variations can also cause vibrations within the system.

Although a large number of teeth is considered desirable for the driving sprocket, in the usual case it is advantageous to obtain as small a sprocket as possible, and this requires one with a small number of teeth. For smooth operation at moderate and high speeds it is considered good practice to use a driving sprocket with at least 17 teeth; 19 or 21 will, of course, give a better life expectancy with less chain noise. Where space limitations are severe or for very slow speeds, smaller tooth numbers may be used by sacrificing the life expectancy of the chain.

Driven sprockets are not made in standard sizes over 120 teeth, because the pitch elongation will eventually cause the chain to “ride” high long before the chain is worn out. The most successful drives have velocity ratios up to 6:1, but higher ratios may be used at the sacrifice of chain life.

Roller chains seldom fail because they lack tensile strength; they more often fail because they have been subjected to a great many hours of service. Actual failure may be due either to wear of the rollers on the pins or to fatigue of the surfaces of the rollers. Roller-chain manufacturers have compiled tables that give the horsepower capacity corresponding to a life expectancy of 15 kh for various sprocket speeds. These capacities are tabulated in Table 17-20 for 17-tooth sprockets. Table 17-21 displays available tooth counts on sprockets of one supplier. Table 17-22 lists the tooth correction factors for other than 17 teeth. Table 17-23 shows the multiple-strand factors  $K_2$ .

The capacities of chains are based on the following:

- 15 000 h at full load
- Single strand
- ANSI proportions
- Service factor of unity
- 100 pitches in length
- Recommended lubrication
- Elongation maximum of 3 percent

- Horizontal shafts
- Two 17-tooth sprockets

The fatigue strength of link plates governs capacity at lower speeds. The American Chain Association (ACA) publication *Chains for Power Transmission and Materials Handling* (1982) gives, for single-strand chain, the nominal power  $H_1$ , link-plate limited, as

$$H_1 = 0.004N_1^{1.08}n_1^{0.9}p^{(3-0.07p)} \quad \text{hp} \quad (17-32)$$

and the nominal power  $H_2$ , roller-limited, as

$$H_2 = \frac{1000K_rN_1^{1.5}p^{0.8}}{n_1^{1.5}} \quad \text{hp} \quad (17-33)$$

where  $N_1$  = number of teeth in the smaller sprocket

$n_1$  = sprocket speed, rev/min

$p$  = pitch of the chain, in

$K_r$  = 29 for chain numbers 25, 35; 3.4 for chain 41; and 17 for chains 40–240

**Table 17-20**

Rated Horsepower  
Capacity of Single-  
Strand Single-Pitch Roller  
Chain for a  
17-Tooth Sprocket

Source: Compiled from ANSI  
B29.1-1975 information  
only section, and from  
B29.9-1958.

Sprocket Speed, rev/min	ANSI Chain Number					
	25	35	40	41	50	60
50	0.05	0.16	0.37	0.20	0.72	1.24
100	0.09	0.29	0.69	0.38	1.34	2.31
150	0.13*	0.41*	0.99*	0.55*	1.92*	3.32
200	0.16*	0.54*	1.29	0.71	2.50	4.30
300	0.23	0.78	1.85	1.02	3.61	6.20
400	0.30*	1.01*	2.40	1.32	4.67	8.03
500	0.37	1.24	2.93	1.61	5.71	9.81
600	0.44*	1.46*	3.45*	1.90*	6.72*	11.6
700	0.50	1.68	3.97	2.18	7.73	13.3
800	0.56*	1.89*	4.48*	2.46*	8.71*	15.0
900	0.62	2.10	4.98	2.74	9.69	16.7
1000	0.68*	2.31*	5.48	3.01	10.7	18.3
1200	0.81	2.73	6.45	3.29	12.6	21.6
1400	0.93*	3.13*	7.41	2.61	14.4	18.1
1600	1.05*	3.53*	8.36	2.14	12.8	14.8
1800	1.16	3.93	8.96	1.79	10.7	12.4
2000	1.27*	4.32*	7.72*	1.52*	9.23*	10.6
2500	1.56	5.28	5.51*	1.10*	6.58*	7.57
3000	1.84	5.64	4.17	0.83	4.98	5.76
Type A		Type B			Type C	

\*Estimated from ANSI tables by linear interpolation.

Note: Type A—manual or drip lubrication; type B—bath or disk lubrication; type C—oil-stream lubrication.

(Continued)

**Table 17-20**

Rated Horsepower  
Capacity of Single-  
Strand Single-Pitch Roller  
Chain for a  
17-Tooth Sprocket  
(Continued)

Sprocket Speed, rev/min		ANSI Chain Number							
		80	100	120	140	160	180	200	240
50	Type A	2.88	5.52	9.33	14.4	20.9	28.9	38.4	61.8
100		5.38	10.3	17.4	26.9	39.1	54.0	71.6	115
150		7.75	14.8	25.1	38.8	56.3	77.7	103	166
200		10.0	19.2	32.5	50.3	72.9	101	134	215
300		14.5	27.7	46.8	72.4	105	145	193	310
400		18.7	35.9	60.6	93.8	136	188	249	359
500	Type B	22.9	43.9	74.1	115	166	204	222	0
600		27.0	51.7	87.3	127	141	155	169	
700		31.0	59.4	89.0	101	112	123	0	
800		35.0	63.0	72.8	82.4	91.7	101		
900		39.9	52.8	61.0	69.1	76.8	84.4		
1000		37.7	45.0	52.1	59.0	65.6	72.1		
1200		28.7	34.3	39.6	44.9	49.9	0		
1400		22.7	27.2	31.5	35.6	0			
1600		18.6	22.3	25.8	0				
1800		15.6	18.7	21.6					
2000		13.3	15.9	0					
2500		9.56	0.40						
3000		7.25	0						

**Type C**

**Type C'**

Note: Type A—manual or drip lubrication; type B—bath or disk lubrication; type C—oil-stream lubrication; type C'—type C, but this is a galling region; submit design to manufacturer for evaluation.

**Table 17-21**

Single-Strand Sprocket Tooth Counts Available from One Supplier\*

No.	Available Sprocket Tooth Counts
25	8-30, 32, 34, 35, 36, 40, 42, 45, 48, 54, 60, 64, 65, 70, 72, 76, 80, 84, 90, 95, 96, 102, 112, 120
35	4-45, 48, 52, 54, 60, 64, 65, 68, 70, 72, 76, 80, 84, 90, 95, 96, 102, 112, 120
41	6-60, 64, 65, 68, 70, 72, 76, 80, 84, 90, 95, 96, 102, 112, 120
40	8-60, 64, 65, 68, 70, 72, 76, 80, 84, 90, 95, 96, 102, 112, 120
50	8-60, 64, 65, 68, 70, 72, 76, 80, 84, 90, 95, 96, 102, 112, 120
60	8-60, 62, 63, 64, 65, 66, 67, 68, 70, 72, 76, 80, 84, 90, 95, 96, 102, 112, 120
80	8-60, 64, 65, 68, 70, 72, 76, 78, 80, 84, 90, 95, 96, 102, 112, 120
100	8-60, 64, 65, 67, 68, 70, 72, 74, 76, 80, 84, 90, 95, 96, 102, 112, 120
120	9-45, 46, 48, 50, 52, 54, 55, 57, 60, 64, 65, 67, 68, 70, 72, 76, 80, 84, 90, 96, 102, 112, 120
140	9-28, 30, 31, 32, 33, 34, 35, 36, 37, 39, 40, 42, 43, 45, 48, 54, 60, 64, 65, 68, 70, 72, 76, 80, 84, 96
160	8-30, 32–36, 38, 40, 45, 46, 50, 52, 53, 54, 56, 57, 60, 62, 63, 64, 65, 66, 68, 70, 72, 73, 80, 84, 96
180	13-25, 28, 35, 39, 40, 45, 54, 60
200	9-30, 32, 33, 35, 36, 39, 40, 42, 44, 45, 48, 50, 51, 54, 56, 58, 59, 60, 63, 64, 65, 68, 70, 72
240	9-30, 32, 35, 36, 40, 44, 45, 48, 52, 54, 60

\*Morse Chain Company, Ithaca, NY, Type B hub sprockets.

**Table 17-22**Tooth Correction  
Factors,  $K_1$ 

Number of Teeth on Driving Sprocket	$K_1$ Pre-extreme Horsepower	$K_1$ Post-extreme Horsepower
11	0.62	0.52
12	0.69	0.59
13	0.75	0.67
14	0.81	0.75
15	0.87	0.83
16	0.94	0.91
17	1.00	1.00
18	1.06	1.09
19	1.13	1.18
20	1.19	1.28
$N$	$(N_1/17)^{1.08}$	$(N_1/17)^{1.5}$

**Table 17-23**Multiple-Strand  
Factors  $K_2$ 

Number of Strands	$K_2$
1	1.0
2	1.7
3	2.5
4	3.3
5	3.9
6	4.6
8	6.0

The constant 0.004 becomes 0.0022 for no. 41 lightweight chain. The nominal horsepower in Table 17-20 is  $H_{\text{nom}} = \min(H_1, H_2)$ . For example, for  $N_1 = 17$ ,  $n_1 = 1000$  rev/min, no. 40 chain with  $p = 0.5$  in, from Eq. (17-32),

$$H_1 = 0.004(17)^{1.08} 1000^{0.9} 0.5^{[3-0.07(0.5)]} = 5.48 \text{ hp}$$

From Eq. (17-33),

$$H_2 = \frac{1000(17)17^{1.5}(0.5^{0.8})}{1000^{1.5}} = 21.64 \text{ hp}$$

The tabulated value in Table 17-20 is  $H_{\text{tab}} = \min(5.48, 21.64) = 5.48 \text{ hp}$ .

It is preferable to have an odd number of teeth on the driving sprocket (17, 19, . . .) and an even number of pitches in the chain to avoid a special link. The approximate length of the chain  $L$  in pitches is

$$\frac{L}{p} \doteq \frac{2C}{p} + \frac{N_1 + N_2}{2} + \frac{(N_2 - N_1)^2}{4\pi^2 C/p} \quad (17-34)$$

The center-to-center distance  $C$  is given by

$$C = \frac{p}{4} \left[ -A + \sqrt{A^2 - 8 \left( \frac{N_2 - N_1}{2\pi} \right)^2} \right] \quad (17-35)$$

where

$$A = \frac{N_1 + N_2}{2} - \frac{L}{p} \quad (17-36)$$

The allowable power  $H_a$  is given by

$$H_a = K_1 K_2 H_{\text{tab}} \quad (17-37)$$

where  $K_1$  = correction factor for tooth number other than 17 (Table 17-22)

$K_2$  = strand correction (Table 17-23)

The horsepower that must be transmitted  $H_d$  is given by

$$H_d = H_{\text{nom}} K_s n_d \quad (17-38)$$

Equation (17-32) is the basis of the pre-extreme power entries (vertical entries) of Table 17-20, and the chain power is limited by link-plate fatigue. Equation (17-33) is the basis for the post-extreme power entries of these tables, and the chain power performance is limited by impact fatigue. The entries are for chains of 100 pitch length and 17-tooth sprocket. For a deviation from this

$$H_2 = 1000 \left[ K_r \left( \frac{N_1}{n_1} \right)^{1.5} p^{0.8} \left( \frac{L_p}{100} \right)^{0.4} \left( \frac{15\,000}{h} \right)^{0.4} \right] \quad (17-39)$$

where  $L_p$  is the chain length in pitches and  $h$  is the chain life in hours. Viewed from a deviation viewpoint, Eq. (17-39) can be written as a trade-off equation in the following form:

$$\frac{H_2^{2.5} h}{N_1^{3.75} L_p} = \text{constant} \quad (17-40)$$

If tooth-correction factor  $K_1$  is used, then omit the term  $N_1^{3.75}$ . Note that  $(N_1^{1.5})^{2.5} = N_1^{3.75}$ .

In Eq. (17-40) one would expect the  $h/L_p$  term because doubling the hours can require doubling the chain length, other conditions constant, for the same number of cycles. Our experience with contact stresses leads us to expect a load (tension) life relation of the form  $F^a L = \text{constant}$ . In the more complex circumstance of roller-bushing impact, the Diamond Chain Company has identified  $a = 2.5$ .

The maximum speed (rev/min) for a chain drive is limited by galling between the pin and the bushing. Tests suggest

$$n_1 \leq 1000 \left[ \frac{82.5}{7.95 p (1.0278)^{N_1} (1.323)^{F/1000}} \right]^{1/(1.59 \log p + 1.873)} \quad \text{rev/min}$$

where  $F$  is the chain tension in pounds.

### EXAMPLE 17-5

Select drive components for a 2:1 reduction, 90-hp input at 300 rev/min, moderate shock, an abnormally long 18-hour day, poor lubrication, cold temperatures, dirty surroundings, short drive  $C/p = 25$ .

#### Solution

Function:  $H_{\text{nom}} = 90$  hp,  $n_1 = 300$  rev/min,  $C/p = 25$ ,  $K_s = 1.3$

Design factor:  $n_d = 1.5$

Sprocket teeth:  $N_1 = 17$  teeth,  $N_2 = 34$  teeth,  $K_1 = 1$ ,  $K_2 = 1, 1.7, 2.5, 3.3$

Chain number of strands:

$$H_{\text{tab}} = \frac{n_d K_s H_{\text{nom}}}{K_1 K_2} = \frac{1.5(1.3)90}{(1)K_2} = \frac{176}{K_2}$$

Form a table:

Number of Strands	176/ $K_2$ (Table 17-23)	Chain Number (Table 17-19)	Lubrication Type
1	$176/1 = 176$	200	C'
2	$176/1.7 = 104$	160	C
3	$176/2.5 = 70.4$	140	B
4	$176/3.3 = 53.3$	140	B

**Decision** 3 strands of number 140 chain ( $H_{\text{tab}}$  is 72.4 hp).

Number of pitches in the chain:

$$\begin{aligned} \frac{L}{p} &= \frac{2C}{p} + \frac{N_1 + N_2}{2} + \frac{(N_2 - N_1)^2}{4\pi^2 C/p} \\ &= 2(25) + \frac{17 + 34}{2} + \frac{(34 - 17)^2}{4\pi^2(25)} = 75.79 \text{ pitches} \end{aligned}$$

**Decision** Use 76 pitches. Then  $L/p = 76$ .

Identify the center-to-center distance: From Eqs. (17-35) and (17-36),

$$\begin{aligned} A &= \frac{N_1 + N_2}{2} - \frac{L}{p} = \frac{17 + 34}{2} - 76 = -50.5 \\ C &= \frac{p}{4} \left[ -A + \sqrt{A^2 - 8 \left( \frac{N_2 - N_1}{2\pi} \right)^2} \right] \\ &= \frac{p}{4} \left[ 50.5 + \sqrt{50.5^2 - 8 \left( \frac{34 - 17}{2\pi} \right)^2} \right] = 25.104p \end{aligned}$$

For a 140 chain,  $p = 1.75$  in. Thus,

$$C = 25.104p = 25.104(1.75) = 43.93 \text{ in}$$

Lubrication: Type B

*Comment:* This is operating on the pre-extreme portion of the power, so durability estimates other than 15 000 h are not available. Given the poor operating conditions, life will be much shorter.

Lubrication of roller chains is essential in order to obtain a long and trouble-free life. Either a drip feed or a shallow bath in the lubricant is satisfactory. A medium or light mineral oil, without additives, should be used. Except for unusual conditions, heavy oils and greases are not recommended, because they are too viscous to enter the small clearances in the chain parts.

## 17-6 Wire Rope

Wire rope is made with two types of winding, as shown in Fig. 17-19. The *regular lay*, which is the accepted standard, has the wire twisted in one direction to form the strands, and the strands twisted in the opposite direction to form the rope. In the completed rope the visible wires are approximately parallel to the axis of the rope. Regular-lay ropes do not kink or untwist and are easy to handle.

*Lang-lay* ropes have the wires in the strand and the strands in the rope twisted in the same direction, and hence the outer wires run diagonally across the axis of the rope. Lang-lay ropes are more resistant to abrasive wear and failure due to fatigue than are regular-lay ropes, but they are more likely to kink and untwist.

Standard ropes are made with a hemp core, which supports and lubricates the strands. When the rope is subjected to heat, either a steel center or a wire-strand center must be used.

Wire rope is designated as, for example, a  $1\frac{1}{8}$ -in  $6 \times 7$  haulage rope. The first figure is the diameter of the rope (Fig. 17-19c). The second and third figures are the number of strands and the number of wires in each strand, respectively. Table 17-24 lists some of the various ropes that are available, together with their characteristics and properties. The area of the metal in standard hoisting and haulage rope is  $A_m = 0.38d^2$ .

When a wire rope passes around a sheave, there is a certain amount of readjustment of the elements. Each of the wires and strands must slide on several others, and presumably some individual bending takes place. It is probable that in this complex action there exists some stress concentration. The stress in one of the wires of a rope passing around a sheave may be calculated as follows. From solid mechanics, we have

$$M = \frac{EI}{\rho} \quad \text{and} \quad M = \frac{\sigma I}{c} \quad (a)$$

where the quantities have their usual meaning. Eliminating  $M$  and solving for the stress gives

$$\sigma = \frac{Ec}{\rho} \quad (b)$$

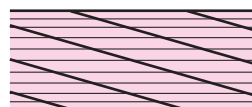
For the radius of curvature  $\rho$ , we can substitute the sheave radius  $D/2$ . Also,  $c = d_w/2$ , where  $d_w$  is the wire diameter. These substitutions give

$$\sigma = E_r \frac{d_w}{D} \quad (c)$$

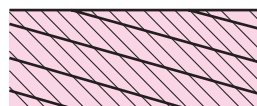
where  $E_r$  is the *modulus of elasticity of the rope*, not the wire. To understand this equation, observe that the individual wire makes a corkscrew figure in space and if you pull on it to determine  $E$  it will stretch or give more than its native  $E$  would suggest. Therefore

**Figure 17-19**

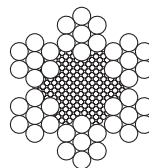
Types of wire rope; both lays are available in either right or left hand.



(a) Regular lay



(b) Lang lay



(c) Section of  
 $6 \times 7$  rope



**Table 17-24**Wire-Rope Data Source: Compiled from *American Steel and Wire Company Handbook*.

Rope	Weight per Foot, lbf	Minimum Sheave Diameter, in	Standard Sizes $d$ , in	Material	Size of Outer Wires	Modulus of Elasticity,* Mpsi	Strength,† kpsi
6 × 7 haulage	$1.50d^2$	$42d$	$\frac{1}{4}$ – $1\frac{1}{2}$	Monitor steel	$d/9$	14	100
				Plow steel	$d/9$	14	88
				Mild plow steel	$d/9$	14	76
6 × 19 standard hoisting	$1.60d^2$	$26d$ – $34d$	$\frac{1}{4}$ – $2\frac{3}{4}$	Monitor steel	$d/13$ – $d/16$	12	106
				Plow steel	$d/13$ – $d/16$	12	93
				Mild plow steel	$d/13$ – $d/16$	12	80
6 × 37 special flexible	$1.55d^2$	$18d$	$\frac{1}{4}$ – $3\frac{1}{2}$	Monitor steel	$d/22$	11	100
				Plow steel	$d/22$	11	88
8 × 19 extra flexible	$1.45d^2$	$21d$ – $26d$	$\frac{1}{4}$ – $1\frac{1}{2}$	Monitor steel	$d/15$ – $d/19$	10	92
				Plow steel	$d/15$ – $d/19$	10	80
7 × 7 aircraft	$1.70d^2$	—	$\frac{1}{16}$ – $\frac{3}{8}$	Corrosion-resistant steel	—	—	124
				Carbon steel	—	—	124
7 × 9 aircraft	$1.75d^2$	—	$\frac{1}{8}$ – $1\frac{3}{8}$	Corrosion-resistant steel	—	—	135
				Carbon steel	—	—	143
19-wire aircraft	$2.15d^2$	—	$\frac{1}{32}$ – $\frac{5}{16}$	Corrosion-resistant steel	—	—	165
				Carbon steel	—	—	165

\*The modulus of elasticity is only approximate; it is affected by the loads on the rope and, in general, increases with the life of the rope.

†The strength is based on the nominal area of the rope. The figures given are only approximate and are based on 1-in rope sizes and  $\frac{1}{4}$ -in aircraft-cable sizes.

$E$  is still the modulus of elasticity of the *wire*, but in its peculiar configuration as part of the rope, its modulus is smaller. For this reason we say that  $E_r$  in Eq. (c) is the modulus of elasticity of the rope, not the wire, recognizing that one can quibble over the name used.

Equation (c) gives the tensile stress  $\sigma$  in the outer wires. The sheave diameter is represented by  $D$ . This equation reveals the importance of using a large-diameter sheave. The suggested minimum sheave diameters in Table 17-24 are based on a  $D/d_w$  ratio of 400. If possible, the sheaves should be designed for a larger ratio. For elevators and mine hoists,  $D/d_w$  is usually taken from 800 to 1000. If the ratio is less than 200, heavy loads will often cause a permanent set in the rope.

A wire rope tension giving the same tensile stress as the sheave bending is called the *equivalent bending load*  $F_b$ , given by

$$F_b = \sigma A_m = \frac{E_r d_w A_m}{D} \quad (17-41)$$

A wire rope may fail because the static load exceeds the ultimate strength of the rope. Failure of this nature is generally not the fault of the designer, but rather that of the operator in permitting the rope to be subjected to loads for which it was not designed.

The first consideration in selecting a wire rope is to determine the static load. This load is composed of the following items:

- The known or dead weight
- Additional loads caused by sudden stops or starts
- Shock loads
- Sheave-bearing friction

When these loads are summed, the total can be compared with the ultimate strength of the rope to find a factor of safety. However, the ultimate strength used in this determination must be reduced by the strength loss that occurs when the rope passes over a curved surface such as a stationary sheave or a pin; see Fig. 17–20.

For an average operation, use a factor of safety of 5. Factors of safety up to 8 or 9 are used if there is danger to human life and for very critical situations. Table 17–25

**Figure 17–20**

Percent strength loss due to different  $D/d$  ratios; derived from standard test data for  $6 \times 19$  and  $6 \times 17$  class ropes. (Materials provided by the Wire Rope Technical Board (WRTB), Wire Rope Users Manual Third Edition, Second printing. Reprinted by permission.)

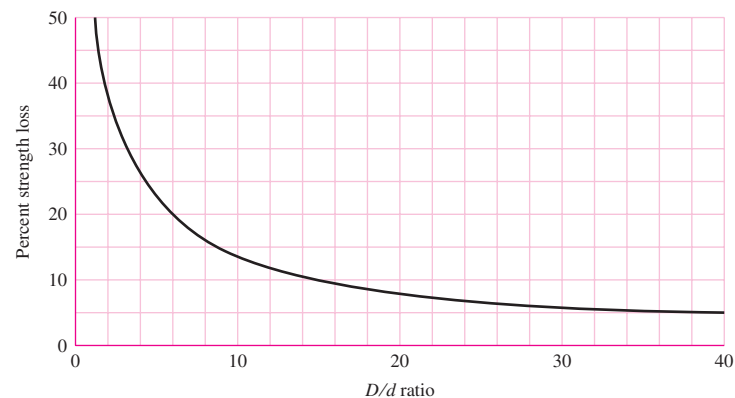


**Table 17–25**

Minimum Factors of  
Safety for Wire Rope\*

Source: Compiled from a  
variety of sources, including  
ANSI A17.1-1978.

Track cables	3.2	Passenger elevators, ft/min:	
Guys	3.5	50	7.60
Mine shafts, ft:		300	9.20
Up to 500	8.0	800	11.25
1000–2000	7.0	1200	11.80
2000–3000	6.0	1500	11.90
Over 3000	5.0	Freight elevators, ft/min:	
Hoisting	5.0	50	6.65
Haulage	6.0	300	8.20
Cranes and derricks	6.0	800	10.00
Electric hoists	7.0	1200	10.50
Hand elevators	5.0	1500	10.55
Private elevators	7.5	Powered dumbwaiters, ft/min:	
Hand dumbwaiter	4.5	50	4.8
Grain elevators	7.5	300	6.6
		500	8.0

\*Use of these factors does not preclude a fatigue failure.

lists minimum factors of safety for a variety of design situations. Here, the factor of safety is defined as

$$n = \frac{F_u}{F_t}$$

where  $F_u$  is the ultimate wire load and  $F_t$  is the largest working tension.

Once you have made a tentative selection of a rope based upon static strength, the next consideration is to ensure that the wear life of the rope and the sheave or sheaves meets certain requirements. When a loaded rope is bent over a sheave, the rope stretches like a spring, rubs against the sheave, and causes wear of both the rope and the sheave. The amount of wear that occurs depends upon the pressure of the rope in the sheave groove. This pressure is called the *bearing pressure*; a good estimate of its magnitude is given by

$$p = \frac{2F}{dD} \quad (17-42)$$

where  $F$  = tensile force on rope

$d$  = rope diameter

$D$  = sheave diameter

The allowable pressures given in Table 17–26 are to be used only as a rough guide; they may not prevent a fatigue failure or severe wear. They are presented here because they represent past practice and furnish a starting point in design.

A fatigue diagram not unlike an  $S$ - $N$  diagram can be obtained for wire rope. Such a diagram is shown in Fig. 17–21. Here the ordinate is the pressure-strength ratio  $p/S_u$ , and  $S_u$  is the ultimate tensile strength of the *wire*. The abscissa is the number of bends that occur in the total life of the rope. The curve implies that a wire rope has a fatigue limit; but this is not true at all. A wire rope that is used over sheaves will eventually fail

**Table 17–26**

Maximum Allowable  
Bearing Pressures of  
Ropes on Sheaves  
(in psi)

Source: Wire Rope Users  
Manual, AISI, 1979.

Rope	Sheave Material				
	Wood <sup>a</sup>	Cast Iron <sup>b</sup>	Cast Steel <sup>c</sup>	Chilled Cast Irons <sup>d</sup>	Manganese Steel <sup>e</sup>
Regular lay:					
6 × 7	150	300	550	650	1470
6 × 19	250	480	900	1100	2400
6 × 37	300	585	1075	1325	3000
8 × 19	350	680	1260	1550	3500
Lang lay:					
6 × 7	165	350	600	715	1650
6 × 19	275	550	1000	1210	2750
6 × 37	330	660	1180	1450	3300

<sup>a</sup>On end grain of beech, hickory, or gum.

<sup>b</sup>For  $H_B$  (min.) = 125.

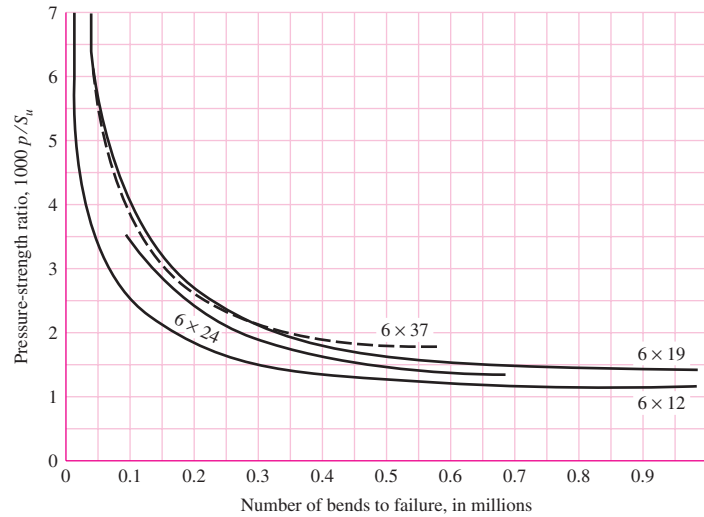
<sup>c</sup>30–40 carbon;  $H_B$  (min.) = 160.

<sup>d</sup>Use only with uniform surface hardness.

<sup>e</sup>For high speeds with balanced sheaves having ground surfaces.

**Figure 17-21**

Experimentally determined relation between the fatigue life of wire rope and the sheave pressure.



in fatigue or in wear. However, the graph does show that the rope will have a long life if the ratio  $p/S_u$  is less than 0.001. Substitution of this ratio in Eq. (17-42) gives

$$S_u = \frac{2000F}{dD} \quad (17-43)$$

where  $S_u$  is the ultimate strength of the *wire*, not the rope, and the units of  $S_u$  are related to the units of  $F$ . This interesting equation contains the wire strength, the load, the rope diameter, and the sheave diameter—all four variables in a single equation! Dividing both sides of Eq. (17-42) by the ultimate strength of the wires  $S_u$  and solving for  $F$  gives

$$F_f = \frac{(p/S_u)S_u d D}{2} \quad (17-44)$$

where  $F_f$  is interpreted as the allowable fatigue tension as the wire is flexed a number of times corresponding to  $p/S_u$  selected from Fig. 17-21 for a particular rope and life expectancy. The factor of safety can be defined in fatigue as

$$n_f = \frac{F_f - F_b}{F_t} \quad (17-45)$$

where  $F_f$  is the rope tension strength under flexing and  $F_t$  is the tension at the place where the rope is flexing. Unfortunately, the designer often has vendor information that tabulates ultimate rope tension and gives no ultimate-strength  $S_u$  information concerning the wires from which the rope is made. Some guidance in strength of individual wires is

Improved plow steel (monitor)	$240 < S_u < 280$ kpsi
Plow steel	$210 < S_u < 240$ kpsi
Mild plow steel	$180 < S_u < 210$ kpsi

In wire-rope usage, the factor of safety has been defined in static loading as  $n = F_u/F_t$  or  $n = (F_u - F_b)/F_t$ , where  $F_b$  is the rope tension that would induce the same outer-wire stress as that given by Eq. (c). The factor of safety in fatigue loading can be defined as in Eq. (17-45), or by using a static analysis and compensating with a large factor of safety applicable to static loading, as in Table 17-25. When using factors of safety expressed in codes, standards, corporate design manuals, or wire-rope manufacturers'

recommendations or from the literature, be sure to ascertain upon which basis the factor of safety is to be evaluated, and proceed accordingly.

If the rope is made of plow steel, the wires are probably hard-drawn AISI 1070 or 1080 carbon steel. Referring to Table 10–3, we see that this lies somewhere between hard-drawn spring wire and music wire. But the constants  $m$  and  $A$  needed to solve Eq. (10–14), p. 505, for  $S_u$  are lacking.

Practicing engineers who desire to solve Eq. (17–43) should determine the wire strength  $S_u$  for the rope under consideration by unraveling enough wire to test for the Brinell hardness. Then  $S_u$  can be found using Eq. (2–17), p. 37. Fatigue failure in wire rope is not sudden, as in solid bodies, but progressive, and shows as the breaking of an outside wire. This means that the beginning of fatigue can be detected by periodic routine inspection.

Figure 17–22 is another graph showing the gain in life to be obtained by using large  $D/d$  ratios. In view of the fact that the life of wire rope used over sheaves is only finite, it is extremely important that the designer specify and insist that periodic inspection, lubrication, and maintenance procedures be carried out during the life of the rope. Table 17–27 gives useful properties of some wire ropes.

For a mine-hoist problem we can develop working equations from the preceding presentation. The wire rope tension  $F_t$  due to load and acceleration/deceleration is

$$F_t = \left( \frac{W}{m} + wl \right) \left( 1 + \frac{a}{g} \right) \quad (17-46)$$

**Figure 17–22**

Service-life curve based on bending and tensile stresses only. This curve shows that the life corresponding to  $D/d = 48$  is twice that of  $D/d = 33$ . (*Materials provided by the Wire Rope Technical Board (WRTB), Wire Rope Users Manual Third Edition, Second printing. Reprinted by permission.*)

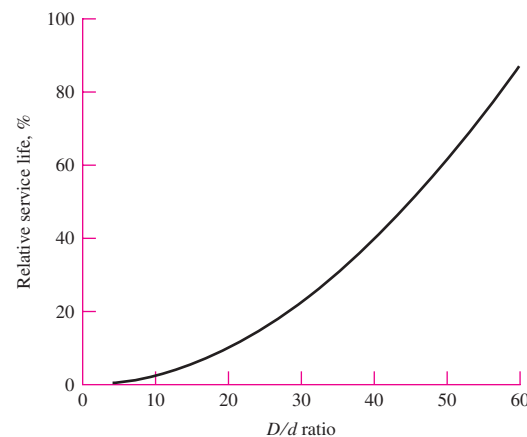


**Table 17–27**

Some Useful Properties of  $6 \times 7$ ,  $6 \times 19$ , and  $6 \times 37$  Wire Ropes

Wire Rope	Weight per Foot $w$ , lbf/ft	Weight per Foot Including Core $w$ , lbf/ft	Minimum Sheave Diameter $D$ , in	Better Sheave Diameter $D$ , in	Diameter of Wires $d_w$ , in	Area of Metal $A_m$ , in <sup>2</sup>	Rope Young's Modulus $E_r$ , psi
$6 \times 7$	$1.50d^2$		$42d$	$72d$	$0.111d$	$0.38d^2$	$13 \times 10^6$
$6 \times 19$	$1.60d^2$	$1.76d^2$	$30d$	$45d$	$0.067d$	$0.40d^2$	$12 \times 10^6$
$6 \times 37$	$1.55d^2$	$1.71d^2$	$18d$	$27d$	$0.048d$	$0.40d^2$	$12 \times 10^6$

where  $W$  = weight at the end of the rope (cage and load), lbf  
 $m$  = number of wire ropes supporting the load  
 $w$  = weight/foot of the wire rope, lbf/ft  
 $l$  = suspended length of rope, ft  
 $a$  = maximum acceleration/deceleration experienced, ft/s<sup>2</sup>  
 $g$  = acceleration of gravity, ft/s<sup>2</sup>

The fatigue tensile strength in pounds for a specified life  $F_f$  is

$$F_f = \frac{(p/S_u)S_u D d}{2} \quad (17-47)$$

where  $(p/S_u)$  = specified life, from Fig. 17-21

$S_u$  = ultimate tensile strength of the wires, psi

$D$  = sheave or winch drum diameter, in

$d$  = nominal wire rope size, in

The equivalent bending load  $F_b$  is

$$F_b = \frac{E_r d_w A_m}{D} \quad (17-48)$$

where  $E_r$  = Young's modulus for the wire rope, Table 17-24 or 17-27, psi

$d_w$  = diameter of the wires, in

$A_m$  = metal cross-sectional area, Table 17-24 or 17-28, in<sup>2</sup>

$D$  = sheave or winch drum diameter, in

The static factor of safety  $n_s$  is

$$n_s = \frac{F_u - F_b}{F_t} \quad (17-49)$$

Be careful when comparing recommended static factors of safety to Eq. (17-49), as  $n_s$  is sometimes defined as  $F_u/F_t$ . The fatigue factor of safety  $n_f$  is

$$n_f = \frac{F_f - F_b}{F_t} \quad (17-50)$$

### EXAMPLE 17-6

Given a  $6 \times 19$  monitor steel ( $S_u = 240$  kpsi) wire rope.

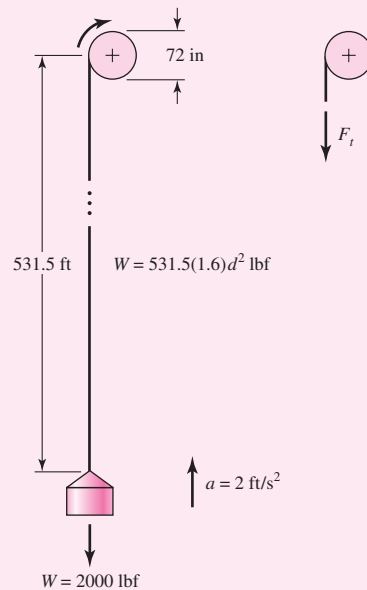
(a) Develop the expressions for rope tension  $F_t$ , fatigue tension  $F_f$ , equivalent bending tensions  $F_b$ , and fatigue factor of safety  $n_f$  for a 531.5-ft, 1-ton cage-and-load mine hoist with a starting acceleration of 2 ft/s<sup>2</sup> as depicted in Fig. 17-23. The sheave diameter is 72 in.

(b) Using the expressions developed in part (a), examine the variation in factor of safety  $n_f$  for various wire rope diameters  $d$  and number of supporting ropes  $m$ .

**Solution** (a) Rope tension  $F_t$  from Eq. (17-46) is given by

**Answer**

$$\begin{aligned} F_t &= \left( \frac{W}{m} + wl \right) \left( 1 + \frac{a}{g} \right) = \left[ \frac{2000}{m} + 1.60d^2(531.5) \right] \left( 1 + \frac{2}{32.2} \right) \\ &= \frac{2124}{m} + 903d^2 \text{ lbf} \end{aligned}$$

**Figure 17-23**Geometry of the mine hoist of  
Ex. 17-6.

From Fig. 17-21, use  $p/S_u = 0.0014$ . Fatigue tension  $F_f$  from Eq. (17-47) is given by

**Answer**

$$F_f = \frac{(p/S_u)S_u D d}{2} = \frac{0.0014(240\,000)72d}{2} = 12\,096d \text{ lbf}$$

Equivalent bending tension  $F_b$  from Eq. (17-48) and Table 17-27 is given by

**Answer**

$$F_b = \frac{E_r d_w A_m}{D} = \frac{12(10^6)0.067d(0.40d^2)}{72} = 4467d^3 \text{ lbf}$$

Factor of safety  $n_f$  in fatigue from Eq. (17-50) is given by

**Answer**

$$n_f = \frac{F_f - F_b}{F_t} = \frac{12\,096d - 4467d^3}{2124/m + 903d^2}$$

(b) Form a table as follows:

$d$	$n_f$			
	$m = 1$	$m = 2$	$m = 3$	$m = 4$
0.25	1.355	2.641	3.865	5.029
0.375	1.910	3.617	5.150	6.536
0.500	2.336	4.263	5.879	7.254
0.625	2.612	4.573	6.099	7.331
0.750	2.731	4.578	5.911	6.918
0.875	2.696	4.330	5.425	6.210
1.000	2.520	3.882	4.736	5.320

Wire rope sizes are discrete, as is the number of supporting ropes. Note that for each  $m$  the factor of safety exhibits a maximum. Predictably the largest factor of safety increases with  $m$ . If the required factor of safety were to be 6, only three or four ropes could meet the requirement. The sizes are different:  $\frac{5}{8}$ -in ropes with three ropes or  $\frac{3}{8}$ -in ropes with four ropes. The costs include not only the wires, but the grooved winch drums.

### 17-7 Flexible Shafts

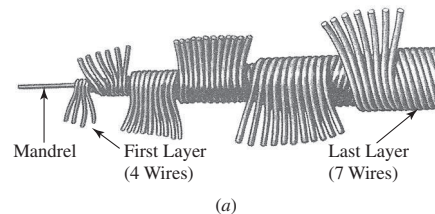
One of the greatest limitations of the solid shaft is that it cannot transmit motion or power around corners. It is therefore necessary to resort to belts, chains, or gears, together with bearings and the supporting framework associated with them. The flexible shaft may often be an economical solution to the problem of transmitting motion around corners. In addition to the elimination of costly parts, its use may reduce noise considerably.

There are two main types of flexible shafts: the power-drive shaft for the transmission of power in a single direction, and the remote-control or manual-control shaft for the transmission of motion in either direction.

The construction of a flexible shaft is shown in Fig. 17-24. The cable is made by winding several layers of wire around a central core. For the power-drive shaft, rotation should be in a direction such that the outer layer is wound up. Remote-control cables

**Figure 17-24**

Flexible shaft: (a) construction details; (b) a variety of configurations. (Courtesy of S. S. White Technologies, Inc.)





have a different lay of the wires forming the cable, with more wires in each layer, so that the torsional deflection is approximately the same for either direction of rotation.

Flexible shafts are rated by specifying the torque corresponding to various radii of curvature of the casing. A 15-in radius of curvature, for example, will give from 2 to 5 times more torque capacity than a 7-in radius. When flexible shafts are used in a drive in which gears are also used, the gears should be placed so that the flexible shaft runs at as high a speed as possible. This permits the transmission of the maximum amount of horsepower.

## PROBLEMS

- 17-1** A 6-in-wide polyamide F-1 flat belt is used to connect a 2-in-diameter pulley to drive a larger pulley with an angular velocity ratio of 0.5. The center-to-center distance is 9 ft. The angular speed of the small pulley is 1750 rev/min as it delivers 2 hp. The service is such that a service factor  $K_s$  of 1.25 is appropriate.
- Find  $F_c$ ,  $F_i$ ,  $F_{1a}$ , and  $F_2$ .
  - Find  $H_a$ ,  $n_{fs}$ , and belt length.
  - Find the dip.

- 17-2** Perspective and insight can be gained by doubling all geometric dimensions and observing the effect on problem parameters. Take the drive of Prob. 17-1, double the dimensions, and compare.

- 17-3** A flat-belt drive is to consist of two 4-ft-diameter cast-iron pulleys spaced 16 ft apart. Select a belt type to transmit 60 hp at a pulley speed of 380 rev/min. Use a service factor of 1.1 and a design factor of 1.0.

- 17-4** In solving problems and examining examples, you probably have noticed some recurring forms:

$$\begin{aligned}
 w &= 12\gamma bt = (12\gamma t)b = a_1 b, \\
 (F_1)_a &= F_a b C_p C_v = (F_a C_p C_v)b = a_0 b \\
 F_c &= \frac{wV^2}{g} = \frac{a_1 b}{32.174} \left( \frac{V}{60} \right)^2 = a_2 b \\
 (F_1)_a - F_2 &= 2T/d = 33\,000 H_d / V = 33\,000 H_{\text{nom}} K_s n_d / V \\
 F_2 &= (F_1)_a - [(F_1)_a - F_2] = a_0 b - 2T/d \\
 f\phi &= \ln \frac{(F_1)_a - F_c}{F_2 - F_c} = \ln \frac{(a_0 - a_2)b}{(a_0 - a_2)b - 2T/d}
 \end{aligned}$$

Show that

$$b = \frac{1}{a_0 - a_2} \frac{33\,000 H_d}{V} \frac{\exp(f\phi)}{\exp(f\phi) - 1}$$

- 17-5** Return to Ex. 17-1 and complete the following.
- Find the torque capacity that would put the drive as built at the point of slip, as well as the initial tension  $F_i$ .
  - Find the belt width  $b$  that exhibits  $n_{fs} = n_d = 1.1$ .
  - For part  $b$  find the corresponding  $F_{1a}$ ,  $F_c$ ,  $F_i$ ,  $F_2$ , power, and  $n_{fs}$ .
  - What have you learned?
- 17-6** Take the drive of Prob. 17-5 and double the belt width. Compare  $F_c$ ,  $F_i$ ,  $F_{1a}$ ,  $F_2$ ,  $H_a$ ,  $n_{fs}$ , and dip.

**17-7** Belted pulleys place loads on shafts, inducing bending and loading bearings. Examine Fig. 17-7 and develop an expression for the load the belt places on the pulley, and then apply it to Ex. 17-2.

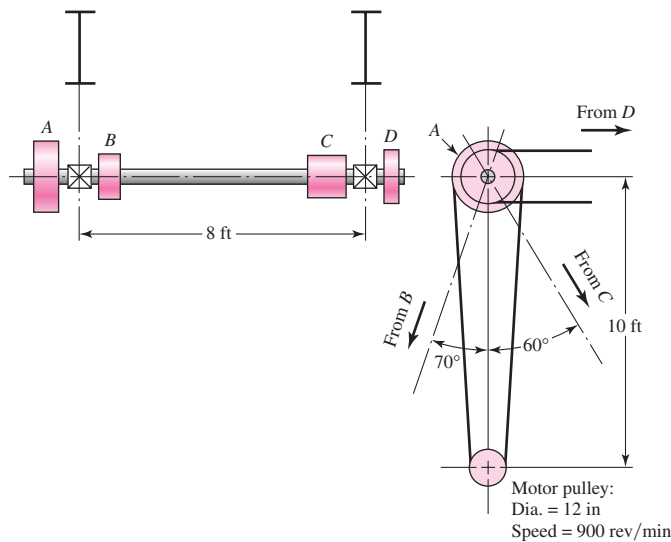
**17-8** Example 17-2 resulted in selection of a 10-in-wide A-3 polyamide flat belt. Show that the value of  $F_1$  restoring  $f$  to 0.80 is

$$F_1 = \frac{(\Delta F + F_c) \exp f \phi - F_c}{\exp f \phi - 1}$$

and compare the initial tensions.

**17-9** The line shaft illustrated in the figure is used to transmit power from an electric motor by means of flat-belt drives to various machines. Pulley  $A$  is driven by a vertical belt from the motor pulley. A belt from pulley  $B$  drives a machine tool at an angle of  $70^\circ$  from the vertical and at a center-to-center distance of 9 ft. Another belt from pulley  $C$  drives a grinder at a center-to-center distance of 11 ft. Pulley  $C$  has a double width to permit belt shifting as shown in Fig. 17-4. The belt from pulley  $D$  drives a dust-extractor fan whose axis is located horizontally 8 ft from the axis of the lineshaft. Additional data are

Machine	Speed, rev/min	Power, hp	Lineshaft Pulley	Diameter, in
Machine tool	400	12.5	$B$	16
Grinder	300	4.5	$C$	14
Dust extractor	500	8.0	$D$	18



Problem 17-9

(Courtesy of Dr. Ahmed F. Abdel  
Azim, Zagazig University,  
Cairo.)

The power requirements, listed above, account for the overall efficiencies of the equipment. The two line-shaft bearings are mounted on hangers suspended from two overhead wide-flange beams. Select the belt types and sizes for each of the four drives. Make provision for replacing belts from time to time because of wear or permanent stretch.

**17-10** Two shafts 20 ft apart, with axes in the same horizontal plane, are to be connected with a flat belt in which the driving pulley, powered by a six-pole squirrel-cage induction motor with a 100 brake hp rating at 1140 rev/min, drives the second shaft at half its angular speed. The driven shaft drives light-shock machinery loads. Select a flat belt.

**17-11** The mechanical efficiency of a flat-belt drive is approximately 98 percent. Because of its high value, the efficiency is often neglected. If a designer should choose to include it, where would he or she insert it in the flat-belt protocol?

**17-12** In metal belts, the centrifugal tension  $F_c$  is ignored as negligible. Convince yourself that this is a reasonable problem simplification.

**17-13** A designer has to select a metal-belt drive to transmit a power of  $H_{\text{nom}}$  under circumstances where a service factor of  $K_s$  and a design factor of  $n_d$  are appropriate. The design goal becomes  $H_d = H_{\text{nom}} K_s n_d$ . Use Eq. (17-8) to show that the minimum belt width is given by

$$b_{\min} = \frac{1}{a} \left( \frac{33\,000 H_d}{V} \right) \frac{\exp f \theta}{\exp f \theta - 1}$$

where  $a$  is the constant from  $F_{1a} = ab$ .

**17-14** Design a friction metal flat-belt drive to connect a 1-hp, four-pole squirrel-cage motor turning at 1750 rev/min to a shaft 15 in away, running at half speed. The circumstances are such that a service factor of 1.2 and a design factor of 1.05 are appropriate. The life goal is  $10^6$  belt passes,  $f = 0.35$ , and the environmental considerations require a stainless steel belt.

**17-15** A beryllium-copper metal flat belt with  $S_f = 56.67$  kpsi is to transmit 5 hp at 1125 rev/min with a life goal of  $10^6$  belt passes between two shafts 20 in apart whose centerlines are in a horizontal plane. The coefficient of friction between belt and pulley is 0.32. The conditions are such that a service factor of 1.25 and a design factor of 1.1 are appropriate. The driven shaft rotates at one-third the motor-pulley speed. Specify your belt, pulley sizes, and initial tension at installation.

**17-16** For the conditions of Prob. 17-15 use a 1095 plain carbon-steel heat-treated belt. Conditions at the driving pulley hub require a pulley outside diameter of 3 in or more. Specify your belt, pulley sizes, and initial tension at installation.

**17-17** A single V belt is to be selected to deliver engine power to the wheel-drive transmission of a riding tractor. A 5-hp single-cylinder engine is used. At most, 60 percent of this power is transmitted to the belt. The driving sheave has a diameter of 6.2 in, the driven, 12.0 in. The belt selected should be as close to a 92-in pitch length as possible. The engine speed is governor-controlled to a maximum of 3100 rev/min. Select a satisfactory belt and assess the factor of safety and the belt life in passes.

**17-18** Two B85 V belts are used in a drive composed of a 5.4-in driving sheave, rotating at 1200 rev/min, and a 16-in driven sheave. Find the power capacity of the drive based on a service factor of 1.25, and find the center-to-center distance.

**17-19** A 60-hp four-cylinder internal combustion engine is used to drive a brick-making machine under a schedule of two shifts per day. The drive consists of two 26-in sheaves spaced about 12 ft apart, with a sheave speed of 400 rev/min. Select a V-belt arrangement. Find the factor of safety, and estimate the life in passes and hours.

**17-20** A reciprocating air compressor has a 5-ft-diameter flywheel 14 in wide, and it operates at 170 rev/min. An eight-pole squirrel-cage induction motor has nameplate data 50 bhp at 875 rev/min.

(a) Design a V-belt drive.

(b) Can cutting the V-belt grooves in the flywheel be avoided by using a V-flat drive?

**17-21** The geometric implications of a V-flat drive are interesting.

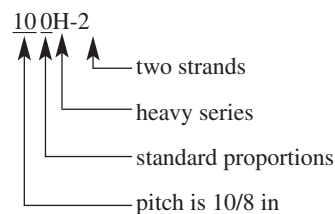
(a) If the earth's equator was an inextensible string, snug to the spherical earth, and you spliced 6 ft of string into the equatorial cord and arranged it to be concentric to the equator, how far off the ground is the string?

(b) Using the solution to part *a*, formulate the modifications to the expressions for  $m_G$ ,  $\theta_d$  and  $\theta_D$ ,  $L_p$ , and  $C$ .

(c) As a result of this exercise, how would you revise your solution to part *b* of Prob. 17–20?

**17–22** A 2-hp electric motor running at 1720 rev/min is to drive a blower at a speed of 240 rev/min. Select a V-belt drive for this application and specify standard V belts, sheave sizes, and the resulting center-to-center distance. The motor size limits the center distance to at least 22 in.

**17–23** The standard roller-chain number indicates the chain pitch in inches, construction proportions, series, and number of strands as follows:



This convention makes the pitch directly readable from the chain number. In Ex. 17–5 ascertain the pitch from the selected chain number and confirm from Table 17–19.

**17–24** Equate Eqs. (17–32) and (17–33) to find the rotating speed  $n_1$  at which the power equates and marks the division between the premaximum and the postmaximum power domains.

(a) Show that

$$n_1 = \left[ \frac{0.25(10^6)K_r N_1^{0.42}}{p^{(2.2-0.07p)}} \right]^{1/2.4}$$

(b) Find the speed  $n_1$  for a no. 60 chain,  $p = 0.75$  in,  $N_1 = 17$ ,  $K_r = 17$ , and confirm from Table 17–20.

(c) At which speeds is Eq. (17–40) applicable?

**17–25** A double-strand no. 60 roller chain is used to transmit power between a 13-tooth driving sprocket rotating at 300 rev/min and a 52-tooth driven sprocket.

(a) What is the allowable horsepower of this drive?

(b) Estimate the center-to-center distance if the chain length is 82 pitches.

(c) Estimate the torque and bending force on the driving shaft by the chain if the actual horsepower transmitted is 30 percent less than the corrected (allowable) power.

**17–26** A four-strand no. 40 roller chain transmits power from a 21-tooth driving sprocket to an 84-tooth driven sprocket. The angular speed of the driving sprocket is 2000 rev/min.

(a) Estimate the chain length if the center-to-center distance has to be about 20 in.

(b) Estimate the tabulated horsepower entry  $H'_{\text{tab}}$  for a 20 000-h life goal.

(c) Estimate the rated (allowable) horsepower that would appear in Table 17–20 for a 20 000-h life.

(d) Estimate the tension in the chain at the allowable power.

**17–27** A 700 rev/min 25-hp squirrel-cage induction motor is to drive a two-cylinder reciprocating pump, out-of-doors under a shed. A service factor  $K_s$  of 1.5 and a design factor of 1.1 are appropriate. The pump speed is 140 rev/min. Select a suitable chain and sprocket sizes.

**17–28** A centrifugal pump is driven by a 50-hp synchronous motor at a speed of 1800 rev/min. The pump is to operate at 900 rev/min. Despite the speed, the load is smooth ( $K_s = 1.2$ ). For a design factor of 1.1 specify a chain and sprockets that will realize a 50 000-h life goal. Let the sprockets be 19T and 38T.

- 17-29** A mine hoist uses a 2-in  $6 \times 19$  monitor-steel wire rope. The rope is used to haul loads of 4 tons from the shaft 480 ft deep. The drum has a diameter of 6 ft, the sheaves are of good-quality cast steel, and the smallest is 3 ft in diameter.
- (a) Using a maximum hoisting speed of 1200 ft/min and a maximum acceleration of  $2 \text{ ft/s}^2$ , estimate the stresses in the rope.
- (b) Estimate the various factors of safety.

- 17-30** A temporary construction elevator is to be designed to carry workers and materials to a height of 90 ft. The maximum estimated load to be hoisted is 5000 lbf at a velocity not to exceed 2 ft/s. For minimum sheave diameters and acceleration of  $4 \text{ ft/s}^2$ , specify the number of ropes required if the 1-in plow-steel  $6 \times 19$  hoisting strand is used.

- 17-31** A 2000-ft mine hoist operates with a 72-in drum using  $6 \times 19$  monitor-steel wire rope. The cage and load weigh 8000 lbf, and the cage is subjected to an acceleration of  $2 \text{ ft/s}^2$  when starting.
- (a) For a single-strand hoist how does the factor of safety  $n = F_f / F_t$  vary with the choice of rope diameter?
- (b) For four supporting strands of wire rope attached to the cage, how does the factor of safety vary with the choice of rope diameter?

- 17-32** Generalize the results of Prob. 17-31 by representing the factor of safety  $n$  as

$$n = \frac{ad}{(b/m) + cd^2}$$

where  $m$  is the number of ropes supporting the cage, and  $a$ ,  $b$ , and  $c$  are constants. Show that the optimal diameter is  $d^* = [b/(mc)]^{1/2}$  and the corresponding maximum attainable factor of safety is  $n^* = a[m/(bc)]^{1/2}/2$ .

- 17-33** From your results in Prob. 17-32, show that to meet a fatigue factor of safety  $n_1$  the optimal solution is

$$m = \frac{4bcn_1}{a^2} \text{ ropes}$$

having a diameter of

$$d = \frac{a}{2cn_1}$$

Solve Prob. 17-31 if a factor of safety of 2 is required. Show what to do in order to accommodate to the necessary discreteness in the rope diameter  $d$  and the number of ropes  $m$ .

- 17-34** For Prob. 17-29 estimate the elongation of the rope if a 9000-lbf loaded mine cart is placed on the cage. The results of Prob. 4-6 may be useful.

### Computer Programs

In approaching the ensuing computer problems, the following suggestions may be helpful:

- Decide whether an analysis program or a design program would be more useful. In problems as simple as these, you will find the programs similar. For maximum instructional benefit, try the design problem.
- Creating a design program without a figure of merit precludes ranking alternative designs but does not hinder the attainment of satisfactory designs. Your instructor can provide the class design library with commercial catalogs, which not only have price information but define available sizes.

- Quantitative understanding and logic of interrelations are required for programming. Difficulty in programming is a signal to you and your instructor to increase your understanding. The following programs can be accomplished in 100 to 500 lines of code.
- Make programs interactive and user-friendly.
- Let the computer do what it can do best; the user should do what a human can do best.
- Assume the user has a copy of the text and can respond to prompts for information.
- If interpolating in a table is in order, solicit table entries in the neighborhood, and let the computer crunch the numbers.
- In decision steps, allow the user to make the necessary decision, even if it is undesirable. This allows learning of consequences and the use of the program for analysis.
- Display a lot of information in the summary. Show the decision set used up-front for user perspective.
- When a summary is complete, adequacy assessment can be accomplished with ease, so consider adding this feature.

**17–35** Your experience with Probs. 17–1 through 17–11 has placed you in a position to write an interactive computer program to design/select flat-belt drive components. A possible decision set is

*A Priori Decisions*

- Function:  $H_{\text{nom}}$ , rev/min, velocity ratio, approximate  $C$
- Design factor:  $n_d$
- Initial tension maintenance: catenary
- Belt material:  $t$ ,  $d_{\text{min}}$ , allowable tension, density,  $f$
- Drive geometry:  $d$ ,  $D$
- Belt thickness:  $t$  (in material decision)

*Design Decisions*

- Belt width:  $b$

**17–36** Problems 17–12 through 17–16 have given you some experience with flat metal friction belts, indicating that a computer program could be helpful in the design/selection process. A possible decision set is

*A Priori Decisions*

- Function:  $H_{\text{nom}}$ , rev/min, velocity ratio approximate  $C$
- Design factor:  $n_d$
- Belt material:  $S_y$ ,  $E$ ,  $\nu$ ,  $d_{\text{min}}$
- Drive geometry:  $d$ ,  $D$
- Belt thickness:  $t$

*Design Decisions*

- Belt width:  $b$
- Length of belt (often standard loop periphery)

**17-37** Problems 17-17 through 17-22 have given you enough experience with V belts to convince you that a computer program would be helpful in the design/selection of V-belt drive components. Write such a program.

**17-38** Experience with Probs. 17-23 through 17-28 can suggest an interactive computer program to help in the design/selection process of roller-chain elements. A possible decision set is

*A Priori Decisions*

- Function: power, speed, space,  $K_s$ , life goal
- Design factor:  $n_d$
- Sprocket tooth counts:  $N_1$ ,  $N_2$ ,  $K_1$ ,  $K_2$

*Design Decisions*

- Chain number
- Strand count
- Lubrication system
- Chain length in pitches

(center-to-center distance for reference)

# 18

## Power Transmission Case Study

### Chapter Outline

- 18-1** Design Sequence for Power Transmission **915**
- 18-2** Power and Torque Requirements **916**
- 18-3** Gear Specification **916**
- 18-4** Shaft Layout **923**
- 18-5** Force Analysis **925**
- 18-6** Shaft Material Selection **925**
- 18-7** Shaft Design for Stress **926**
- 18-8** Shaft Design for Deflection **926**
- 18-9** Bearing Selection **927**
- 18-10** Key and Retaining Ring Selection **928**
- 18-11** Final Analysis **931**



Transmission of power from a source, such as an engine or motor, through a machine to an output actuation is one of the most common machine tasks. An efficient means of transmitting power is through rotary motion of a shaft that is supported by bearings. Gears, belt pulleys, or chain sprockets may be incorporated to provide for torque and speed changes between shafts. Most shafts are cylindrical (solid or hollow), and include stepped diameters with shoulders to accommodate the positioning and support of bearings, gears, etc.

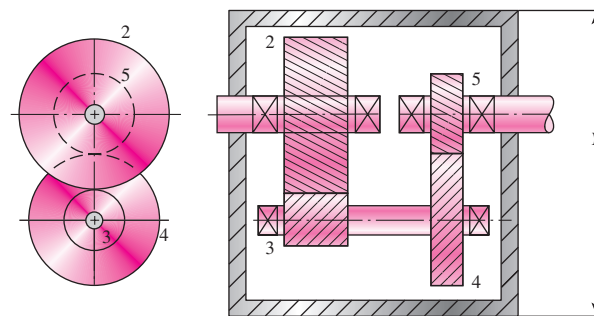
The design of a system to transmit power requires attention to the design and selection of individual components (gears, bearings, shaft, etc.). However, as is often the case in design, these components are not independent. For example, in order to design the shaft for stress and deflection, it is necessary to know the applied forces. If the forces are transmitted through gears, it is necessary to know the gear specifications in order to determine the forces that will be transmitted to the shaft. But stock gears come with certain bore sizes, requiring knowledge of the necessary shaft diameter. It is no surprise that the design process is interdependent and iterative, but where should a designer start?

The nature of machine design textbooks is to focus on each component separately. This chapter will focus on an overview of a power transmission system design, demonstrating how to incorporate the details of each component into an overall design process. A typical two-stage gear reduction such as shown in Fig. 18–1 will be assumed for this discussion. The design sequence is similar for variations of this particular transmission system.

The following outline will help clarify a logical design sequence. Discussion of how each part of the outline affects the overall design process will be given in sequence in this chapter. Details on the specifics for designing and selecting major components are covered in separate chapters, particularly Chap. 7 on shaft design, Chap. 11 on bearing selection, and Chaps. 13 and 14 on gear specification. A complete case study is presented as a specific vehicle to demonstrate the process.

**Figure 18–1**

A compound reverted gear train.



## CASE STUDY PART 1 PROBLEM SPECIFICATION

Section 1-16, p. 23, presents the background for this case study involving a speed reducer. A two-stage, compound reverted gear train such as shown in Fig. 18-1 will be designed. In this chapter, the design of the intermediate shaft and its components is presented, taking into account the other shafts as necessary.

A subset of the pertinent design specifications that will be needed for this part of the design are given here.

*Power to be delivered:* 20 hp  
*Input speed:* 1750 rpm  
*Output speed:* 82–88 rev/min  
 Usually low shock levels, occasional moderate shock  
 Input and output shafts extend 4 in outside gearbox  
*Maximum gearbox size:* 22 in × 14 in × 14 in  
 Output shaft and input shaft in-line  
 Gear and bearing life > 12 000 hours; infinite shaft life

## 18–1 Design Sequence for Power Transmission

There is not a precise sequence of steps for any design process. By nature, design is an iterative process in which it is necessary to make some tentative choices, and to build a skeleton of a design, and to determine which parts of the design are critical. However, much time can be saved by understanding the dependencies between the parts of the problem, allowing the designer to know what parts will be affected by any given change. In this section, only an outline is presented, with a short explanation of each step. Further details will be discussed in the following sections.

- *Power and torque requirements.* Power considerations should be addressed first, as this will determine the overall sizing needs for the entire system. Any necessary speed or torque ratio from input to output must be determined before addressing gear/pulley sizing.
- *Gear specification.* Necessary gear ratios and torque transmission issues can now be addressed with selection of appropriate gears. Note that a full force analysis of the shafts is not yet needed, as only the transmitted loads are required to specify the gears.
- *Shaft layout.* The general layout of the shaft, including axial location of gears and bearings must now be specified. Decisions on how to transmit the torque from the gears to the shaft need to be made (keys, splines, etc.), as well as how to hold gears and bearings in place (retaining rings, press fits, nuts, etc.). However, it is not necessary at this point to size these elements, since their standard sizes allow estimation of stress concentration factors.
- *Force analysis.* Once the gear/pulley diameters are known, and the axial locations of the gears and bearings are known, the free-body, shear force, and bending moment diagrams for the shafts can be produced. Forces at the bearings can be determined.
- *Shaft material selection.* Since fatigue design depends so heavily on the material choice, it is usually easier to make a reasonable material selection first, then check for satisfactory results.
- *Shaft design for stress (fatigue and static).* At this point, a stress design of the shaft should look very similar to a typical design problem from the shaft chapter (Chap. 7). Shear force and bending moment diagrams are known, critical locations can be predicted, approximate stress concentrations can be used, and estimates for shaft diameters can be determined.

- *Shaft design for deflection.* Since deflection analysis is dependent on the entire shaft geometry, it is saved until this point. With all shaft geometry now estimated, the critical deflections at the bearing and gear locations can be checked by analysis.
- *Bearing selection.* Specific bearings from a catalog may now be chosen to match the estimated shaft diameters. The diameters can be adjusted slightly as necessary to match the catalog specifications.
- *Key and retaining ring selection.* With shaft diameters settling in to stable values, appropriate keys and retaining rings can be specified in standard sizes. This should make little change in the overall design if reasonable stress concentration factors were assumed in previous steps.
- *Final analysis.* Once everything has been specified, iterated, and adjusted as necessary for any specific part of the task, a complete analysis from start to finish will provide a final check and specific safety factors for the actual system.

## 18-2 Power and Torque Requirements

Power transmission systems will typically be specified by a power capacity, for example, a 40-horsepower gearbox. This rating specifies the combination of torque and speed that the unit can endure. Remember that, in the ideal case, *power in* equals *power out*, so that we can refer to the power being the same throughout the system. In reality, there are small losses due to factors like friction in the bearings and gears. In many transmission systems, the losses in the rolling bearings will be negligible. Gears have a reasonably high efficiency, with about 1 to 2 percent power loss in a pair of meshed gears. Thus, in the double-reduction gearbox in Fig. 18-1, with two pairs of meshed gears the output power is likely to be about 2 to 4 percent less than the input power. Since this is a small loss, it is common to speak of simply the power of the system, rather than input power and output power. Flat belts and timing belts have efficiencies typically in the mid to upper 90 percent range. V belts and worm gears have efficiencies that may dip much lower, requiring a distinction between the necessary input power to obtain a desired output power.

Torque, on the other hand, is typically not constant throughout a transmission system. Remember that power equals the product of torque and speed. Since *power in* = *power out*, we know that for a gear train

$$H = T_i \omega_i = T_o \omega_o \quad (18-1)$$

With a constant power, a gear ratio to decrease the angular velocity will simultaneously increase torque. The gear ratio, or train value, for the gear train is

$$e = \omega_o / \omega_i = T_i / T_o \quad (18-2)$$

A typical power transmission design problem will specify the desired power capacity, along with either the input and output angular velocities, or the input and output torques. There will usually be a tolerance specified for the output values. After the specific gears are specified, the actual output values can be determined.

## 18-3 Gear Specification

With the gear train value known, the next step is to determine appropriate gears. As a rough guideline, a train value of up to 10 to 1 can be obtained with one pair of gears. Greater ratios can be obtained by compounding additional pairs of gears (See Sec. 13-13, p. 678). The compound reverted gear train in Fig. 18-1 can obtain a train value of up to 100 to 1.

Since numbers of teeth on gears must be integers, it is best to design with teeth numbers rather than diameters. See Ex. 13–3, 13–4, and 13–5, pp. 680–682, for details on designing appropriate numbers of teeth to satisfy the gear train value and any necessary geometry condition, such as in-line condition of input and output shaft. Care should be taken at this point to find the best combination of teeth numbers to minimize the overall package size. If the train value only needs to be approximate, use this flexibility to try different options of teeth numbers to minimize the package size. A difference of one tooth on the smallest gear can result in a significant increase in size of the overall package.

If designing for large production quantities, gears can be purchased in large enough quantities that it is not necessary to worry about preferred sizes. For small lot production, consideration should be given to the tradeoffs between smaller gearbox size and extra cost for odd gear sizes that are difficult to purchase off the shelf. If stock gears are to be used, their availability in prescribed numbers of teeth with anticipated diametral pitch should be checked at this time. If necessary, iterate the design for numbers of teeth that are available.

## CASE STUDY PART 2 SPEED, TORQUE, AND GEAR RATIOS

Continue the case study by determining appropriate tooth counts to reduce the input speed of  $\omega_i = 1750$  rev/min to an output speed within the range

$$82 \text{ rev/min} < \omega_o < 88 \text{ rev/min}$$

Once final tooth counts are specified, determine values of

- (a) Speeds for the intermediate and output shafts
- (b) Torques for the input, intermediate and output shafts, to transmit 20 hp.

### Solution

Use the notation for gear numbers from Fig. 18-1. Choose mean value for initial design,  $\omega_5 = 85$  rev/min.

$$e = \frac{\omega_5}{\omega_2} = \frac{85}{1750} = \frac{1}{20.59} \quad \text{Eq. (18-2)}$$

For a compound reverted geartrain,

$$e = \frac{1}{20.59} = \frac{N_2 N_4}{N_3 N_5} \quad \text{Eq. (13-30), p. 679}$$

For smallest package size, let both stages be the same reduction. Also, by making the two stages identical, the in-line condition on the input and output shaft will automatically be satisfied.

$$\frac{N_2}{N_3} = \frac{N_4}{N_5} = \sqrt{\frac{1}{20.59}} = \frac{1}{4.54}$$

For this ratio, the minimum number of teeth from Eq. (13-11), p. 666, is 16.

$$N_2 = N_4 = 16 \text{ teeth}$$

$$N_3 = 4.54(N_2) = 72.64$$

Try rounding down and check if  $\omega_5$  is within limits.

$$\omega_5 = \left(\frac{16}{72}\right) \left(\frac{16}{72}\right) (1750) = 86.42 \text{ rev/min} \quad \text{Acceptable}$$

Proceed with

$$N_2 = N_4 = 16 \text{ teeth}$$

$$N_3 = N_5 = 72 \text{ teeth}$$

$$e = \left(\frac{16}{72}\right) \left(\frac{16}{72}\right) = \frac{1}{20.25}$$

$$\omega_5 = 86.42 \text{ rev/min}$$

$$\omega_3 = \omega_4 = \left(\frac{16}{72}\right) (1750) = 388.9 \text{ rev/min}$$

To determine the torques, return to the power relationship,

$$H = T_2 \omega_2 = T_5 \omega_5$$

Eq. (18-1)

$$T_2 = H / \omega_2 = \left(\frac{20 \text{ hp}}{1750 \text{ rev/min}}\right) \left(550 \frac{\text{ft-lbf/s}}{\text{hp}}\right) \left(\frac{1 \text{ rev}}{2\pi \text{ rad}}\right) \left(60 \frac{\text{s}}{\text{min}}\right)$$

$$T_2 = 60.0 \text{ lbf} \cdot \text{ft}$$

$$T_3 = T_2 \frac{\omega_2}{\omega_3} = 60.0 \frac{1750}{388.9} = 270 \text{ lbf} \cdot \text{ft}$$

$$T_5 = T_2 \frac{\omega_2}{\omega_5} = 60.0 \frac{1750}{86.42} = 1215 \text{ lbf} \cdot \text{ft}$$

If a maximum size for the gearbox has been specified in the problem specification, a minimum diametral pitch (maximum tooth size) can be estimated at this point by writing an expression for gearbox size in terms of gear diameters, and converting to numbers of teeth through the diametral pitch. For example, from Fig. 18-1, the overall height of the gearbox is

$$Y = d_3 + d_2/2 + d_5/2 + 2/P + \text{clearances} + \text{wall thicknesses}$$

where the  $2/P$  term accounts for the addendum height of the teeth on gears 2 and 5 that extend beyond the pitch diameters. Substituting  $d_i = N_i/P$  gives

$$Y = N_3/P + N_2/(2P) + N_5/(2P) + 2/P + \text{clearances} + \text{wall thicknesses}$$

Solving this for  $P$ , we find

$$P = (N_3 + N_2/2 + N_5/2 + 2)/(Y - \text{clearances} - \text{wall thicknesses}) \quad (18-3)$$

This is the minimum value that can be used for diametral pitch, and therefore the maximum tooth size, to stay within the overall gearbox constraint. It should be rounded *up* to the next standard diametral pitch, which reduces the maximum tooth size.

The AGMA approach, as described in Chap. 14, for both bending and contact stress should be applied next to determine suitable gear parameters. The primary design parameters to be specified by the designer include material, diametral pitch, and face width. A recommended procedure is to start with an estimated diametral pitch. This allows determination of gear diameters ( $d = N/P$ ), pitch-line velocities [Eq. (13–34), p. 687], and transmitted loads [Eq. (13–35) or (13–36), p. 687]. Typical spur gears are available with face widths from 3 to 5 times the circular pitch  $p$ . Using an average of 4, a first estimate can be made for face width  $F = 4p = 4\pi/P$ . Alternatively, the designer can simply perform a quick search of on-line gear catalogs to find available face widths for the diametral pitch and number of teeth.

Next, the AGMA equations in Chap. 14 can be used to determine appropriate material choices to provide desired safety factors. It is generally most efficient to attempt to analyze the most critical gear first, as it will determine the limiting values of diametral pitch and material strength. Usually, the critical gear will be the smaller gear, on the high-torque (low-speed) end of the gearbox.

If the required material strengths are too high, such that they are either too expensive or not available, iteration with a smaller diametral pitch (larger tooth) will help. Of course, this will increase the overall gearbox size. Often the excessive stress will be in one of the small gears. Rather than increase the tooth size for all gears, it is sometimes better to reconsider the design of tooth counts, shifting more of the gear ratio to the pair of gears with less stress, and less ratio to the pair of gears with the excessive stress. This will allow the offending gear to have more teeth and therefore larger diameter, decreasing its stress.

If contact stress turns out to be more limiting than bending stress, consider gear materials that have been heat treated or case hardened to increase the surface strength. Adjustments can be made to the diametral pitch if necessary to achieve a good balance of size, material, and cost. If the stresses are all much lower than the material strengths, a larger diametral pitch is in order, which will reduce the size of the gears and the gearbox.

Everything up to this point should be iterated until acceptable results are obtained, as this portion of the design process can usually be accomplished independently from the next stages of the process. The designer should be satisfied with the gear selection before proceeding to the shaft. Selection of specific gears from catalogs at this point will be helpful in later stages, particularly in knowing overall width, bore size, recommended shoulder support, and maximum fillet radius.

## CASE STUDY PART 3 GEAR SPECIFICATION

Continue the case study by specifying appropriate gears, including pitch diameter, diametral pitch, face width, and material. Achieve safety factors of at least 1.2 for wear and bending.

### Solution

Estimate the minimum diametral pitch for overall gearbox height = 22 in.

From Eq. (18-3) and Fig. 18-1,

$$P_{\min} = \frac{\left(N_3 + \frac{N_2}{2} + \frac{N_5}{2} + 2\right)}{(Y - \text{clearances} - \text{wall thickness})}$$

Allow 1.5 in for clearances and wall thicknesses:

$$P_{\min} = \frac{\left(72 + \frac{16}{2} + \frac{72}{2} + 2\right)}{(22 - 1.5)} = 5.76 \text{ teeth/in}$$

Start with  $P = 6 \text{ teeth/in}$

$$\begin{aligned} d_2 = d_4 = N_2/P &= 16/6 = 2.67 \text{ in} \\ d_3 = d_5 = 72/6 &= 12.0 \text{ in} \end{aligned}$$

Shaft speeds were previously determined to be

$$\omega_2 = 1750 \text{ rev/min} \quad \omega_3 = \omega_4 = 388.9 \text{ rev/min} \quad \omega_5 = 86.4 \text{ rev/min}$$

Get pitch-line velocities and transmitted loads for later use.

$$V_{23} = \frac{\pi d_2 \omega_2}{12} = \frac{\pi (2.67)(1750)}{12} = 1223 \text{ ft/min} \quad \text{Eq. (13-34), p. 687}$$

$$V_{45} = \frac{\pi d_5 \omega_5}{12} = 271.5 \text{ ft/min}$$

$$W'_{23} = 33000 \frac{H}{V_{23}} = 33000 \left( \frac{20}{1223} \right) = 540.0 \text{ lbf} \quad \text{Eq. (13-35), p. 687}$$

$$W'_{45} = 33000 \frac{H}{V_{45}} = 2431 \text{ lbf}$$

Start with gear 4, since it is the smallest gear, transmitting the largest load. It will likely be critical. Start with wear by contact stress, since it is often the limiting factor.

### Gear 4 Wear

$$I = \frac{\cos 20^\circ \sin 20^\circ}{2(1)} \left( \frac{4.5}{4.5 + 1} \right) = 0.1315 \quad \text{Eq. (14-23), p. 735}$$

$$\text{For } K_v, \text{ assume } Q_v = 7, B = 0.731, A = 65.1 \quad \text{Eq. (14-29), p. 736}$$

$$K_v = \left( \frac{65.1 + \sqrt{271.5}}{65.1} \right)^{0.731} = 1.18 \quad \text{Eq. (14-27), p. 736}$$

Face width  $F$  is typically from 3 to 5 times circular pitch. Try

$$F = 4 \left( \frac{\pi}{P} \right) = 4 \left( \frac{\pi}{6} \right) = 2.09 \text{ in.}$$

Since gear specifications are readily available on the Internet, we might as well check for commonly available face widths. On [www.globalspec.com](http://www.globalspec.com), entering  $P = 6$  teeth/in and  $d = 2.67$  in, stock spur gears from several sources have face widths of 1.5 in or 2.0 in. These are also available for the meshing gear 5 with  $d = 12$  in.

Choose  $F = 2.0 \text{ in.}$

$$\text{For } K_m, \quad C_{pf} = 0.0624 \quad \text{Eq. (14-32), p. 740}$$



$$C_{mc} = 1 \text{ uncrowned teeth} \quad \text{Eq. (14-31), p. 740}$$

$$C_{pm} = 1 \text{ straddle-mounted} \quad \text{Eq. (14-33), p. 740}$$

$$C_{ma} = 0.15 \text{ commercial enclosed unit} \quad \text{Eq. (14-34), p. 740}$$

$$C_e = 1 \quad \text{Eq. (14-35), p. 740}$$

$$K_m = 1.21 \quad \text{Eq. (14-30), p. 739}$$

$$C_p = 2300 \quad \text{Table 14-8, p. 737}$$

$$K_o = K_s = C_f = 1$$

$$\sigma_c = 2300 \sqrt{\frac{2431(1.18)(1.21)}{2.67(2)(0.1315)}} = 161\,700 \text{ psi} \quad \text{Eq. (14-16), p. 726}$$

Get factors for  $\sigma_{c,all}$ . For life factor  $Z_N$ , get number of cycles for specified life of 12 000 h.

$$L_4 = (12\,000 \text{ h}) \left( 60 \frac{\text{min}}{\text{h}} \right) \left( 389 \frac{\text{rev}}{\text{min}} \right) = 2.8 \times 10^8 \text{ rev}$$

$$Z_N = 0.9 \quad \text{Fig. 14-15, p. 743}$$

$$K_R = K_T = C_H = 1$$

For a design factor of 1.2,

$$\sigma_{c,all} = S_c Z_N / S_H = \sigma_c \quad \text{Eq. (14-18), p. 730}$$

$$S_c = \frac{S_H \sigma_c}{Z_N} = \frac{1.2(161\,700)}{0.9} = 215\,600 \text{ psi}$$

From Table 14-6, p. 731, this strength is achievable with Grade 2 carburized and hardened with  $S_c = 225\,000 \text{ psi}$ . To find the achieved factor of safety,  $n_c = \sigma_{c,all} / \sigma_c$  with  $S_H = 1$ . The factor of safety for wear of gear 4 is

$$n_c = \frac{\sigma_{c,all}}{\sigma_c} = \frac{S_c Z_N}{\sigma_c} = \frac{225\,000(0.9)}{161\,700} = 1.25$$

### Gear 4 Bending

$$J = 0.27 \quad \text{Fig. 14-6, p. 733}$$

$$K_B = 1$$

Everything else is the same as before.

$$\sigma = W_t K_v \frac{P_d K_m}{F J} = (2431)(1.18) \left( \frac{6}{2} \right) \left( \frac{1.21}{0.27} \right) \quad \text{Eq. (14-15), p. 726}$$

$$\sigma = 38\,570 \text{ psi}$$

$$Y_N = 0.9 \quad \text{Fig. 14-14, p. 743}$$



Using Grade 2 carburized and hardened, same as chosen for wear, find  $S_t = 65\,000$  psi (Table 14-3, p. 728).

$$\sigma_{\text{all}} = S_t Y_N = 58\,500 \text{ psi}$$

The factor of safety for bending of gear 4 is

$$n = \frac{\sigma_{\text{all}}}{\sigma} = \frac{58\,500}{38\,570} = 1.52$$

### Gear 5 Bending and Wear

Everything is the same as for gear 4, except  $J$ ,  $Y_N$ , and  $Z_N$ .

$$J = 0.41$$

Fig. 14-6, p. 733

$$L_5 = (12\,000 \text{ h})(60 \text{ min/h})(86.4 \text{ rev/min}) = 6.2 \times 10^7 \text{ rev}$$

$$Y_N = 0.97$$

Fig. 14-14, p. 743

$$Z_N = 1.0$$

Fig. 14-15, p. 743

$$\sigma_c = 2300 \sqrt{\frac{2431(1.18)(1.21)}{12(2)(0.1315)}} = 76\,280 \text{ psi}$$

$$\sigma = (2431)(1.18) \left(\frac{6}{2}\right) \left(\frac{1.21}{0.41}\right) = 25\,400 \text{ psi}$$

Choose a Grade 1 steel, through-hardened to  $250 H_B$ . From Fig. 14-2, p. 727,  $S_t = 32\,000$  psi and from Fig. 14-5, p. 730,  $S_c = 110\,000$  psi.

$$n_c = \frac{\sigma_{c,\text{all}}}{\sigma_c} = \frac{110\,000}{76\,280} = 1.44$$

$$n = \frac{\sigma_{\text{all}}}{\sigma} = \frac{32\,000(.97)}{25\,400} = 1.22$$

### Gear 2 Wear

Gears 2 and 3 are evaluated similarly. Only selected results are shown.

$$K_v = 1.37$$

Try  $F = 1.5$  in, since the loading is less on gears 2 and 3.

$$K_m = 1.19$$

All other factors are the same as those for gear 4.

$$\sigma_c = 2300 \sqrt{\frac{(539.7)(1.37)(1.19)}{2.67(1.5)(0.1315)}} = 94\,000 \text{ psi}$$

$$L_2 = (12\,000 \text{ h})(60 \text{ min/h})(1750 \text{ rev/min}) = 1.26 \times 10^9 \text{ rev} \quad Z_N = 0.8$$

Try grade 1 flame-hardened,  $S_c = 170\,000$  psi

$$n_c = \frac{\sigma_{c,\text{all}}}{\sigma_c} = \frac{170\,000(0.8)}{94\,000} = 1.40$$

### Gear 2 Bending

$$J = 0.27 \quad Y_N = 0.88$$

$$\sigma = 539.7(1.37) \frac{(6)(1.19)}{(1.5)(0.27)} = 13\,040 \text{ psi}$$

$$n = \frac{\sigma_{\text{all}}}{\sigma} = \frac{45\,000(0.88)}{13\,040} = 3.04$$

### Gear 3 Wear and Bending

$$J = 0.41 \quad Y_N = 0.9 \quad Z_N = 0.9$$

$$\sigma_c = 2300 \sqrt{\frac{(539.7)(1.37)(1.19)}{12(1.5)(0.1315)}} = 44\,340 \text{ psi}$$

$$\sigma = 539.7(1.37) \frac{(6)(1.19)}{1.5(0.41)} = 8584 \text{ psi}$$

Try Grade 1 steel, through-hardened to 200  $H_B$ . From Fig. 14-2, p. 727,  $S_t = 28\,000$  psi and from Fig. 14-5, p. 730,  $S_c = 90\,000$  psi.

$$n_c = \frac{90\,000(0.9)}{44\,340} = 1.83$$

$$n = \frac{\sigma_{\text{all}}}{\sigma} = \frac{28\,000(0.9)}{8584} = 2.94$$

In summary, the resulting gear specifications are:

All gears,  $P = 6$  teeth/in

Gear 2, Grade 1 flame-hardened,  $S_c = 170\,000$  psi and  $S_t = 45\,000$  psi

$d_2 = 2.67$  in, face width = 1.5 in

Gear 3, Grade 1 through-hardened to 200  $H_B$ ,  $S_c = 90\,000$  psi and  $S_t = 28\,000$  psi

$d_3 = 12.0$  in, face width = 1.5 in

Gear 4, Grade 2 carburized and hardened,  $S_c = 225\,000$  psi and  $S_t = 65\,000$  psi

$d_4 = 2.67$  in, face width = 2.0 in

Gear 5, Grade 1 through-hardened to 250  $H_B$ ,  $S_c = 110\,000$  psi and  $S_t = 31\,000$  psi

$d_5 = 12.0$  in, face width = 2.0 in

## 18-4 Shaft Layout

The general layout of the shafts, including axial location of gears and bearings, must now be specified in order to perform a free-body force analysis and to obtain shear force and bending moment diagrams. If there is no existing design to use as a starter, then the determination of the shaft layout may have many solutions. Section 7-3, p. 349, discusses the issues involved in shaft layout. In this section the focus will be on how the decisions relate to the overall process.

A free-body force analysis can be performed without knowing shaft diameters, but can not be performed without knowing axial distances between gears and bearings. It is extremely important to keep axial distances small. Even small forces can create large bending moments if the moment arms are large. Also, recall that beam deflection equations typically include length terms raised to the third power.

It is worth examining the entirety of the gearbox at this time, to determine what factors drive the length of the shaft and the placement of the components. A rough sketch, such as shown in Fig. 18-2, is sufficient for this purpose.

Sketch for shaft layout. Dimensions are in inches.

Wider face widths on gears require more shaft length. Originally, gears with hubs were considered for this design to allow the use of set screws instead of high-stress-concentration retaining rings. However, the extra hub lengths added several inches to the shaft lengths and the gearbox housing.

Several points are worth noting in the layout in Fig. 18–2. The gears and bearings are positioned against shoulders, with retaining rings to hold them in position. While it is desirable to place gears near the bearings, a little extra space is provided between them to accommodate any housing that extends behind the bearing, and to allow for a bearing puller to have space to access the back of the bearing. The extra change in diameter between the bearings and the gears allows the shoulder height for the bearing and the bore size for the gear to be different. This diameter can have loose tolerances and large fillet radius.

Each bearing is restrained axially on its shaft, but only one bearing on each shaft is axially fixed in the housing, allowing for slight axial thermal expansion of the shafts.

## 18–5 Force Analysis

Once the gear diameters are known, and the axial locations of the components are set, the free-body diagrams and shear force and bending moment diagrams for the shafts can be produced. With the known transmitted loads, determine the radial and axial loads transmitted through the gears (see Secs. 13–14 through 13–17, pp. 685–694). From summation of forces and moments on each shaft, ground reaction forces at the bearings can be determined. For shafts with gears and pulleys, the forces and moments will usually have components in two planes along the shaft. For rotating shafts, usually only the resultant magnitude is needed, so force components at bearings are summed as vectors. Shear force and bending moment diagrams are usually obtained in two planes, then summed as vectors at any point of interest. A torque diagram should also be generated to clearly visualize the transfer of torque from an input component, through the shaft, and to an output component.

See the beginning of Ex. 7–2, p. 361, for the force analysis portion of the case study for the intermediate shaft. The bending moment is largest at gear 4. This is predictable, since gear 4 is smaller, and must transmit the same torque that entered the shaft through the much larger gear 3.

While the force analysis is not difficult to perform manually, if beam software is to be used for the deflection analysis, it will necessarily calculate reaction forces, along with shear force and bending moment diagrams in the process of calculating deflections. The designer can enter guessed values for diameters into the software at this point, just to get the force information, and later enter actual diameters to the same model to determine deflections.

## 18–6 Shaft Material Selection

A trial material for the shaft can be selected at any point before the stress design of the shaft, and can be modified as necessary during the stress design process. Section 7–2, p. 348, provides details for decisions regarding material selection. For the case study, an inexpensive steel, 1020 CD, is initially selected. After the stress analysis, a slightly higher strength 1050 CD is chosen to reduce the critical stresses without further increasing the shaft diameters.

## 18-7 Shaft Design for Stress

The critical shaft diameters are to be determined by stress analysis at critical locations. Section 7-4, p. 354, provides a detailed examination of the issues involved in shaft design for stress.

### CASE STUDY PART 5 DESIGN FOR STRESS

Proceed with the next phase of the case study design, in which appropriate diameters for each section of the shaft are estimated, based on providing sufficient fatigue and static stress capacity for infinite life of the shaft, with minimum safety factor of 1.5.

#### Solution

The solution to this phase of the design is presented in Ex. 7-2, p. 361.

Since the bending moment is highest at gear 4, potentially critical stress points are at its shoulder, keyway, and retaining ring groove. It turns out that the keyway is the critical location. It seems that shoulders often get the most attention. This example demonstrates the danger of neglecting other stress concentration sources, such as keyways.

The material choice was changed in the course of this phase, choosing to pay for a higher strength to limit the shaft diameter to 2 in. If the shaft were to get much bigger, the small gear would not be able to provide an adequate bore size. If it becomes necessary to increase the shaft diameter any more, the gearing specification will need to be redesigned.

## 18-8 Shaft Design for Deflection

Section 7-5, p. 367, provides a detailed discussion of deflection considerations for shafts. Typically, a deflection problem in a shaft will not cause catastrophic failure of the shaft, but will lead to excess noise and vibration, and premature failure of the gears or bearings.

### CASE STUDY PART 6 DEFLECTION CHECK

Proceed with the next phase of the case study by checking that deflections and slopes at the gears and bearings on the intermediate shaft are within acceptable ranges.

#### Solution

The solution to this phase of the design is presented in Ex. 7-3, p. 368.

It turns out that in this problem all the deflections are within recommended limits for bearings and gears. This is not always the case, and it would be a poor choice to neglect the deflection analysis. In a first iteration of this case study, with longer shafts due to using gears with hubs, the deflections were more critical than the stresses.

## 18–9 Bearing Selection

Bearing selection is straightforward now that the bearing reaction forces and the approximate bore diameters are known. See Chap. 11 for general details on bearing selection. Rolling-contact bearings are available with a wide range of load capacities and dimensions, so it is usually not a problem to find a suitable bearing that is close to the estimated bore diameter and width.

### CASE STUDY PART 7 BEARING SELECTION

Continue the case study by selecting appropriate bearings for the intermediate shaft, with a reliability of 99 percent. The problem specifies a design life of 12 000 h. The intermediate shaft speed is 389 rev/min. The estimated bore size is 1 in, and the estimated bearing width is 1 in.

#### Solution

From the free-body diagram (see Ex. 7-2, p. 361),

$$R_{Az} = 115.0 \text{ lbf} \quad R_{Ay} = 356.7 \text{ lbf} \quad R_A = 375 \text{ lbf}$$

$$R_{Bz} = 1776.0 \text{ lbf} \quad R_{By} = 725.3 \text{ lbf} \quad R_B = 1918 \text{ lbf}$$

At the shaft speed of 389 rev/min, the design life of 12 000 h correlates to a bearing life of  $L_D = (12\,000 \text{ h})(60 \text{ min/h})(389 \text{ rev/min}) = 2.8 \times 10^8 \text{ rev}$ .

Start with bearing B since it has the higher loads and will likely raise any lurking problems. From Eq. (11-7), p. 558, assuming a ball bearing with  $a = 3$  and  $L = 2.8 \times 10^6 \text{ rev}$ ,

$$F_{RB} = 1918 \left[ \frac{2.8 \times 10^8 / 10^6}{0.02 + 4.439(1 - 0.99)^{1/1.483}} \right]^{1/3} = 20\,820 \text{ lbf}$$

A check on the Internet for available bearings ([www.globalspec.com](http://www.globalspec.com) is one good starting place) shows that this load is relatively high for a ball bearing with bore size in the neighborhood of 1 in. Try a cylindrical roller bearing. Recalculating  $F_{RB}$  with the exponent  $a = 3/10$  for roller bearings, we obtain

$$F_{RB} = 16\,400 \text{ lbf}$$

Cylindrical roller bearings are available from several sources in this range. A specific one is chosen from SKF, a common supplier of bearings, with the following specifications:

Cylindrical roller bearing at right end of shaft

$C = 18\,658 \text{ lbf}$ , ID = 1.181 1 in, OD = 2.834 6 in,  $W = 1.063 \text{ in}$

Shoulder diameter = 1.45 in to 1.53 in, and maximum fillet radius = 0.043 in

For bearing *A*, again assuming a ball bearing,

$$F_{RA} = 375 \left[ \frac{2.8 \times 10^8 / 10^6}{0.02 + 4.439(1 - 0.99)^{1/1.483}} \right]^{1/3} = 407 \text{ lbf}$$

A specific ball bearing is chosen from the SKF Internet catalog.

Deep-groove ball bearing at left end of shaft

$C = 5058 \text{ lbf}$ , ID = 1.000 in, OD = 2.500 in,  $W = 0.75 \text{ in}$

Shoulder diameter = 1.3 in to 1.4 in, and maximum fillet radius = 0.08 in

At this point, the actual bearing dimensions can be checked against the initial assumptions. For bearing *B* the bore diameter of 1.1811 in is slightly larger than the original 1.0 in. There is no reason for this to be a problem as long as there is room for the shoulder diameter. The original estimate for shoulder support diameters was 1.4 in. As long as this diameter is less than 1.625 in, the next step of the shaft, there should not be any problem. In the case study, the recommended shoulder support diameters are within the acceptable range. The original estimates for stress concentration at the bearing shoulder assumed a fillet radius such that  $r/d = 0.02$ . The actual bearings selected have ratios of 0.036 and 0.080. This allows the fillet radii to be increased from the original design, decreasing the stress concentration factors.

The bearing widths are close to the original estimates. Slight adjustments should be made to the shaft dimensions to match the bearings. No redesign should be necessary.

## 18–10 Key and Retaining Ring Selection

The sizing and selection of keys is discussed in Sec. 7–7, p. 376, with an example in Ex. 7–6, p. 382. The cross-sectional size of the key will be dictated to correlate with the shaft size (see Tables 7–6 and 7–8, pp. 379, 381), and must certainly match an integral keyway in the gear bore. The design decision includes the length of the key, and if necessary an upgrade in material choice.

The key could fail by shearing across the key, or by crushing due to bearing stress. For a square key, it turns out that checking only the crushing failure is adequate, since the shearing failure will be less critical according to the distortion energy failure theory, and equal according to the maximum shear stress failure theory. Check Ex. 7–6 to investigate why.

## CASE STUDY PART 8 KEY DESIGN

Continue the case study by specifying appropriate keys for the two gears on the intermediate shaft to provide a factor of safety of 2. The gears are to be custom bored and keyed to the required specifications. Previously obtained information includes the following:

Transmitted torque:  $T = 3240 \text{ lbf-in}$

Bore diameters:  $d_3 = d_4 = 1.625 \text{ in}$

Gear hub lengths:  $l_3 = 1.5 \text{ in}$ ,  $l_4 = 2.0 \text{ in}$

### Solution

From Table 7-6, p. 379, for a shaft diameter of 1.625 in, choose a square key with side dimension  $t = \frac{3}{8}$  in. Choose 1020 CD material, with  $S_y = 57$  kpsi. The force on the key at the surface of the shaft is

$$F = \frac{T}{r} = \frac{3240}{1.625/2} = 3988 \text{ lbf}$$

Checking for failure by crushing, we find the area of one-half the face of the key is used.

$$n = \frac{S_y}{\sigma} = \frac{S_y}{F/(tl/2)}$$

Solving for  $l$  gives

$$l = \frac{2Fn}{tS_y} = \frac{2(3988)(2)}{(0.375)(57000)} = 0.75 \text{ in}$$

Since both gears have the same bore diameter and transmit the same torque, the same key specification can be used for both.

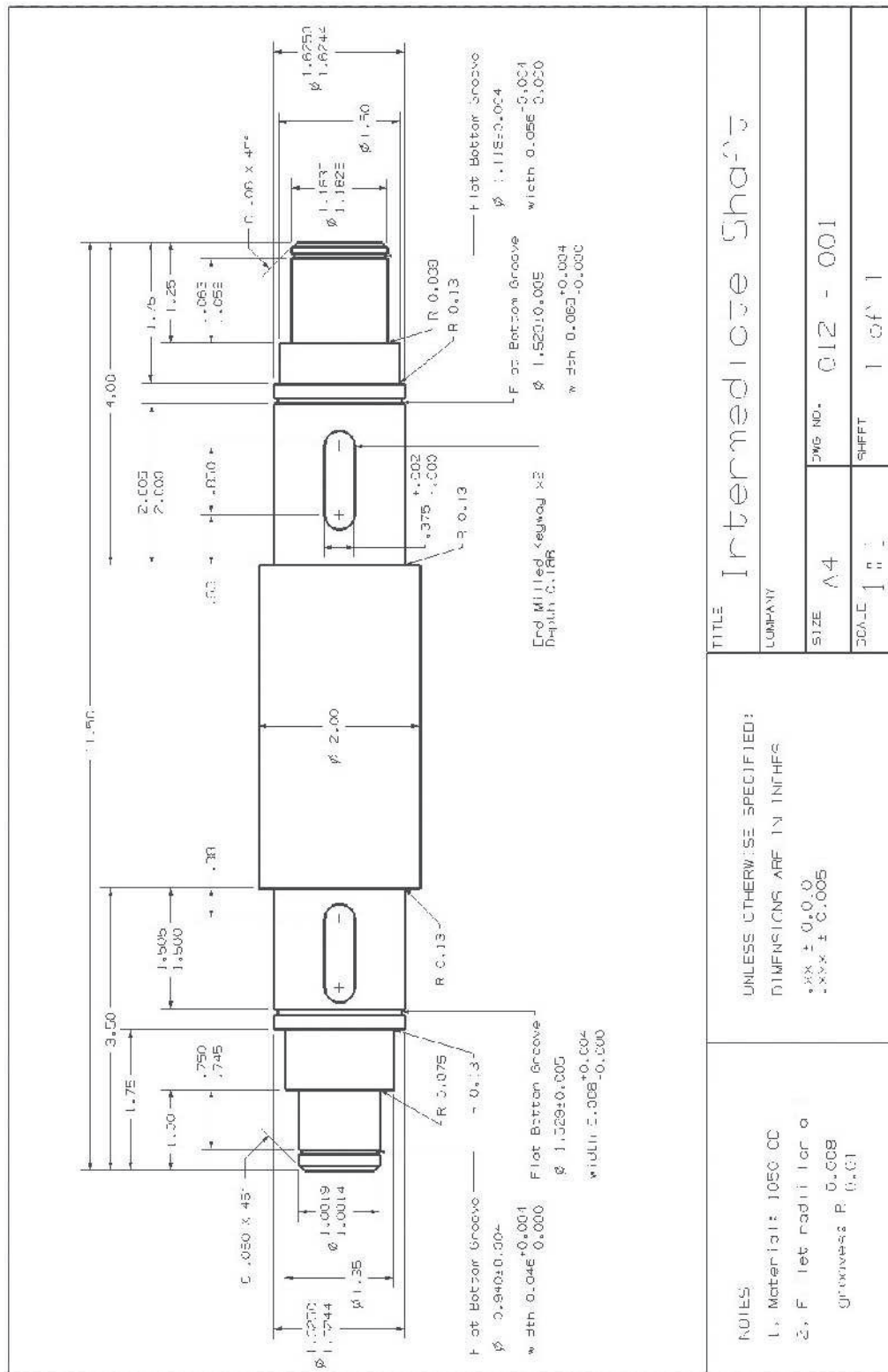
Retaining ring selection is simply a matter of checking catalog specifications. The retaining rings are listed for nominal shaft diameter, and are available with different axial load capacities. Once selected, the designer should make note of the depth of the groove, the width of the groove, and the fillet radius in the bottom of the groove. The catalog specification for the retaining ring also includes an edge margin, which is the minimum distance to the next smaller diameter change. This is to ensure support for the axial load carried by the ring. It is important to check stress concentration factors with actual dimensions, as these factors can be rather large. In the case study, a specific retaining ring was already chosen during the stress analysis (see Ex. 7-2, p. 361) at the potentially critical location of gear 4. The other locations for retaining rings were not at points of high stress, so it is not necessary to worry about the stress concentration due to the retaining rings in these locations. Specific retaining rings should be selected at this time to complete the dimensional specifications of the shaft.

For the case study, retaining rings specifications are entered into globalspec, and specific rings are selected from Truarc Co., with the following specifications:

	Both Gears	Left Bearing	Right Bearing
Nominal Shaft diameter	1.625 in	1.000 in	1.181 in
Groove diameter	$1.529 \pm 0.005$ in	$0.940 \pm 0.004$ in	$1.118 \pm 0.004$ in
Groove width	$0.068^{+0.004}_{-0.000}$ in	$0.046^{+0.004}_{-0.000}$ in	$0.046^{+0.004}_{-0.000}$ in
Nominal groove depth	0.048 in	0.030 in	0.035 in
Max groove fillet radius	0.010 in	0.010 in	0.010 in
Minimum edge margin	0.144 in	0.105 in	0.105 in
Allowable axial thrust	11 850 lbf	6 000 lbf	7 000 lbf

These are within the estimates used for the initial shaft layout, and should not require any redesign. The final shaft should be updated with these dimensions.





## 18–12 Final Analysis

At this point in the design, everything seems to check out. Final details include determining dimensions and tolerances for appropriate fits with the gears and bearings. See Section 7–8, p. 383, for details on obtaining specific fits. Any small changes from the nominal diameters already specified will have negligible effect on the stress and deflection analysis. However, for manufacturing and assembly purposes, the designer should not overlook the tolerance specification. Improper fits can lead to failure of the design. The final drawing for the intermediate shaft is shown in Fig. 18–3.

For documentation purposes, and for a check on the design work, the design process should conclude with a complete analysis of the final design. Remember that analysis is much more straightforward than design, so the investment of time for the final analysis will be relatively small.

## PROBLEMS

- 18–1** For the case study problem, design the input shaft, including complete specification of the gear, bearings, key, retaining rings, and shaft.
- 18–2** For the case study problem, design the output shaft, including complete specification of the gear, bearings, key, retaining rings, and shaft.
- 18–3** For the case study problem, use helical gears and design the intermediate shaft. Compare your results with the spur gear design presented in this chapter.
- 18–4** Perform a final analysis for the resulting design of the intermediate shaft of the case study problem presented in this chapter. Produce a final drawing with dimensions and tolerances for the shaft. Does the final design satisfy all the requirements? Identify the critical aspects of the design with the lowest factor of safety.
- 18–5** For the case study problem, change the power requirement to 40 horsepower. Design the intermediate shaft, including complete specification of the gears, bearings, keys, retaining rings, and shaft.